

**Modelling and Simulation of Oil Production Tubing Dynamic and
Static Characteristics due to Fluid Dynamic Loading**

by

HO CHIT SIONG

Dissertation submitted in partial fulfillment of

the requirements for the

Bachelor of Engineering (Hons)

Mechanical Engineering

AUGUST 2013

Universiti Teknologi PETRONAS

Bandar Seri Iskandar

31750 Tronoh

Perak Darul Ridzuan

CERTIFICATION OF APPROVAL

Modelling and Simulation of Oil Production Tubing Dynamic and Static Characteristics due to Fluid Dynamic Loading

by

Ho Chit Siong

A project dissertation submitted to the
Mechanical Engineering Programme
Universiti Teknologi PETRONAS
in partial fulfillment of the requirement for the
BACHELOR OF ENGINEERING (HONS)
MECHANICAL ENGINEERING

Approved by,

(IR. DR. IDRIS BIN IBRAHIM)

UNIVERSITI TEKNOLOGI PETRONAS

TRONOH, PERAK

AUGUST 2013

CERTIFICATION OF ORIGINALITY

This is to certify that I am responsible for the work submitted in this project, that the original work is my own except as specified in the references and acknowledgements, and that the original work contained herein have not been undertaken or done by unspecified sources or persons.

HO CHIT SIONG

ABSTRACT

This report outlines the modelling and simulation of oil production tubing to investigate the dynamic and static characteristics of the tubing due to fluid dynamic loading with respect to different production rates. The fluid-structure interaction between the tubing and the contained oil are modeled and simulated using Ansys. Pressure difference between the wellhead choke and bottomhole forces the oil to move upwards in the tubing, thus exert fluid dynamic loading onto the tubing, which in turn creates the static and dynamic characteristics of the tubing due to fluid loading. At different production rate, different pressure difference between wellhead choke and bottomhole is generated, which produces variation in the static and dynamic characteristics of the tubing due to fluid loading. Therefore, there is a need to investigate the static and dynamic characteristics of the tubing with respect to different production rates. Due to confidentiality, the name of the oil company that provides the data is kept secret and the company will be referred as “the oil company” throughout the report. The scope for the tubing length is resized to 50m only, which is the depth for one oil production zone, focusing on the region from bottomhole to the subsequent upward 50m depth, which is critical in oil production system, since the location of the oil production zone is the critical region where the production tubing receives the highest fluid loading from the oil production. The simulation focuses on single phase incompressible oil flow with constant viscosity in an isothermal environment. Experimental validation is excluded, instead, simulation validation is needed to verify that the model case built is acceptable and produces results in agreement with the data from the oil company. Literature review is conducted at the early stage of this project, followed by validation of the model case through modelling and simulation. Upon validation, the settings of the model case are applied for different production rates, followed by the simulation of the dynamic and static characteristics of the tubing due to fluid loading, whereby the results are analysed and interpreted. The results show that the pressure, stress and deformation occurring on the tubing increases as the production rate increases. For lower modes of vibration, the natural frequencies also increase with increasing production rates.

ACKNOWLEDGEMENT

Firstly, I would like to express my greatest gratitude towards my supervisor, Ir. Dr. Idris Bin Ibrahim for assisting me throughout my whole final year project duration. His guidance and advice have helped me to move forward while conducting my final year project up to the completion stage. Besides that, he is willing to solve my doubts patiently from day one until the day of completion my final year project.

Secondly, I would like to express my gratitude towards Ms. Raja Rajeswary for her guidance and aid throughout my whole final year project duration. She have helped me a lot in clearing my doubts about the petroleum production system, so that I can complete my final year project successfully.

Besides that, I would like to express my gratitude towards Dr. Tadimalla Rao for his guidance and aid throughout my whole final year project duration. He have helped me a lot in clearing my doubts, especially regarding the dynamic characteristics aspect of the tubing for me to get some insight in continuing my final year project.

Besides that, I would like to express my gratitude towards Ms. Chin Yee Sing for her guidance and aid throughout my whole final year project duration. She have helped me a lot in clearing my doubts about Ansys Fluent and have given constructive suggestions so that my final year project can be completed successfully.

I also wish to express my thank you to my family, friends and anyone who have helped me throughout my whole final year project duration. Their aid and help have helped me in my final year project undertaking, so that I can complete my final year project successfully.

Lastly, I wish to express my gratitude towards Universiti Teknologi PETRONAS (UTP) for giving me this opportunity to pursue this Final Year Project Course as one of the requirements to complete my Bachelor of Engineerng (Hons) in Mechanical Engineering. This has made me more familiar with Ansys Software and enhances my problem solving skills as well as preparing me for my future career.

TABLE OF CONTENTS

CERTIFICATION OF APPROVAL	i
CERTIFICATION OF ORIGINALITY	ii
ABSTRACT	iii
ACKNOWLEDGEMENT	iv
TABLE OF CONTENTS.....	v
LIST OF FIGURES	vii
LIST OF TABLES.....	xiv
NOMENCLATURE.....	xv
CHAPTER 1	1
INTRODUCTION	1
1.1 BACKGROUND OF STUDY	1
1.1.1 OVERVIEW OF PRODUCTION EQUIPMENTS USED IN PETROLEUM PRODUCTION	1
1.1.2 OVERVIEW OF PRODUCTION FLUID PRODUCED (CRUDE OIL).....	3
1.1.3 OVERVIEW OF DIFFERENT TYPES OF CRUDE OIL	4
1.1.4 IMPORTANCE OF CRUDE OIL TO HUMAN CIVILIZATION	5
1.2 PROBLEM STATEMENT	6
1.3 OBJECTIVES	6
1.4 SCOPE OF STUDY	7
1.5 RELEVANCY OF THE PROJECT.....	8
1.6 FEASIBILITY OF THE PROJECT WITHIN THE SCOPE AND TIME FRAME.....	8
CHAPTER 2	9
LITERATURE REVIEW	9
2.1 OVERVIEW OF SINGLE PHASE FLUID FLOW IN PIPE	9
2.2 OVERVIEW OF THE SIMULATION PARAMETERS USED	12
2.3 OVERVIEW OF STATIC AND DYNAMIC CHARACTERISTICS OF THE TUBING DUE TO FLUID DYNAMIC LOADING	19
CHAPTER 3	22
METHODOLOGY.....	22
3.1 RESEARCH METHODOLOGY	22

3.2	PROJECT ACTIVITIES.....	24
3.2.1	MODELLING ACTIVITIES	25
3.2.2	SIMULATION ACTIVITIES.....	26
3.3	GANTT CHART (FYP 1).....	29
3.4	GANTT CHART (FYP 2).....	30
3.5	KEY MILESTONES.....	31
3.6	TOOLS.....	32
CHAPTER 4		33
RESULTS AND DISCUSSIONS		33
4.1	VALIDATION OF MODEL CASE	33
4.2	SIMULATION OF FLUID FLOW FOR DIFFERENT PRODUCTION RATES	37
4.2.1	SIMULATION PARAMETERS APPLIED FOR DIFFERENT PRODUCTION RATES	37
4.2.2	VELOCITY VECTORS PROFILES FOR DIFFERENT PRODUCTION RATES	39
4.3	SIMULATION OF STATIC CHARACTERISTICS OF THE TUBING FOR DIFFERENT PRODUCTION RATES.....	44
4.3.1	PRESSURE EXERTED ON THE TUBING	44
4.3.2	DEFORMATION AND STRESS OCCURRING ON THE TUBING FOR DIFFERENT PRODUCTION RATES.....	48
4.4	SIMULATION OF DYNAMIC CHARACTERISTICS OF THE TUBING FOR DIFFERENT PRODUCTION RATES.....	60
4.4.2	DEFORMATION ON THE DIFFERENT LOCATIONS OF THE TUBING WITH RESPECT TO THE NATURAL FREQUENCIES	79
CHAPTER 5		84
CONCLUSION.....		84
5.1	CONCLUSION	84
5.2	RECOMMENDATIONS FOR FUTURE WORK AND CONTINUATION.....	85
REFERENCES.....		86
APPENDICES		88

LIST OF FIGURES

Figure 1.1: Schematic Diagram of Oil and Gas Production Inlet Wellbore-----	2
Figure 1.2: Paraffin Molecule-----	4
Figure 1.3: Naphthene Molecule-----	4
Figure 1.4: Aromatic Molecule-----	5
Figure 2.1: Moody Chart-----	10
Figure 2.2: Parabolic Shapes of Laminar and Turbulent Velocity Profiles-----	11
Figure 2.3: Completion schematic of the oil field-----	12
Figure 3.1: Flow Chart Describing the Research Methodology-----	23
Figure 3.2: The Project Activities for Modelling and Simulation-----	24
Figure 3.3: The Locations of Outlet and Inlet in the Simulation-----	26
Figure 3.4: Meshing at the Packer Region -----	27
Figure 3.5: Meshing at the Outlet Region-----	27
Figure 4.1: The Graph of Pressure vs Length for the Model Case-----	33
Figure 4.2: Velocity Vectors Profile of the Model Case at the Entrance Region of Fluid Flow where Developing Flow Forms-----	35
Figure 4.3: Velocity Vectors Profile of the Model Case at the Region After the Entrance Region of the Fluid Flow where Fully Developed Flow Forms-----	36
Figure 4.4: Velocity Vectors Profile of Developing Flow for 5000bbl/day-----	39
Figure 4.5: Velocity Vectors Profile of Developing Flow for 5500bbl/day-----	40
Figure 4.6: Velocity Vectors Profile of Developing Flow for 6000bbl/day-----	40

Figure 4.7: Velocity Vectors Profile of Developing Flow for 6500bbl/day	-----41
Figure 4.8: Velocity Vectors Profile of Fully Developed Flow for 5000bbl/day	-----42
Figure 4.9: Velocity Vectors Profile of Fully Developed Flow for 5500bbl/day	-----42
Figure 4.10: Velocity Vectors Profile of Fully Developed Flow for 6000bbl/day	-----43
Figure 4.11: Velocity Vectors Profile of Fully Developed Flow for 6500bbl/day	-----43
Figure 4.12: Pressure Exerted on the Tubing for Production Rate of 5000bbl/day	-----44
Figure 4.13: Pressure Exerted on the Tubing for Production Rate of 5000bbl/day at the Outlet Region	-----45
Figure 4.14: Pressure Exerted on the Tubing for Production Rate of 5500bbl/day at the Outlet Region	-----45
Figure 4.15: Pressure Exerted on the Tubing for Production Rate of 6000bbl/day at the Outlet Region	-----46
Figure 4.16: Pressure Exerted on the Tubing for Production Rate of 6500bbl/day at the Outlet Region	-----46
Figure 4.17: The Graph of Difference of Pressure Exerted on Tubing at Different Production Rates	-----47
Figure 4.18: Von-Mises Stress Occurring on the Tubing for Production Rate=5000bbl/day at the Packer Region	-----49
Figure 4.19: Shear Stress Occurring on the Tubing for Production Rate=5000bbl/day at the Packer Region	-----49

Figure 4.20: Principal Stress Occurring on the Tubing for Production Rate=5000bbl/day at the Packer Region-----	50
Figure 4.21: Deformation Occurring on the Tubing for Production Rate=5000bbl/day at the Inlet Region-----	50
Figure 4.22: Von-Mises Stress Occurring on the Tubing for Production Rate=5500bbl/day at the Packer Region-----	51
Figure 4.23: Shear Stress Occurring on the Tubing for Production Rate=5500bbl/day at the Packer Region-----	51
Figure 4.24: Prinipal Stress Occurring on the Tubing for Production Rate=5500bbl/day at the Packer Region-----	52
Figure 4.25: Deformation Occurring on the Tubing for Production Rate=5500bbl/day at the Inlet Region-----	52
Figure 4.26: Von-Mises Stress Occurring on the Tubing for Production Rate=6000bbl/day at the Packer Region-----	53
Figure 4.27: Shear Stress Occurring on the Tubing for Production Rate=6000bbl/day at the Packer Region-----	53
Figure 4.28: Prinipal Stress Occurring on the Tubing for Production Rate=6000bbl/day at the Packer Region-----	54
Figure 4.29: Deformation Occurring on the Tubing for Production Rate=6000bbl/day at the Inlet Region-----	54
Figure 4.30: Von-Mises Stress Occurring on the Tubing for Production Rate=6500bbl/day at the Packer Region-----	55
Figure 4.31: Shear Stress Occurring on the Tubing for Production Rate=6500bbl/day at the Packer Region-----	55

Figure 4.32: Principal Stress Occurring on the Tubing for Production Rate=6500bbl/day at the Packer Region-----	56
Figure 4.33: Deformation Occurring on the Tubing for Production Rate=6500bbl/day at the Inlet Region-----	56
Figure 4.34: The Graph of Maximum Stress on the Tubing vs Production Rate-----	58
Figure 4.35: The Graph of Maximum Deformation vs Production Rate-----	59
Figure 4.36: The Graph of Mode Natural Frequencies vs Production rate-----	60
Figure 4.37: The Graph of Maximum Deformation of Different Modes vs Different Production rates-----	61
Figure 4.38: Deformation at Natural Frequency of Mode 1 at Production rate=5000bbl/day at Packer Region-----	62
Figure 4.39: Deformation at Natural Frequency of Mode 1 at Production rate=5000bbl/day for the Whole 50m Tubing Length-----	62
Figure 4.40: Deformation at Natural Frequency of Mode 2 at Production rate=5000bbl/day at Packer Region-----	63
Figure 4.41: Deformation at Natural Frequency of Mode 2 at Production rate=5000bbl/day for the Whole 50m Tubing Length-----	63
Figure 4.42: Deformation at Natural Frequency of Mode 3 at Production rate=5000bbl/day at Packer Region-----	64
Figure 4.43: Deformation at Natural Frequency of Mode 3 at Production rate=5000bbl/day for the Whole 50m Tubing Length-----	64
Figure 4.44: Deformation at Natural Frequency of Mode 4 at Production rate=5000bbl/day at Packer Region-----	65

Figure 4.45: Deformation at Natural Frequency of Mode 4 at Production rate=5000bbl/day for the Whole 50m Tubing Length-----	65
Figure 4.46: Deformation at Natural Frequency of Mode 1 at Production rate=5500bbl/day at Packer Region-----	66
Figure 4.47: Deformation at Natural Frequency of Mode 1 at Production rate=5500bbl/day for the Whole 50m Tubing Length-----	66
Figure 4.48: Deformation at Natural Frequency of Mode 2 at Production rate=5500bbl/day at Packer Region-----	67
Figure 4.49: Deformation at Natural Frequency of Mode 2 at Production rate=5500bbl/day for the Whole 50m Tubing Length-----	67
Figure 4.50: Deformation at Natural Frequency of Mode 3 at Production rate=5500bbl/day at Packer Region-----	68
Figure 4.51: Deformation at Natural Frequency of Mode 3 at Production rate=5500bbl/day for the Whole 50m Tubing Length-----	68
Figure 4.52: Deformation at Natural Frequency of Mode 4 at Production rate=5500bbl/day at Packer Region-----	69
Figure 4.53: Deformation at Natural Frequency of Mode 4 at Production rate=5500bbl/day for the Whole 50m Tubing Length-----	69
Figure 4.54: Deformation at Natural Frequency of Mode 1 at Production rate=6000bbl/day at Packer Region-----	70
Figure 4.55: Deformation at Natural Frequency of Mode 1 at Production rate=6000bbl/day for the Whole 50m Tubing Length-----	70
Figure 4.56: Deformation at Natural Frequency of Mode 2 at Production rate=6000bbl/day at Packer Region-----	71

Figure 4.57: Deformation at Natural Frequency of Mode 2 at Production rate=6000bbl/day for the Whole 50m Tubing Length-----	71
Figure 4.58: Deformation at Natural Frequency of Mode 3 at Production rate=6000bbl/day at Packer Region-----	72
Figure 4.59: Deformation at Natural Frequency of Mode 3 at Production rate=6000bbl/day for the Whole 50m Tubing Length-----	72
Figure 4.60: Deformation at Natural Frequency of Mode 4 at Production rate=6000bbl/day at Packer Region-----	73
Figure 4.61: Deformation at Natural Frequency of Mode 4 at Production rate=6000bbl/day for the Whole 50m Tubing Length-----	73
Figure 4.62: Deformation at Natural Frequency of Mode 1 at Production rate=6500bbl/day at Packer Region-----	74
Figure 4.63: Deformation at Natural Frequency of Mode 1 at Production rate=6500bbl/day for the Whole 50m Tubing Length-----	74
Figure 4.64: Deformation at Natural Frequency of Mode 2 at Production rate=6500bbl/day at Packer Region-----	75
Figure 4.65: Deformation at Natural Frequency of Mode 2 at Production rate=6500bbl/day for the Whole 50m Tubing Length-----	75
Figure 4.66: Deformation at Natural Frequency of Mode 3 at Production rate=6500bbl/day at Packer Region-----	76
Figure 4.67: Deformation at Natural Frequency of Mode 3 at Production rate=6500bbl/day for the Whole 50m Tubing Length-----	76
Figure 4.68: Deformation at Natural Frequency of Mode 4 at Production rate=6500bbl/day at Packer Region-----	80

Figure 4.69: Deformation at Natural Frequency of Mode 4 at Production rate=6500bbl/day for the Whole 50m Tubing Length-----	81
Figure 4.70: The Positioning of the Support between the Packer and the Inlet-----	82
Figure 4.71: Graph of Deformations at Different Locations on the Tubing between the Packer and the Inlet vs Natural Frequencies-----	83
Figure 4.72: The Positioning of the Support between the Packer and the Outlet -----	79
Figure 4.73: Graph of Deformations at Different Locations on the Tubing between the Packer and the Outlet vs Natural Frequencies -----	80

LIST OF TABLES

Table 1.1: Chemical Composition of Typical Crude Oil-----	3
Table 1.2: Average and Range of Hydrocarbon Series Molecules in Crude Oil-----	3
Table 1.3: Energy Density of Different Energy Sources -----	5
Table 2.1: Data from the oil company-----	13
Table 2.2: Simulation Parameters for Validation of Model Case-----	17
Table 2.3: The Tubing Properties -----	20
Table 3.1: The Modelling Parameters for Tubing and Packer-----	25
Table 3.2: The Average Skewness and Aspect Ratio of the Meshing-----	28
Table 3.3: Gantt Chart for FYP 1-----	29
Table 3.4: Gantt Chart for FYP 2-----	30
Table 3.5: Key Milestones-----	31
Table 3.6: Tools Used for Simulation-----	32
Table 4.1: The Pressure Exerted on the Tubing at Different Production Rates-----	47
Table 4.2: The Stress Occurring on the Tubing at Different Production Rates-----	57
Table 4.3: The Deformation Occurring on the Tubing at Different Production Rates-----	58
Table 4.4: Natural Frequencies of First Four Modes for Different Production Rates-----	60
Table 4.5: The Maximum Deformation of Different Modes at Different Production rates-----	78

Table 4.6: The Deformation at Different Locations on the Tubing at
 Different Natural Frequencies between the Inlet and the Packer-----80

Table 4.7: The Deformation at Different Locations on the Tubing at
 Different Natural Frequencies between the Packer and the Outlet-----82

NOMENCLATURE

Symbol	Meaning	Unit
Δp_f	Pressure loss due to friction	Pa
f	Friction factor	-
ρ	Density	kg/m ³
V	Velocity	m/s
D	Diameter	m
Δp_z	Pressure loss due to elevation	Pa
g	Gravitational acceleration	m/s ²
Re	Reynolds number	-
μ	Dynamic viscosity	kg/m.s
ε	Absolute roughness	m/m
A	Cross-sectional area	m ²
K	Relative roughness	m/m
p_{outlet}	Pressure at outlet	Pa
p_{bottom}	Pressure at bottomhole	Pa
q	Volume Flow Rate	m ³ /s

CHAPTER 1

INTRODUCTION

1.1 BACKGROUND OF STUDY

1.1.1 OVERVIEW OF PRODUCTION EQUIPMENTS USED IN PETROLEUM PRODUCTION

In petroleum production, production equipments are used to extract the petroleum from the reservoir. For this project, the petroleum production equipments which are related are production tubing and packer. This is because production tubing is the main focus in this project, while packer provides support to the production tubing during the petroleum production.

Production tubing, which is shown in Figure 1.1, is a small diameter pipe used for petroleum production that provides continuous bore from the production zone to the wellhead [1]. Moreover, production tubing is also used to protect the wellbore casing from wear, tear and corrosion by the produced fluids. As a matter of fact, it is hard to repair the casing because it has been cemented in the well. This is when another functionality of the production tubing is displayed since by being suspended in the well, it can be easily removed from the well for repair and replacement during a workover, such as when leakage occurs. The material of the tubing is steel, which comes with diameter ranging from 1.25 in to 4.25 in [2]. Thus, it is recommended to have a diameter between 1.25 in and 4.25 in for tubing diameter to be used for modeling purpose.

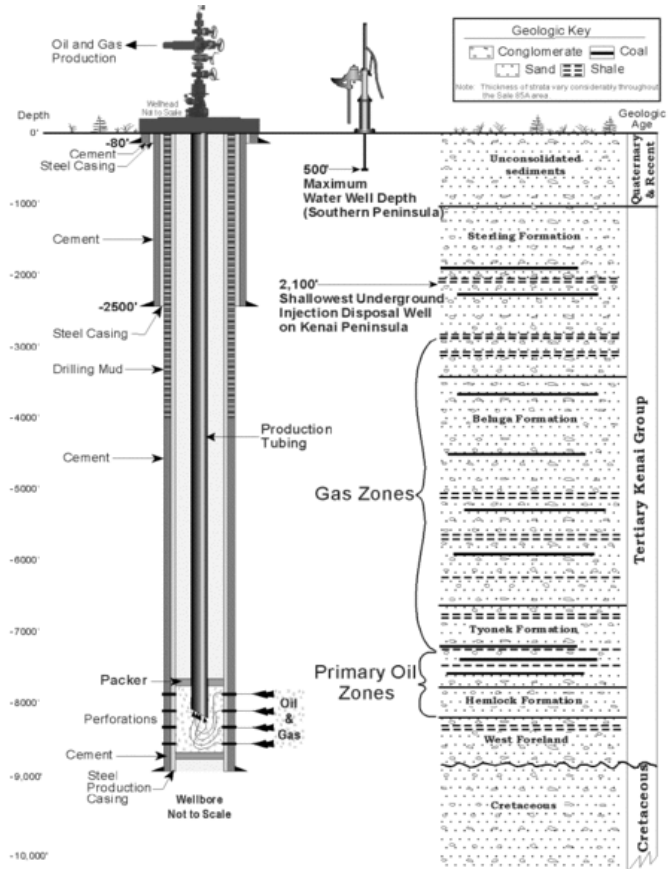


Figure 1.1: Schematic Diagram of Oil and Gas Production Inlet Wellbore

1.1.2 OVERVIEW OF PRODUCTION FLUID PRODUCED (CRUDE OIL)

Crude oil is a naturally occurring and flammable liquid which is composed of hydrocarbons, which can be found in underground geological formations [3]. In other words, crude oil is mixtures of molecules formed by carbon and hydrogen atoms. A typical crude oil has elements of carbon, hydrogen, sulfur, nitrogen and oxygen, which is shown in Table 1.1. Crude oil can be divided into 4 types, which are paraffins, naphthenes, aromatics and asphaltics, as shown in Table 1.2 [2].

Table 1.1: Chemical Composition of Typical Crude Oil

Element	Composition Percentage
Carbon	84-87%
Hydrogen	11-14%
Sulfur	0.06-2%
Nitrogen	0.1-2%
Oxygen	0.1-2%

Table 1.2: Average and Range of Hydrocarbon Series Molecules in Crude Oil

	Weight Percent	Percent Range
Paraffins	30	15-60
Naphthenes	49	30-60
Aromatics	15	3-30
Asphaltics	6	Remainder

1.1.3 OVERVIEW OF DIFFERENT TYPES OF CRUDE OIL

From Table 1.2, it can be shown that there are four types of hydrocarbon series, with different relative percentage of molecules that occur in each crude oil. For paraffin, it is a straight chain of five carbon atoms and longer in length with saturated (single) bonds between the carbon atoms (Fig 1.2) which uses the general formula of C_nH_{2n+2} .

From the table, it can be shown that there are four types of hydrocarbon series with different relative percentage of molecules that occur in each crude oil. For paraffin, it is a straight chain of five carbon atoms and longer in length with saturated (single) bonds between the carbon atoms (Fig 1.2) which uses the general formula of C_nH_{2n+2} .

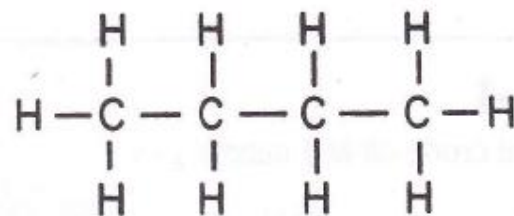


Figure 1.1: Paraffin Molecule

Naphthene molecule is a closed circle that consists of five carbon atoms and longer in length with saturated bonds between the carbon atoms (Fig 1.3) which uses the general formula of C_nH_{2n} .

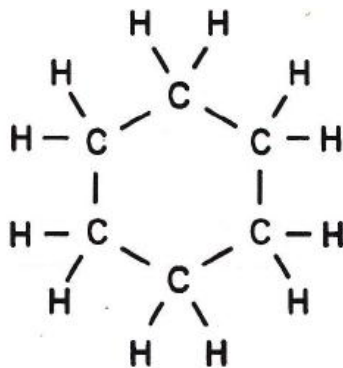


Figure 1.2: Naphthene Molecule

Aromatic molecule is a closed ring of six carbon atoms and longer in length with some unsaturated (double) bonds between carbon atoms (Fig 1.4) which uses the general formula of C_nH_{2n-6} . At the refinery, an aromatic-rich crude oil yields the highest –octane gasoline, which makes it a valuable feedstock for the petrochemical industry.

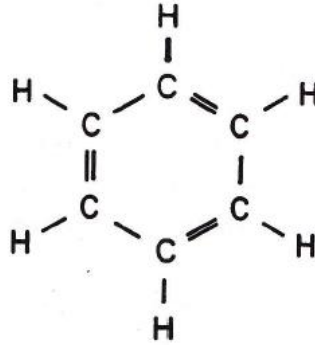


Figure 1.3: Aromatic Molecule

For asphaltic molecule, it has 40 to more than 60 carbon atoms and has a high boiling point with brown to black in color. An asphalt-based crude oil contains little or no paraffin wax that yields a large percentage of paraffin wax, high quality lubricating oil and kerosene when refined.

1.1.4 IMPORTANCE OF CRUDE OIL TO HUMAN CIVILIZATION

Crude Oil is an extremely vital source of energy for human civilization. Processed crude oil is used massively for transportation vehicles and as source of energy for power generation. The reason of massive usage of processed crude oil is because crude oil has high energy density, as shown in Table 1.3 [4].

Table 1.3: Energy Density of Different Energy Sources

Energy Source	Energy Density(J/m ³)
Oil	45×10^9
Natural Gas	40×10^6
Geothermal	0.05
Solar	0.0000015

1.2 PROBLEM STATEMENT

During petroleum production, the crude oil flows through production tubing from the reservoir to the wellhead. The flow of crude oil to the wellhead from reservoir is due to pressure difference between wellhead choke and bottomhole. This pressure difference excites the motion of the production tubing due to fluid dynamic loading, which in turn produces dynamic and static characteristics of the tubing.

Usually, engineer adjusts the valve opening to control the production rate of the crude oil. By varying the choke valve opening, different choke pressure is produced, which later produces different pressure difference between wellhead choke and bottomhole, which in turn produces different production rate. Thus, different pressure difference corresponds to different production rate. And the different pressure difference at different production rate excites the production tubing differently; consequently, different dynamic and static characteristics of the tubing are produced. Therefore, study of dynamic and static characteristics of the production tubing with respect to different production rate is needed because the results can be used to further research on the improvement that can be made on the existing oil and gas production system, and also to provide the engineers with additional knowledge about production tubing characteristics in order to reduce the time for decision-making process in case emergency occurs.

1.3 OBJECTIVES

The objectives of this project are:

- To study the dynamic characteristics of the production tubing due to fluid dynamic loading caused by petroleum production with respect to different production rate.
- To study the static characteristics of the production tubing due to fluid dynamic loading caused by petroleum production with respect to different production rate.

1.4 SCOPE OF STUDY

The scopes of study of this project are:

- Conduct the modelling and simulation of the production tubing loaded by the fluid dynamic loading using Ansys Fluent, Ansys Static Strcutural and Ansys Modal.
- The experimental validation is excluded from the scope; instead simulation validation is needed to ensure that the model case built is acceptable by producing results that are in agreement with the data from the oil company.
- The simulation focuses on single phase incompressible fluid flow with constant viscosity in an isothermal environment.
- Get the technical data needed from the oil company, especially details of the production tubing and its operating parameters and the petroleum production parameters, so that the model case for the simulation can be built.
- The scope for the production tubing length is resized from the original tubing length of 1635m to the length covering one oil zone only. The oil zone is zone J70 with the length of the tubing covering this zone to be 50m, which is from the bottomhole depth of 1635m to 1585m, and this oil zone is chosen because it is the most critical region in the production system, since at this zone, the pressure on the tubing is the highest, which means that this zone receives the highest fluid dynamic loading from the oil flow.
- Study the dynamic and static characteristics of the production tubing at different production rate.

1.5 RELEVANCY OF THE PROJECT

This project entitled “Modelling and Simulation of Oil Production Tubing Static and Dynamic Characteristics due to Fluid Dynamic Loading” is relevant to the oil and gas industry since this project investigates the dynamic and static characteristics of the tubing due to fluid dynamic loading, which can help in reducing time for decision-making process. Plus, this project is important as a foundation stone to further improve on the existing oil production system.

1.6 FEASIBILITY OF THE PROJECT WITHIN THE SCOPE AND TIME FRAME

This project is expected to be finished in 2 semesters time, which is around seven to eight months. This project is feasible and manageable within the time frame, because the software needed is available at the computer lab at Block 17. Therefore, the students can conduct this project from Monday to Friday, during the working hours time. Plus, only simulation validation is needed due to the exclusion of experimental validation.

CHAPTER 2

LITERATURE REVIEW

2.1 OVERVIEW OF SINGLE PHASE FLUID FLOW IN PIPE

During the production of hydrocarbon, the hydrocarbon flows upward in the production tubing. For the hydrocarbon flow, it is a basic entity that must be dealt with, since the hydrocarbon flow forms the core of all flow problems. When the fluid is moving upwards in the production tubing, there will be pressure drop created. The total pressure drop created in the production tubing is the sum of hydrostatic pressure drop, acceleration pressure drop and frictional pressure drop [5][6]. In vertical fluid flow, the gravitational term or hydrostatic term is the dominant element which contributes to most of the pressure drop, while frictional term contributes the rest, with acceleration term being very small and considered as negligible [7]. For simplicity, Darcy-Weisbach equation (Eq. 1) will be used to evaluate the pressure losses due to friction, while the hydrostatic pressure losses (Eq. 2) will be evaluated using the elevation change between the inlet and outlet of the tubing [8].

Darcy-Weisbach Equation:

Pressure losses due to friction:

$$\Delta p_f = f \frac{\rho L V^2}{2D} \quad (1)$$

Pressure losses due to elevation change:

$$\Delta p_z = \rho g h \quad (2)$$

For Darcy-Weisbach equation, friction factor is the main element which needs to be determined. However, to determine friction factor, the state of flow as to whether the flow is turbulent or laminar needs to be verified using Reynolds number. Reynolds number is a function of density of fluid, velocity of fluid, diameter and dynamic viscosity. For laminar flow, the Reynolds number is less than 2100, while for turbulent flow, the Reynolds number exceeds 4000 [9]. Generally, there are two most commonly

used methods to determine friction factor for laminar flow, which are determination of the friction factor by using Moody Chart (Fig. 2.1) and the determination of the friction factor by using Hagen- Poiseuille equation (Eq.4). On the other hands, for turbulent flow, the friction factor can be determined by using Moody Chart and by using Colebrook-White equation (Eq. 5) [9].

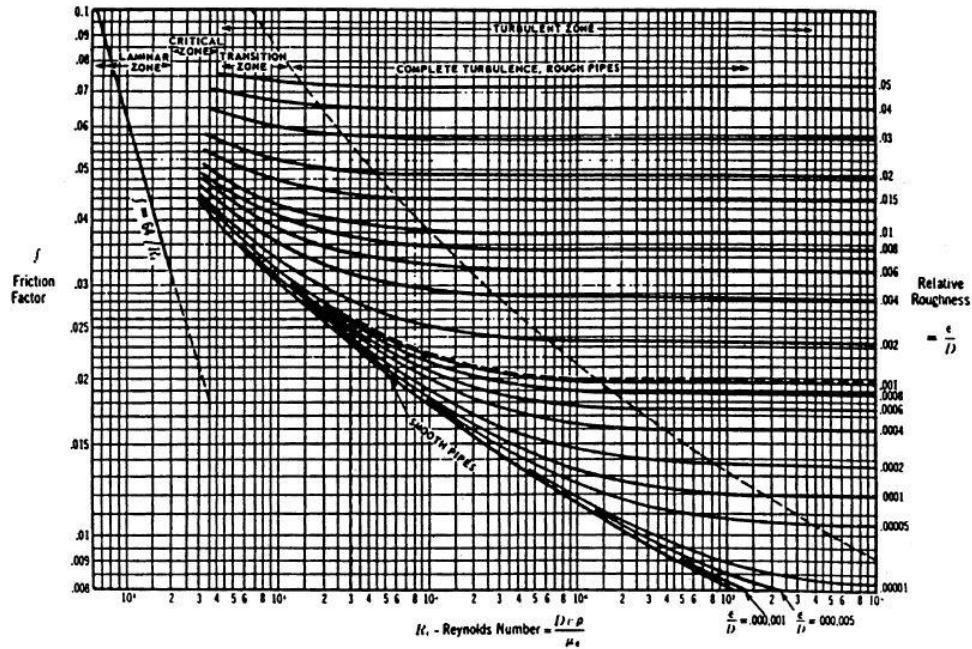


Figure 2.1: Moody Chart

Reynolds number:

$$Re = \frac{\rho V D}{\mu} \quad (3)$$

Hagen-Poiseuille equation:

$$f = \frac{64}{Re} \text{ for } Re < 2100 \quad (4)$$

Colebrook-White equation:

$$\frac{1}{\sqrt{f}} = -2 \log \left[\frac{\frac{\epsilon}{D}}{3.71} + \frac{2.52}{Re \sqrt{f}} \right] \text{ for } 4000 < Re < 10^8 \quad (5)$$

For fluid flow related problems, continuity equation can also be applied as one of the main equations to be used for fluid flow analysis. Continuity equation (Eq.6) states that the volumetric flow rate at the inlet is equivalent to the volumetric flow rate at the outlet [10]. In other words, when the cross-sectional area is constant, the velocity of fluid flow at the inlet is equal to the velocity of the fluid flow at the outlet. However, if there is change in diameter, then there will be change in velocity with the smaller cross-sectional area having higher velocity, while the bigger cross-sectional area having smaller velocity.

Continuity equation:

$$q = VA \tag{6}$$

For single phase fluid flow, the velocity profile is always started with parabolic-shaped developing flow, which later developed into fully developed flow. For laminar and turbulent flow, they produce velocity profiles that are symmetric about the axis of the tubing with maximum velocity at the centre of the tubing, and the difference between turbulent and laminar velocity profiles lies in the flatness of the parabolic shape of the velocity profiles. For laminar flow, the velocity profile at the entrance region of the flow is parabolic, while for the turbulent flow, the velocity profile yields the shape of a much flatter parabolic shape across the core of the flow, with the mean velocity is closer to the centre-line velocity in the flow (as shown in Fig. 2.2).

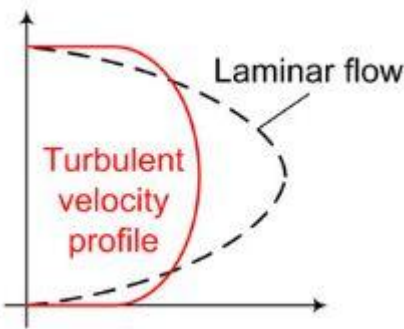


Figure 2.2: Parabolic Shapes of Laminar and Turbulent Velocity Profiles

2.2 OVERVIEW OF THE SIMULATION PARAMETERS USED

The Figure 2.3 is showing the completion schematic of the oil field, obtained from the oil company.



Figure 2.3: Completion schematic of the oil field

Due to confidentiality, the name of the oil company will not be revealed; instead the oil company will be referred to as “the oil company”. The production tubing is the straight pipe inside the casing, with packer located between the tubing itself and the casing. The zone of interest is zone J70, where the depth is from 1585m to 1635m (highlighted in blue region in Figure 2.3). The data obtained from the oil company is as shown in the Table 2.1.

Table 2.1: Data from the oil company

Field Data Parameter	Value
<i>The condition at Zone J70</i>	
Bottom hole pressure	2226.3 psig (equivalent to 15349798 Pa)
Production rate (bbl/day)	5165 (equivalent to $9.5043 \times 10^{-3} \text{ m}^3/\text{s}$)
<i>The properties of the oil</i>	
Density (kg/m^3)	704
Viscosity ($\text{kg}/\text{m}\cdot\text{s}$)	0.0034
Number of Phase	Single phase (no gas is present)
Type of oil	Sweet oil (no hydrogen sulfide is present)
<i>The properties of tubing</i>	
Tubing Inner Diameter	2.441in (equivalent to 0.0620014m)
Tubing Outer Diameter (in)	2.875
Tubing Material	Steel
Length of Tubing	50m (from 1585m to 1635m)
Absolute Roughness	0.006
<i>The properties of packer</i>	
Packer Inner Diameter (in)	2.875
Packer Outer Diameter (in)	4.720
Packer Material	Steel
Length of Packer	0.1397m (located 17m from the depth of 1635m)

The scope for the tubing length is resized to 50m only, which is the depth for one oil production zone, focusing on the region from bottomhole to the subsequent upward 50m depth, which is critical in oil production system, since the location of the oil production zone is the critical region where the production tubing receives the highest fluid loading from the oil production. Therefore, the static and dynamic characteristics of the tubing at this region will be significant, as compared to the static and dynamic characteristics of the tubing at other production zones that are above the 1585m depth.

The simulation focuses on three main items which are the tubing itself, packer and the oil. The depth of the tubing and the oil is 50m, which is covering the entire depth of the Zone J70, while the packer that is located 17m from the bottomhole depth of 1635m has small depth of only 0.1397m. In the simulation, the oil acts as the fluid, and the tubing acts as the solid, with packer acting as the support to hold the tubing.

The simulation scheme used is velocity inlet- pressure outlet scheme, where velocity inlet will be used as the boundary condition at the inlet (positioned at bottomhole), while pressure outlet will be used as the boundary condition at the outlet (located 50m above the bottomhole). Velocity inlet- pressure outlet scheme is chosen because it is the most commonly used scheme for simulation of fluid flow. Velocity inlet is determined from the continuity equation, while the pressure outlet is determined from the Darcy-Weisbach equation. It is a known fact that the pressure at the bottomhole is the largest pressure exerted on the tubing and the pressure decreases as the elevation increases, until it reaches the outlet pressure at the outlet region. Therefore, the outlet pressure is less than the inlet pressure and the factors that contribute to the drop in pressure are elevation change and frictional pressure loss, as according to Darcy-Weisbach Equation. However, the friction factor and Reynolds number have to be determined. Colebrook Equation is used to calculate the friction factor, but because it is an implicit function, so Matlab software is used to compute the friction factor with absolute roughness of the tubing used is 0.006.

$$A = \frac{\pi D^2}{4} \quad (7)$$

$$A = \frac{\pi D^2}{4} = \frac{\pi(0.0620014)^2}{4} = 0.00302m^2$$

$$V = \frac{Q}{A} = \frac{9.5043 \times 10^{-3}}{0.00302} = 3.15 \frac{m}{s}$$

Pressure at Outlet:

$$p_{outlet} = p_{bottom} - \Delta p_f - \Delta p_z \quad (8)$$

Colebrook Equation:

$$\frac{1}{\sqrt{f}} = -2 \log \left[\frac{\frac{\varepsilon}{D}}{3.71} + \frac{2.52}{Re\sqrt{f}} \right]$$

$$K = \frac{\varepsilon}{D} \tag{9}$$

$$K = \frac{\varepsilon}{D} = \frac{0.006}{0.0620014} = 0.0968$$

$$Re = \frac{\rho V D}{\mu} = \frac{704(3.15)(0.0620014)}{0.0034} = 40440 > 4000 \text{ (Turbulent)}$$

Matlab Codes used as M-File:

```
function F = colebrook(R,K)
% F = COLEBROOK(R,K)
%
%          1          |          K          2.52          |
%  -----  = -2 * Log_10 |  ----- + -----  |
%  sqrt(F)          |  3.71          R * sqrt(F)  |
%
% INPUT:
%  R : Reynolds' number (should be >= 2300).
%  K : Equivalent sand roughness height divided by the
%      hydraulic diameter (default K=0).
%
% OUTPUT:
%  F : Friction factor.
%
% Check for errors.
if any(R(:)<2300) == 1,
    warning('The Colebrook equation is valid for Reynolds''
numbers >= 2300.');
```

```
end,
if nargin == 1 || isempty(K) == 1,
    K = 0;
end,
if any(K(:)<0) == 1,
    warning('The relative sand roughness must be non-negative.');
```

```
end,

% Initialization.
X1 = K .* R * 0.123968186335417556;          % X1 <- K * R *
log(10) / 18.574.
X2 = log(R) - 0.779397488455682028;          % X2 <- log( R
* log(10) / 5.02 );
% Initial guess.
```

```

F = X2 - 0.2;

% First iteration.
E = ( log(X1+F) - 0.2 ) ./ ( 1 + X1 + F );
F = F - (1+X1+F+0.5*E) .* E .* (X1+F) ./ (1+X1+F+E.*(1+E/3));

% Second iteration (remove the next two lines for moderate
accuracy).
E = ( log(X1+F) + F - X2 ) ./ ( 1 + X1 + F );
F = F - (1+X1+F+0.5*E) .* E .* (X1+F) ./ (1+X1+F+E.*(1+E/3));

% Finalized solution.
F = 1.151292546497022842 ./ F; % F <- 0.5 *
log(10) / F; % F <- Friction
F = F .* F; % F <- Friction
factor.

```

Matlab Commands Used inside Matlab Editor:

R=40440;

K=0.0968;

F=Colebrook(R,K);

From the Matlab, the friction factor is determined to be 0.1002.

$$\Delta p_f = f \frac{\rho L V^2}{2D} = \frac{0.1002(704)(50)(3.15)^2}{2(0.0620014)} = 282228 \text{ Pa}$$

$$\Delta p_z = \rho g h = 704(9.81)(50) = 345312 \text{ Pa}$$

$$p_{outlet} = p_{bottom} - \Delta p_f - \Delta p_z = 15349798 - 282228 - 345312 = 14722258 \text{ Pa}$$

After the pressure outlet is determined, the simulation parameters to be used for the validation of the model case are finalized. Model case is built based on the data given from the oil company with the application of theoretical fluid mechanics equation. The simulation parameters used for the validation are shown in Table 2.2.

Table 2.2: Simulation Parameters for Validation of Model Case

Parameter	Value
Production Rate	5165 bbl/day
Simulation Scheme	Velocity Inlet- Pressure Outlet
Velocity Inlet	3.15m/s
Outlet Pressure	14722258 Pa
Inlet Pressure	2226.3 psig (equivalent to 15349798 Pa)
Reynolds Number	40440 (Turbulent)
Turbulent Setting	K-epsilon
Effect of Gravity	Present, because the oil flows upward under the influence of gravity

And there are a few assumptions made for the simulation of model case:

1. The oil flow is incompressible. In other words, the density of the oil is kept constant at 704kg/m^3 .
2. The viscosity of the oil flow is kept constant at 0.0034 kg/m.s .
3. The temperature is kept constant at bottomhole temperature of 206°F .
4. The bottomhole pressure is constant because it is reservoir pressure.

For the validation of the model case, the percentage error (Eq.10) for the simulation result as compared to the data from the oil company and theoretical equations application, will be calculated to determine whether the simulation result is in agreement with the expected result. Validation of model case is important because it proves that the simulation parameters used are acceptable, and the simulation settings used for the proven model case will be applied for production rate of 5000, 5500, 6000 and 6500 bbl/day, since the main objective of this project is to determine the static and dynamic characteristics of the tubing at different production rate.

$$\% \text{ Error} = \frac{|Theoretical \ value - Simulation \ Value|}{Theoretical \ Value} \times 100\% \quad (10)$$

Later, simulation settings for the proven model case are applied for the production rates of 5000, 5500, 6000 and 6500 bbl/day by using Ansys Fluent Software. For each of the production rates, the results from the Ansys Fluent simulation are transferred to Ansys Static Structural to determine the static characteristics of the tubing under fluid dynamic load. The results transferred from the Ansys Fluent to Ansys Static Structural are pressure exerted onto the tubing, since the pressure exerted on the tubing creates the fluid dynamic loading on the tubing. The static characteristics that need to be determined are stress and deformation.

Then, the results from the Ansys Fluent simulation are transferred to the Ansys Modal to determine the dynamic characteristics of the tubing under fluid dynamic loading. The dynamic characteristic that needs to be determined is the natural frequencies of the tubing at different modes.

2.3 OVERVIEW OF STATIC AND DYNAMIC CHARACTERISTICS OF THE TUBING DUE TO FLUID DYNAMIC LOADING

The tubing receives pressure from the flowing fluid, and the pressure produces fluid loading to tubing, which eventually leads to the motion of the tubing. Therefore, tubing and liquid system cannot be treated separately in analysis and their interaction mechanisms have to be taken into consideration. This interaction is known as Fluid Structure Interaction [11].

Fluid Structure Interaction (FSI) in piping system consists of the transfer of momentum and forces between the pipe and the contained liquid during unsteady flow, which is caused by the changes in flow and pressure. As a result, static and dynamic characteristics of the tubing are produced, such as vibration in the piping system, which can lead to disastrous consequences for the system if not taken care of properly [12].

Generally, for Fluid Structure Interaction, there are three types of coupling, which are Poisson Coupling, Friction Coupling and Junction Coupling. Friction coupling is created by the liquid shear stresses acting on the pipe wall, while junction coupling is due to changes in liquid momentum at discrete locations in the pipe, such as bend and tee. Poisson coupling is due to normal forces acting at the interface between pipe wall and the fluid [13]. For this project, only two types of coupling are present, which are Poisson coupling and friction coupling, since there are liquid shear stresses and normal forces acting on the pipe due to fluid loading. However, since there is no change in the diameter of the pipe used and only vertical straight pipe configuration is used, no junction coupling occurs in the pipe.

For simulation using Ansys software, Finite Element Method (FEM) is a powerful problem-solving method which can be applied, given that the FSI coupling conditions are taken into consideration [14]. For modelling of fluid flow, fluid parameters and pipe parameters are needed [15]. In combination, the parameters needed are density and viscosity of the fluid, material, internal diameter, outer diameter and length of the pipe as well as the material, internal diameter, outer diameter and length of the packer. Using the parameters, the steps for simulation using Ansys software such as modelling,

meshing, apply boundary condition and input fluid properties and many more can be executed [16].

For the tubing, the static characteristics investigated are deformation and stress occurring on the tubing, while the dynamic characteristics investigated are the natural frequencies at different modes. For stress, maximum Von Mises stress, principal stress and shear stress are investigated. Maximum shear stress is defined as the maximum stress component that acts in the plane of the sectioned area, while maximum principal stress represents the maximum normal stress at the body, and deformation is the change in size and shape due to the force applied on the body [18]. In this project, due to fluid dynamic loading applied on the tubing, deformation will occur on the tubing, but as to whether the deformation is permanent or elastic, it depends on the magnitude of the applied loading and the yield strength of the material. If the applied loading exceeds the yield strength, deformation is permanent, and for elastic deformation, the applied loading is less than the yield strength.

For the tubing, the material used is L80 steel (its properties are as shown in Table 2.3). In oil and gas industry, the L80 steel used is ductile steel, which means that it is capable of absorbing shock or energy, and if it becomes overloaded, it will exhibit large deformation before failing. After L80 steel undergoes permanent deformation, it begins to experience strain hardening until it reaches the ultimate tensile stress.

Table 2.3: The Tubing Properties

Tubing Properties	Value
Density (kg/m ³)	7660
Yield strength (psi)	Minimum 80000
Ultimate tensile strength (psi)	95000
Poisson Ratio	0.30
Young Modulus (Pa)	2.02E+11

Natural frequencies at different modes are also one important characteristic investigated in this project. When the tubing achieves its natural frequencies, it will start to breakdown and the deformation occurring on the tubing is irreversible at this stage. At different modes, different natural frequencies are produced; in which higher modes will have higher magnitude of natural frequencies. This means that the natural frequency at second mode should be bigger than the natural frequency at the first mode, and the natural frequency at the third mode should be bigger than the natural frequencies at the second and first mode. And the natural frequency at the fourth mode should be bigger than the natural frequencies at the third, second and first mode. And the expected results are at lower modes, the natural frequencies increase as the production rate increases[18].

CHAPTER 3

METHODOLOGY

3.1 RESEARCH METHODOLOGY

The flow chart describing the research methodology is shown in Fig. 3.1. The research is started with literature review after the research topic is finalized between the lecturer and the student. Literature review is conducted to gather information related to the project by referring to various sources, such as journals, publications and books.

Later, the data is obtained from the oil company, where the technical parameters are obtained to model the tubing. The technical parameters are the dimensions of the packer and tubing, the material of the packer and tubing and the properties of the material. From the data from the oil company, the oil production parameters and the oil properties are obtained for the oil flow simulation. The oil production parameters are the production rate and the properties of the single phase oil at the oil production zone to be applied for the validation of the model case. In the case that the validation of the model case is not successful, different settings of Fluent are applied until the correct settings for Ansys Fluent is obtained, so that the model case is validated by having acceptable percentage error for the interested parameters, which are outlet velocity and inlet pressure. Then the production rates to be investigated are finalized, which are 5000, 5500, 6000 and 6500bbl/day.

Then, the simulation of fluid flow, static and dynamic characteristics of the tubing is conducted for the production rates using the settings from the validated model case. Then, the results are analysed and interpreted, which followed by documentation and reporting of the whole research project. Finally, the project ends.

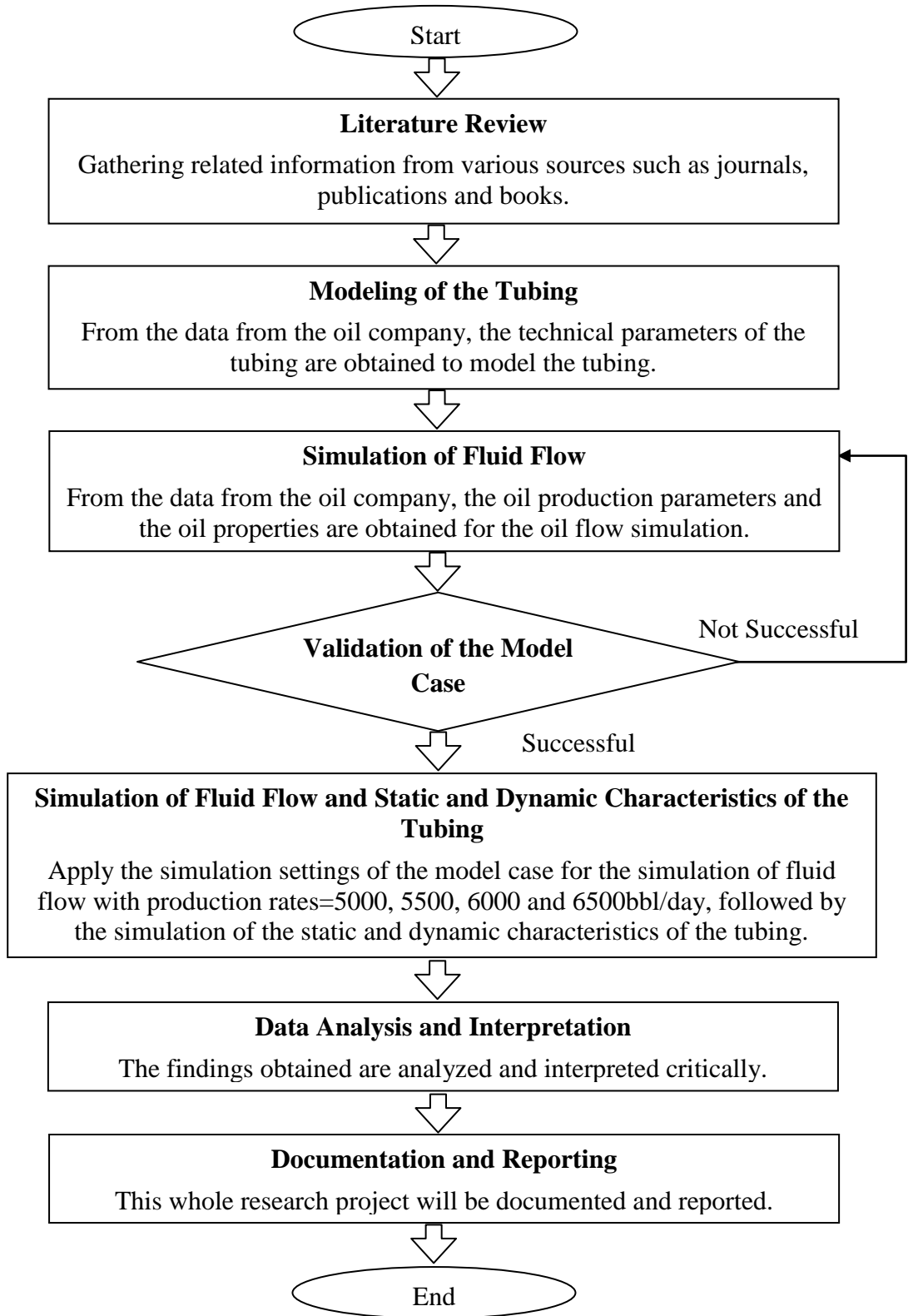


Figure 3.1: Flow Chart Describing the Research Methodology

3.2 PROJECT ACTIVITIES

The modelling and simulation activities are as shown below in Fig. 3.2.

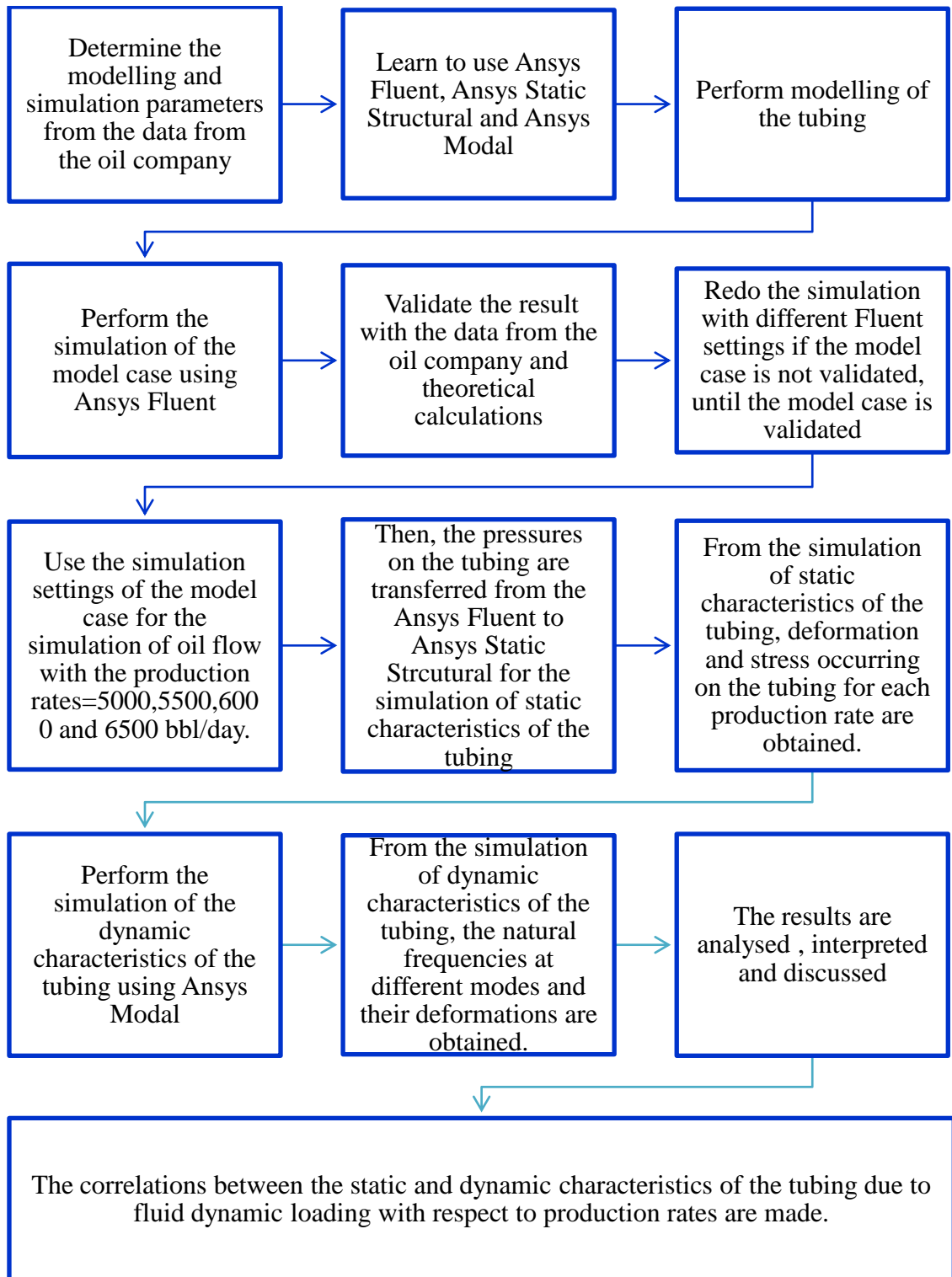


Figure 3.2: The Project Activities for Modelling and Simulation

3.2.1 MODELLING ACTIVITIES

The modelling of the tubing is started with determining the modelling parameters from the data from the oil company. The modelling parameters are the length and the inner and outer diameter of the packer with the length and the inner and out diameter of the tubing. The modelling parameters are as shown below in Table 3.1.

Table 3.1: The Modelling Parameters for Tubing and Packer

The Modelling Parameters of Tubing	
Tubing Inner Diameter	2.441in (equivalent to 0.0620014m)
Tubing Outer Diameter (in)	2.875
Tubing Material	Steel
Length of Tubing	50m (from 1585m to 1635m)
Absolute Roughness	0.006
The Modelling Parameters for Packer	
Packer Inner Diameter (in)	2.875
Packer Outer Diameter (in)	4.720
Packer Material	Steel
Length of Packer	0.1397m (located 17m from the depth of 1635m)

Then, the tubing, packer and the fluid are drawn with Catia software. The tubing is drawn as a body, while the packer is drawn as another body, and the fluid is drawn as another body, which forms a geometry (as shown below in Fig. 3.3) consisting of three different bodies.

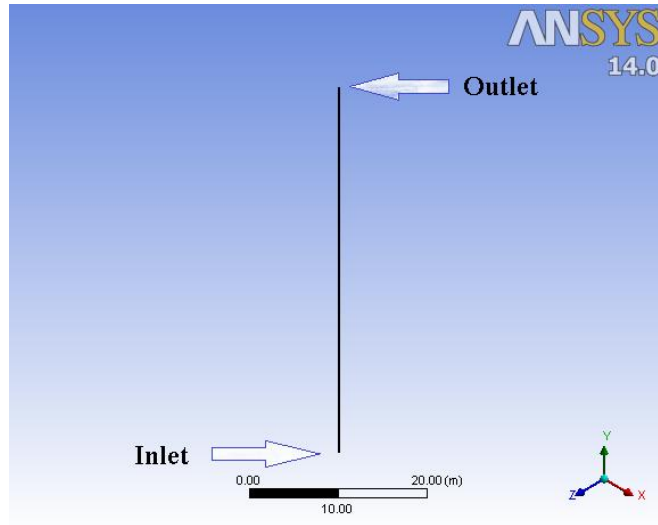


Figure 3.3: The Locations of Outlet and Inlet in the Simulation

The functions used for drawing the bodies are circle, diameter and extrude, whereby the circle is drawn first, and then later, the diameter of the circle is specified, and then later the circle is extruded to form solid body. Subtract function is also used to produce the packer and tubing, which is hollow in the middle cross section. After that, the geometry is saved in Fluent-Compatible format to allow the geometry to be imported into Fluent for fluid flow simulation.

3.2.2 SIMULATION ACTIVITIES

Using the geometry imported from Catia software, the simulation is conducted. The meshing is conducted at this stage. Meshing of the geometry (as shown below in Fig. 3.3 and 3.4) is one core process in conducting simulation because poor meshing will produce inaccurate and poor result.

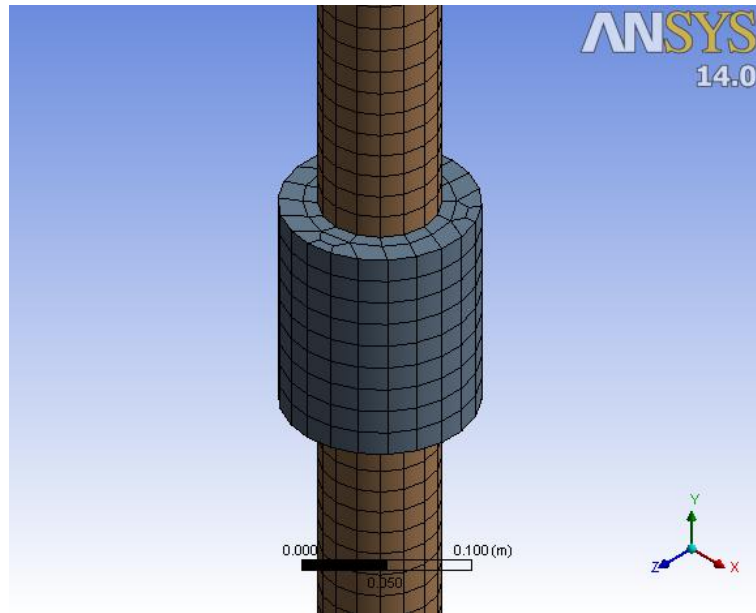


Figure 3.4: Meshing at the Packer Region

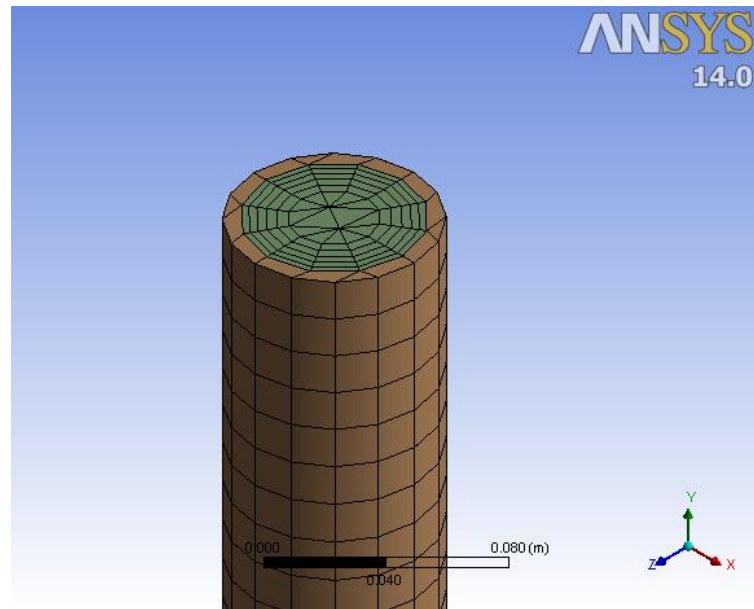


Figure 3.5: Meshing at the Outlet Region

For meshing, there are a few requirements that need to be met, which are skewness value of <0.7 and aspect ratio value of <10 . From the meshing conducted, the result is satisfactory (as shown below in Table 3.2) because the skewness and aspect ratio requirements are being fulfilled.

Table 3.2: The Average Skewness and Aspect Ratio of the Meshing

Parameter	Value	Value is acceptable?
Average skewness	0.3135	Yes, since $0.3135 < 0.7$
Average aspect ratio	3.6267	Yes, since $3.6267 < 10$

After meshing, the boundary condition is applied, whereby the boundary conditions specified are velocity inlet and pressure outlet, followed by specifying the fluid properties and the material of the solid inside the Material Section. Later on, the settings are set up and the simulation is started. Then, the results are checked for validation. If the validation of the model case is successful, then the fluid flow simulation for the model case has ended. Then, the simulation for the production rate of 5000, 5500, 6000 and 6500 bbl/day are started and by applying the same settings as the model case, the simulation is conducted with the velocity inlet and pressure outlet values set as according to the theoretical calculations made. Then, the velocity vectors profile are obtained.

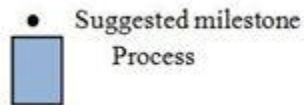
Then, for solid structural simulation, the pressure from the Fluent is imported into Solid Structural. Then, inside the Engineering Data Section, the properties of steel are changed to the properties of steel obtained from the data from the oil company. Then, boundary condition is applied, where the supports for the tubing are specified. Then, the required stress and deformation of the tubing are obtained for different production rates.

Then, for modal simulation, the boundary condition is applied, where the supports for the tubing are specified. Then, the simulation is run in order to obtain the natural frequencies at different modes for different production rate of 5000, 5500, 6000 and 6500 bbl/day.

3.3 GANTT CHART (FYP 1)

Table 3.3 : Gantt Chart for FYP 1

NO	DETAIL	WEEK															
		1	2	3	4	5	6	7		8	9	10	11	12	13	14	
1	Selection of Project Title	■	■	■					M I D S E M E S T E R B R E A K								
2	Literature Review				■	■	■										
3	Submission of Extended Proposal							●									
4	Determine the modelling and simulation parameters from the data from the oil company							■		■	■						
5	Preparation for Oral Proposal Defense									■							
6	Proposal Defense Presentation										■						
7	Detailed Literature Review										■	■	■	■			
8	Learn to use Ansys Fluent, Static Structural and Modal										■	■	■	■	■	■	
9	Perform modelling of tubing using ANSYS													■	■	■	
10	Submission of Interim Draft Report															●	
11	Submission of Interim Final Report																●



3.4 GANTT CHART (FYP 2)

Table 3.4: Gantt Chart for FYP 2

NO	DETAIL	WEEK							M I D S E M E S T E R	B R E A K											
		1	2	3	4	5	6	7			8	9	10	11	12	13	14				
1	Perform the simulation of the model case and validate the model case	■	■	■	■	■	■	■													
2	Use the simulation settings of the model case for the simulation of oil flow with different production rates					■	■	■		■											
3	Perform simulation of the static characteristics of the tubing due to fluid loading									■	■	■									
4	Submission of Progress Report																				
5	Perform simulation of the static characteristics of the tubing due to fluid loading									■	■	■									
6	Analyse and interpret the results										■	■									
7	Make conclusion for the results											■	■								
6	Pre-SEDEX																			●	
7	Submission of Draft Report																				●
8	Submission of Dissertation (Soft Bound)																				●
9	Submission of Technical Report																				●
10	Oral Presentation																				●
11	Submission of Dissertation (Hard Bound)																				●

● Suggested milestone
 ■ Process

3.5 KEY MILESTONES

Key milestones (Fig. 3.5) serve as reminder for the students to keep track of their project progress carefully, to ensure that the project can be completed on time.

Table 3.5: Key Milestones

No	Key Milestones	Timeline
1	Extended proposal submission	FYP 1 Week 7
2	Proposal defense	FYP 1 Week 9
3	Determine the modelling and simulation parameters from the data from the oil company	FYP 1 Week 9
4	Submission of Interim Draft Report	FYP 1 Week 13
5	Submission of Interim Final Report	FYP 1 Week 14
6	Learn to use Ansys Fluent, Static Structural and Modal	FYP 1 Week 14
7	Perform modelling of tubing using Ansys	FYP 1 Week 14
8	Perform the simulation of the model case and validate the model case	FYP 2 Week 7
9	Use the simulation settings of the model case for the simulation of oil flow with different production rates	FYP 2 Week 8
10	Submission of Progress Report	FYP 2 Week 9
11	Perform simulation of the static characteristics of the tubing due to fluid loading	FYP 2 Week 10
12	Perform simulation of the dynamic characteristics of the tubing due to fluid loading	FYP 2 Week 10
13	Analyse and interpret the results	FYP 2 Week 10
14	Make conclusion for the results	FYP 2 Week 11
15	Pre-SEDEX	FYP 2 Week 12
16	Submission of Draft Report	FYP 2 Week 13
17	Submission of Soft Bound Dissertation	FYP 2 Week 13
18	Submission of Technical Paper	FYP 2 Week 13
19	Oral Presentation	FYP 2 Week 14
20	Submission of Hard Bound Dissertation	FYP 2 Week 14

3.6 TOOLS

The tools applied are as shown below in Table 3.6.

Table 3.6: Tools Used for Simulation

Simulation Scope	Tools
Simulation of oil flow	Ansys Fluent
Simulation of the static characteristics of the tubing due to fluid loading	Ansys Static Structural
Simulation of the dynamic characteristics of the tubing due to fluid loading	Ansys Modal

CHAPTER 4

RESULTS AND DISCUSSIONS

4.1 VALIDATION OF MODEL CASE

The graph of pressure vs length of tubing for the model case is as shown below in Figure 4.1. From Fig. 4.1, the pressure decreases as the elevation increases. This is due to the pressure loss inside the tubing, and as elevation increases, the cumulative pressure loss continue to increase, which cause the pressure to drop.

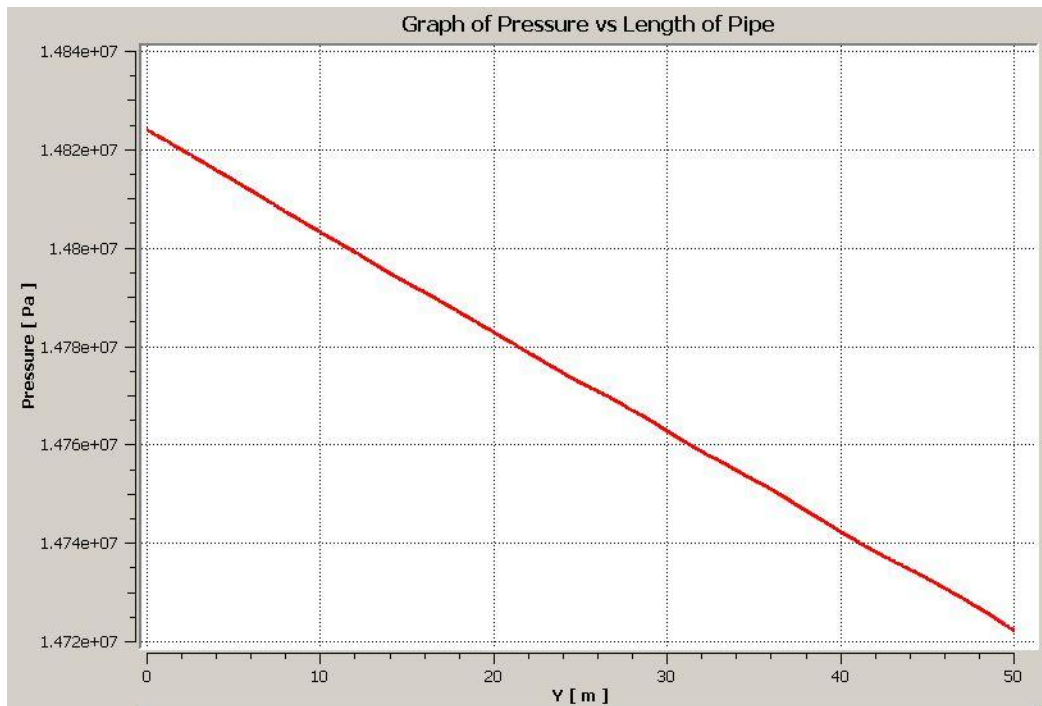


Figure 4.1: The Graph of Pressure versus Length for the Model Case

From Fig. 4.1, the inlet pressure is 1.4824E+7Pa, which is different than the expected inlet pressure of 1.5349798PA. The percentage error obtained (as shown by % Error below) is 3.43%, which is acceptable considering that the viscosity is kept constant for simplification of the problem.

$$\% \text{ Error} = \frac{|Theoretical \ value - \ Simulation \ Value|}{Theoretical \ Value} \times 100\%$$

$$\% \text{ Error} = \frac{|P_{\text{Inlet (Company data)}} - P_{\text{Inlet (Simulation Result)}}|}{P_{\text{Inlet (Company data)}}} \times 100\%$$

$$\% \text{ Error} = \frac{|15349798 - 14824000|}{15349798} \times 100\% = 3.43\%$$

In real situation, the temperature affects the viscosity of the fluid with piecewise-linear relationship. In other words, change in temperature will cause the viscosity of the fluid to change. However, for simplification of the problem, the viscosity is kept constant since the temperature is assumed to be constant at bottomhole temperature. Therefore, the percentage error computed is acceptable.

Based on continuity equation, the volume flow rate is a function of cross-sectional area and velocity of fluid flow, as shown below. Since there is no diameter change, the cross-sectional area is constant, thus, it can be deduced that the velocity at outlet is equal to velocity at inlet. By taking into consideration that the total length of the tubing is 1635m, and the length of the tubing used for the simulation is only 50m, which is the exact length for zone J70. Therefore, the application of continuity equation is acceptable, since Ansys Fluent also considers continuity equation for the simulation.

Continuity Equation:

$$Q = A_1 V_1 = A_2 V_2$$

$$Q = AV_1 = AV_2$$

$$V_1 = V_2$$

After simulation, the velocity at the outlet is 3.068m/s, which is different than the expected 3.15m/s. The percentage error is 2.60%, which is acceptable considering that viscosity is kept constant for simplification of the problem.

$$\% \text{ Error} = \frac{|Theoretical \text{ value} - Experimental \text{ Value}|}{Theoretical \text{ Value}}$$

$$\% \text{ Error} = \frac{|V_{\text{Outlet (Theoretical)}} - V_{\text{Outlet (Simulation Result)}}|}{V_{\text{Outlet (Theoretical)}}} \times 100\%$$

$$\% \text{ Error} = \frac{|3.15 - 3.068|}{3.15} \times 100\% = 2.60\%$$

The Velocity Vectors Profile of the Model Case at the Entrance Region of Fluid Flow where Developing Flow Forms is as shown below in Figure 4.2. From Fig. 4.2, it can be seen that there is parabolic shape at the entrance of the flow region (Fig. 4.2). This parabolic shape indicates that the flow is having developing flow, which is commonly seen in single phase fluid flow. For the developing flow, the velocity vectors are a bit scattered and not organized. This is because the oil molecules are entering the tubing with turbulent state of flow, which makes the flow to be a bit chaotic in motion. And as the flow developed, the organization of the velocity vectors becomes more organized.

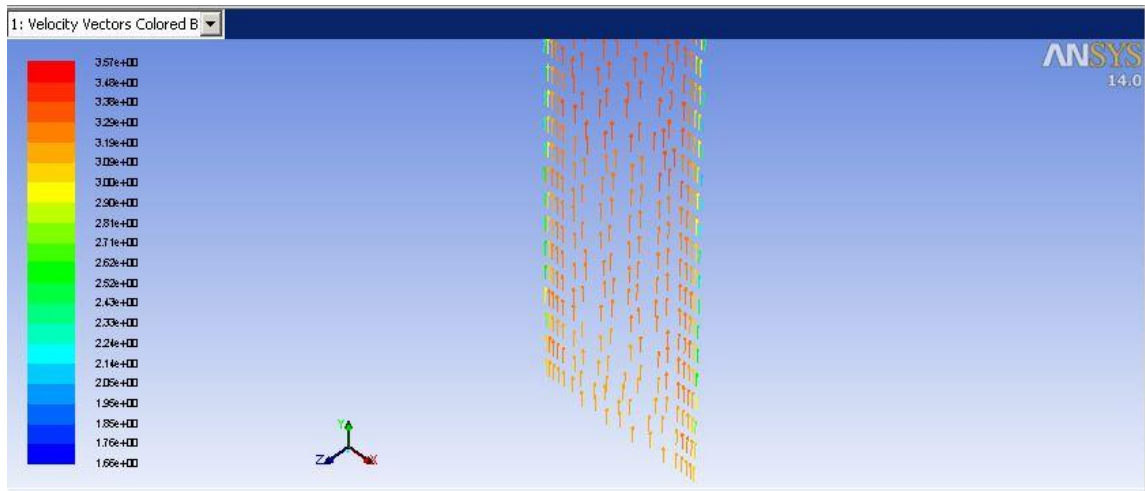


Figure 4.2: Velocity Vectors Profile of the Model Case at the Entrance Region of Fluid Flow where Developing Flow Forms

However, soon after that, the developing flow developed into fully developed flow (as shown in Fig. 4.3 below), where the velocity vectors are more organized. Plus, the velocity vectors at the wall (highlighted by blue velocity vectors in the Figure 4.3) are having minimum velocity, followed by velocity vectors with greater velocity magnitude until finally, at the middle of the tubing, the maximum velocity vectors (highlighted by red velocity vectors in the Figure 4.3) are obtained. This velocity vectors profile matches perfectly the velocity vectors profile in a single phase fluid flow.

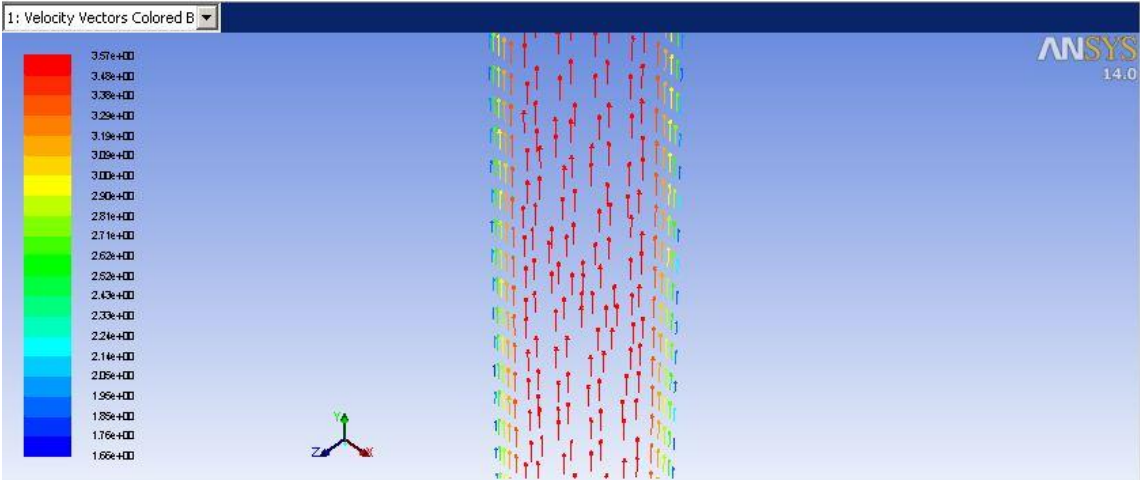


Figure 4.3: Velocity Vectors Profile of the Model Case at the Region After the Entrance Region of the Fluid Flow where Fully Developed Flow Forms

Thus, the results from the simulation is reasonable and in agreement with the data from the oil company. The model case is validated and the simulation settings for this proven model case will be used for production rates of 5000, 5500, 6000 and 6500bbl/day.

4.2 SIMULATION OF FLUID FLOW FOR DIFFERENT PRODUCTION RATES

4.2.1 SIMULATION PARAMETERS APPLIED FOR DIFFERENT PRODUCTION RATES

The simulation is conducted using velocity inlet-pressure outlet scheme. Therefore, by using the data from the oil company and theoretical fluid mechanics equations, the simulation parameters for the different production rates (as shown in Table 4.1 below) are determined.

Table 4.1: The Simulation Parameters for Production Rates of 5000, 5500, 6000 and 6500bbl/day

Parameters	Production Rate			
	5000bbl/day	5500bbl/day	6000bbl/day	6500bbl/day
Bottomhole Pressure (Pa)	15349798	15349798	15349798	15349798
Outlet Pressure (Pa)	14739629	14685282	14623472	14558451
Inlet Velocity (m/s)	3.05	3.35	3.66	3.96
Reynolds Number	39156 (Turbulent)	43007 (Turbulent)	46934 (Turbulent)	50838 (Turbulent)
Relative Roughness	0.0968	0.0968	0.0968	0.0968
Friction Factor	0.1003	0.1002	0.1002	0.1002

The sample calculations for the production rate of 5000bbl/day are shown below whereby the velocity inlet, pressure outlet, friction factor, relative roughness and Reynolds number are calculated.

Calculation for inlet velocity for production rate=5000bbl/day=9.2007 x 10⁻³ m/s,

$$A = \frac{\pi D^2}{4} = \frac{\pi(0.0620014)^2}{4} = 0.00302m^2$$

$$V = \frac{Q}{A} = \frac{9.2007 \times 10^{-3}}{0.00302} = 3.05 \frac{m}{s}$$

Calculation for Reynolds Number for production rate=5000bbl/day,

$$Re = \frac{\rho VD}{\mu} = \frac{704(3.05)(0.0620014)}{0.0034} = 39156 > 4000 \text{ (Turbulent)}$$

Calculation for Outlet Pressure for production rate=5000bbl/day,

$$\Delta p_f = f \frac{\rho LV^2}{2D} = \frac{0.1003(704)(50)(3.05)^2}{2(0.0620014)} = 264857 Pa$$

$$\Delta p_z = \rho gh = 704(9.81)(50) = 345312 Pa$$

$$p_{outlet} = p_{bottom} - \Delta p_f - \Delta p_z = 15349798 - 264857 - 345312 = 14739629 Pa$$

Calculation for Friction Factor for production rate=5000bbl/day,

Colebrook Equation is used to calculate the friction factor by using Matlab Software.

$$K = \frac{\varepsilon}{D} = \frac{0.006}{0.0620014} = 0.0968$$

$$\frac{1}{\sqrt{f}} = -2 \log \left[\frac{\frac{\varepsilon}{D}}{3.7} + \frac{2.51}{Re\sqrt{f}} \right]$$

$$\frac{1}{\sqrt{f}} = -2 \log \left[\frac{0.0968}{3.7} + \frac{2.51}{39156\sqrt{f}} \right]$$

$$f = 0.1003$$

4.2.2 VELOCITY VECTORS PROFILES FOR DIFFERENT PRODUCTION RATES

After simulation is conducted for each of the production rates, their velocity vectors profiles (as shown in Fig. 4.4 up to Fig. 4.11) are obtained. Basically, all of the velocity vectors profiles for production rates of 5000, 5500, 6000 and 6500bbl/day follow similar flow pattern as the velocity vectors profile of the model case. The flow starts with developing flow (as shown in Fig. 4.4, 4.5, 4.6 and 4.7) at the entrance region of the flow. For the developing flow, the velocity vectors are a bit scattered and not organized. This is because the oil molecules are entering the tubing with turbulent state of flow, which makes the flow to be a bit chaotic in motion. And as the flow developed, the organization of the velocity vectors becomes more organized.

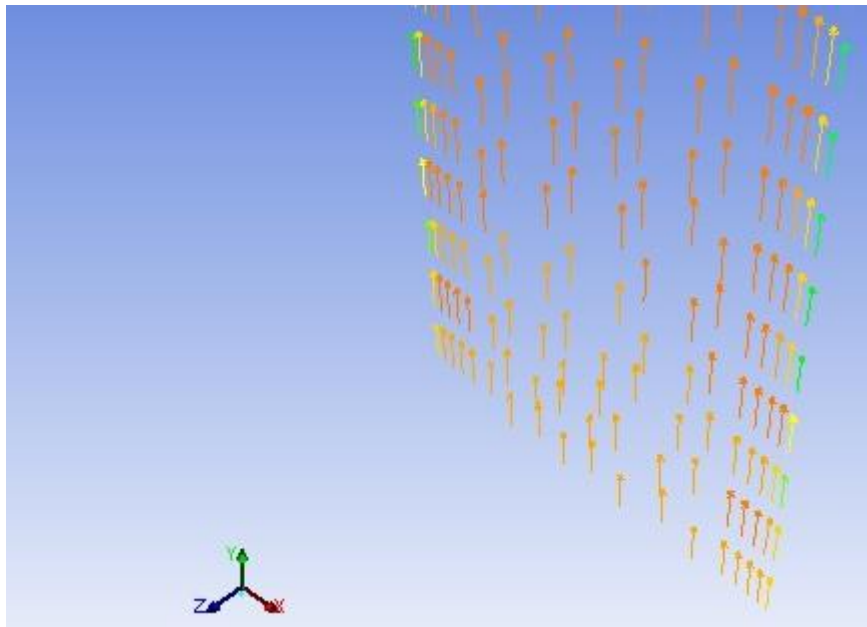


Figure 4.4: Velocity Vectors Profile of Developing Flow for 5000bbl/day at the Entrance Region of the Flow

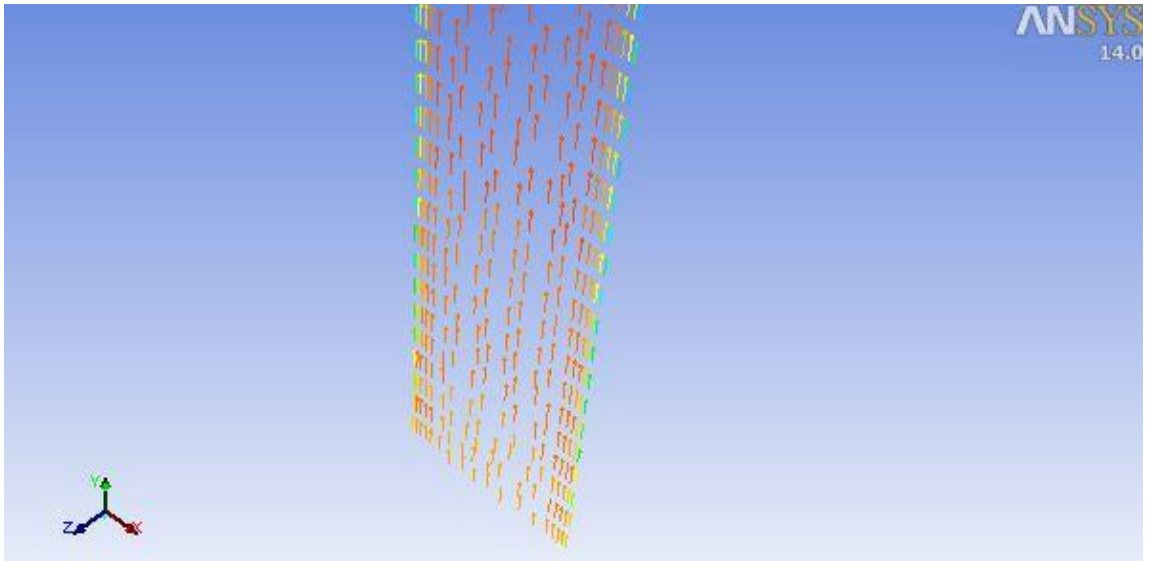


Figure 4.5: Velocity Vectors Profile of Developing Flow for 5500bbl/day at the Entrance Region of the Flow

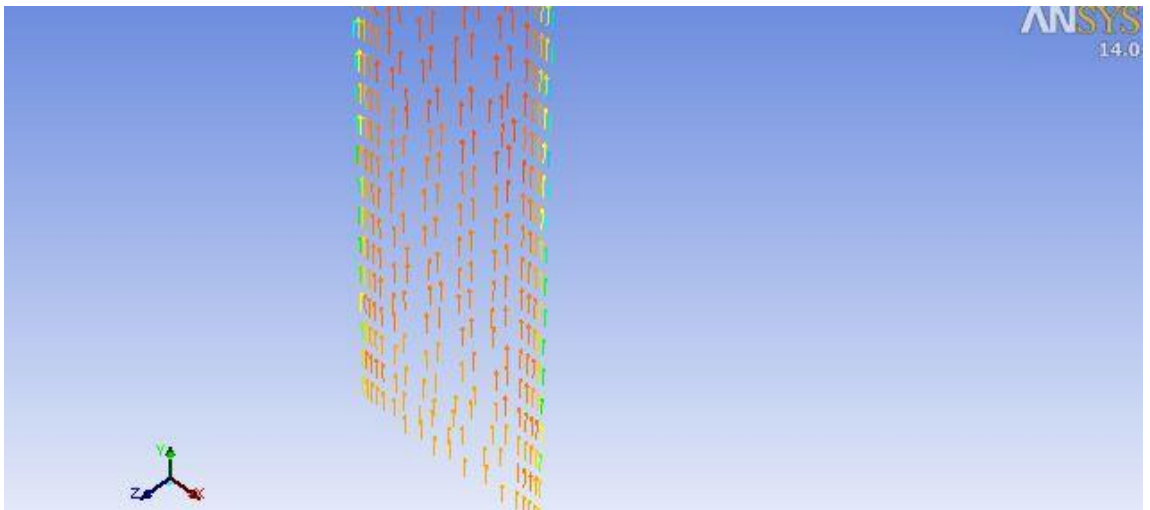


Figure 4.6: Velocity Vectors Profile of Developing Flow for 6000bbl/day at the Entrance Region of the Flow

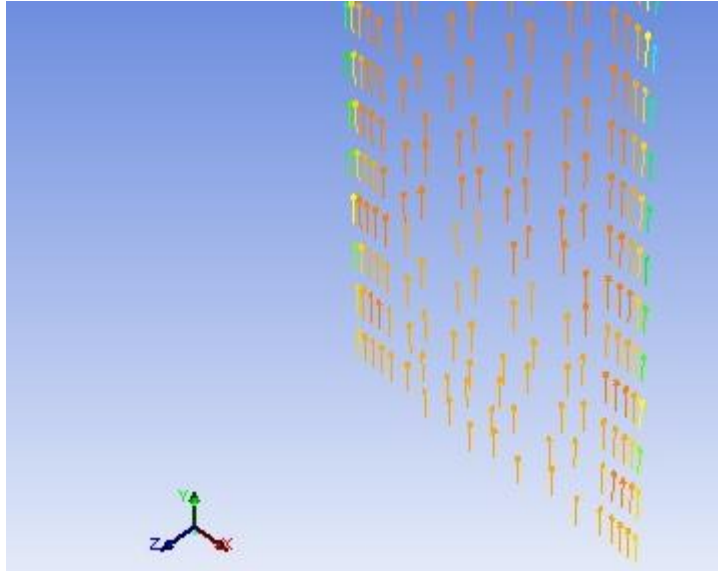


Figure 4.7: Velocity Vectors Profile of Developing Flow for 6500bbl/day at the Entrance Region of the Flow

Later the developing flow developed to become fully developed flow (as shown in Fig. 4.8, 4.9, 4.10 and 4.11). The fully developed flow does not experience any significant changes in the velocity vectors profile until the outlet region of the flow. The velocity vectors are also having minimum velocity at the wall, which increases in magnitude until it achieves maximum velocity magnitude at the middle of the tubing. It can be concluded that, regardless of the change in the production rate, all of the velocity vectors profile exhibit similar flow characteristics because their fluid content only consists of single phase oil.

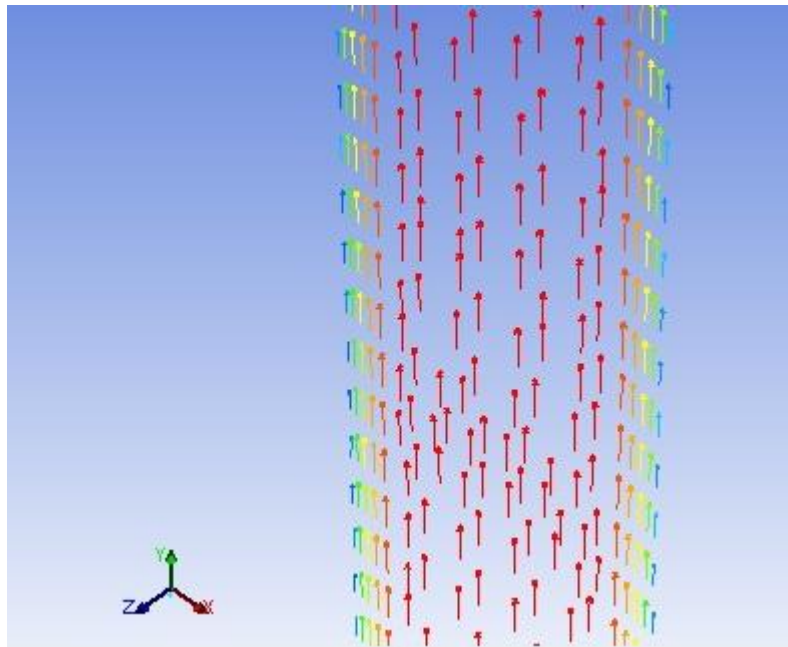


Figure 4.8: Velocity Vectors Profile of Fully Developed Flow for 5000bbl/day at the Region after the Entrance Region of the Flow

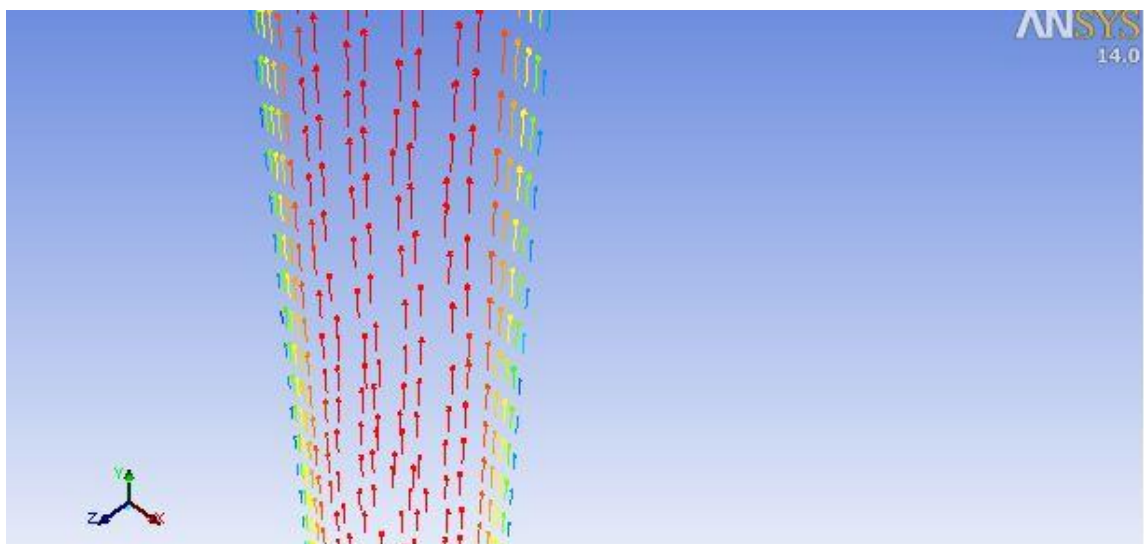


Figure 4.9: Velocity Vectors Profile of Fully Developed Flow for 5500bbl/day at the Region after the Entrance Region of the Flow

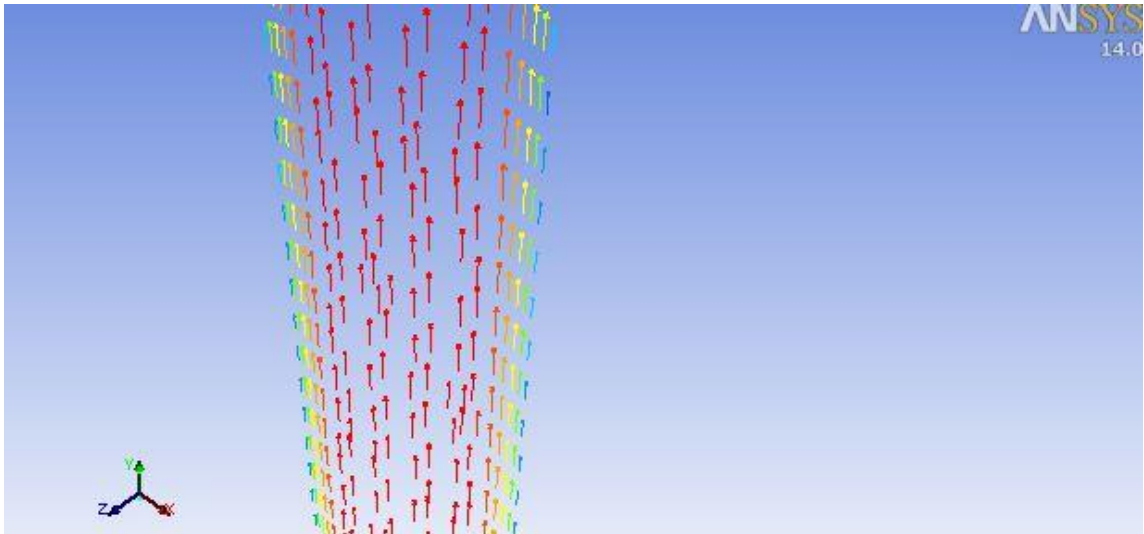


Figure 4.10: Velocity Vectors Profile of Fully Developed Flow for 6000bbl/day at the Region after the Entrance Region of the Flow

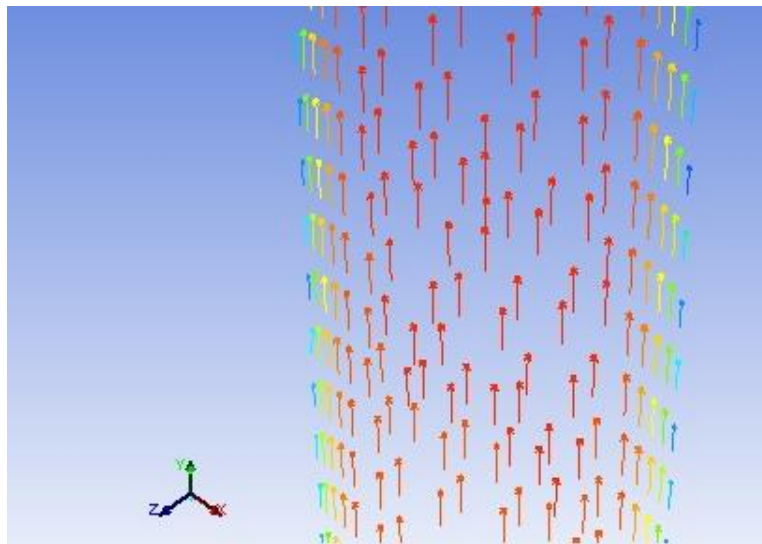


Figure 4.11: Velocity Vectors Profile of Fully Developed Flow for 6500bbl/day at the Region after the Entrance Region of the Flow

4.3 SIMULATION OF STATIC CHARACTERISTICS OF THE TUBING FOR DIFFERENT PRODUCTION RATES

4.3.1 PRESSURE EXERTED ON THE TUBING

After the simulation of fluid flow is finished, the pressure exerted on the tubing (as shown in Fig. 4.12 up to 4.16) is transferred from the Ansys Fluent to Ansys Static Structural so that the static characteristics of the tubing can be determined.

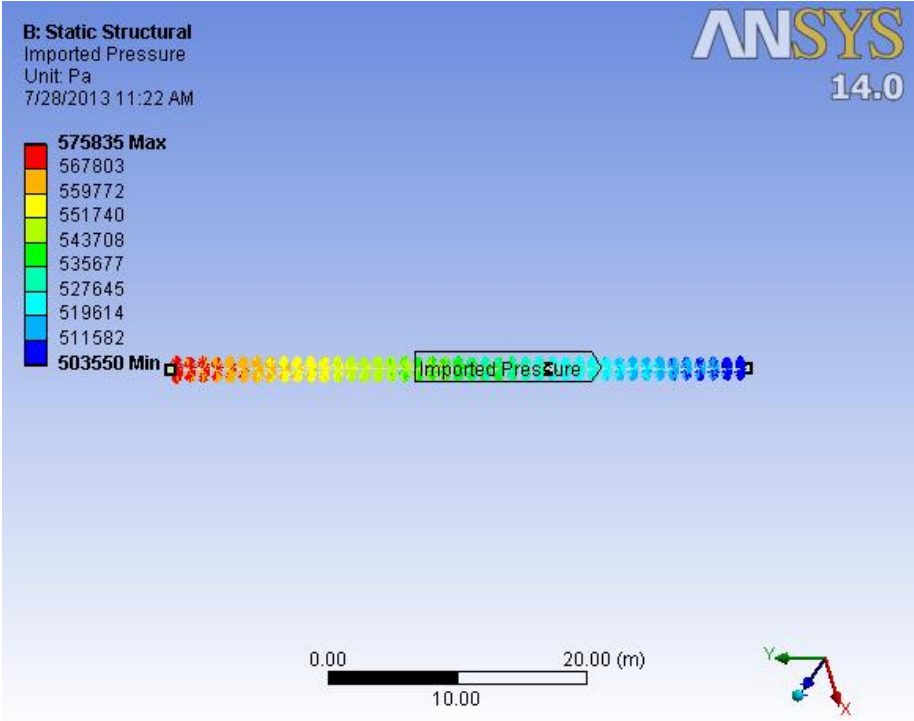


Figure 4.12: Pressure Exerted on the Tubing for Production Rate of 5000bbl/day for the whole 50m tubing length

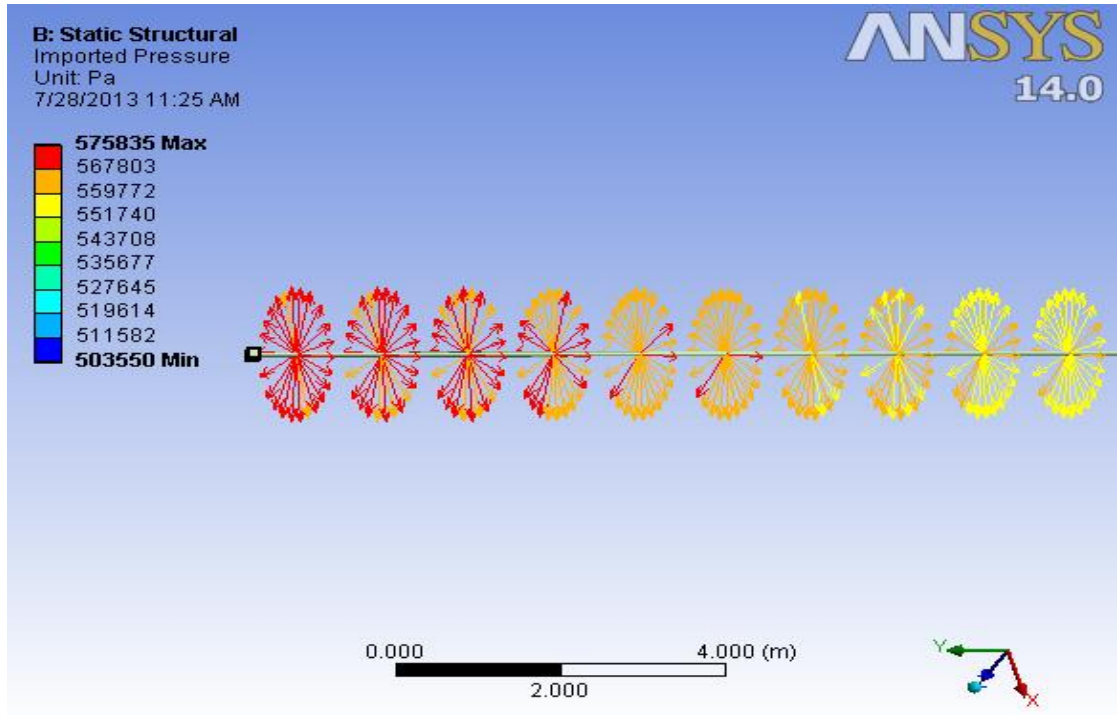


Figure 4.13: Pressure Exerted on the Tubing for Production Rate of 5000bbl/day at the Outlet Region

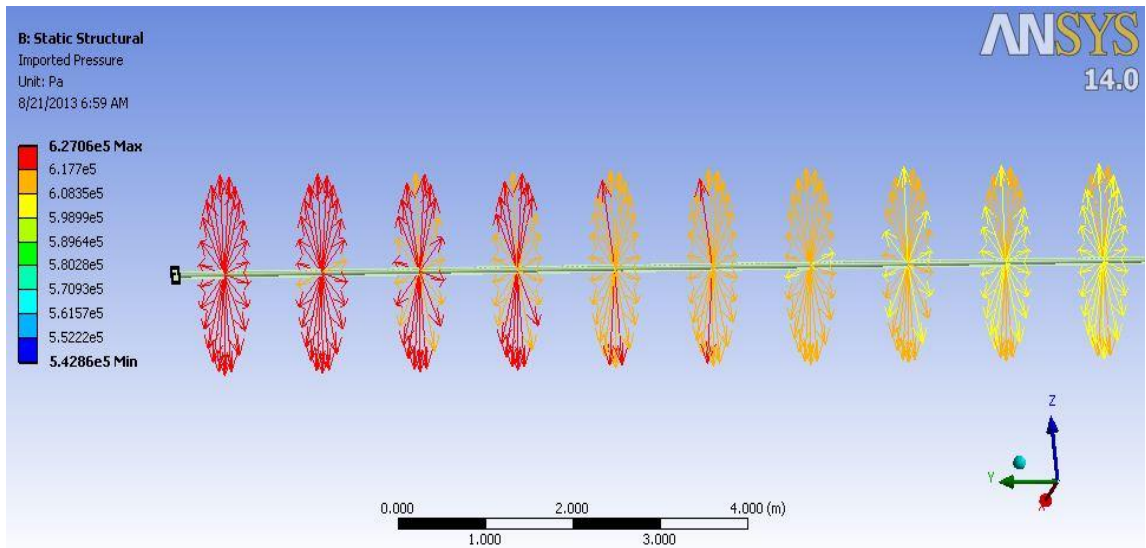


Figure 4.14: Pressure Exerted on the Tubing for Production Rate of 5500bbl/day at the Outlet Region

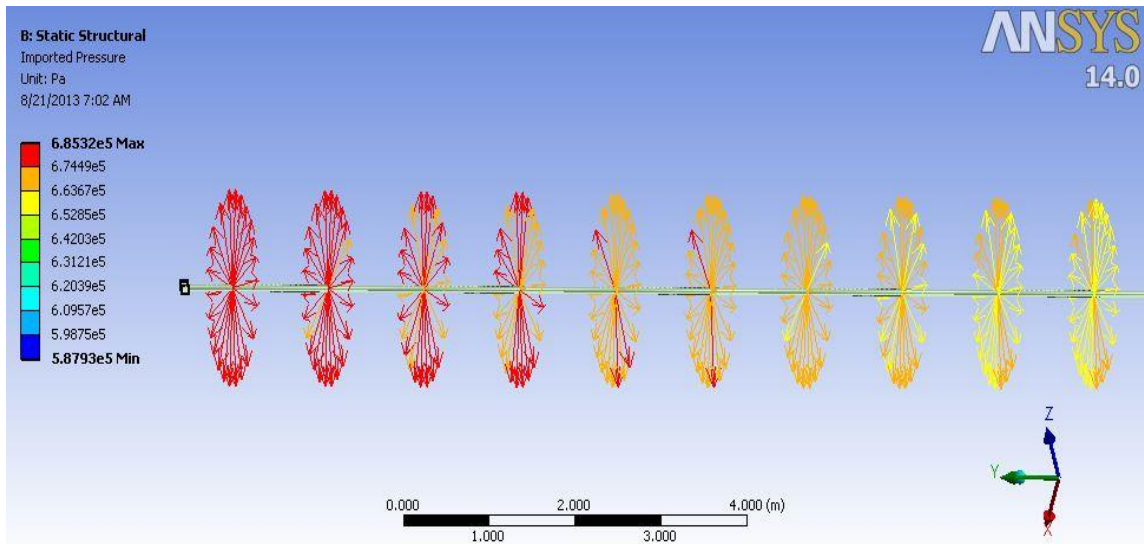


Figure 4.15: Pressure Exerted on the Tubing for Production Rate of 6000bbl/day at the Outlet Region

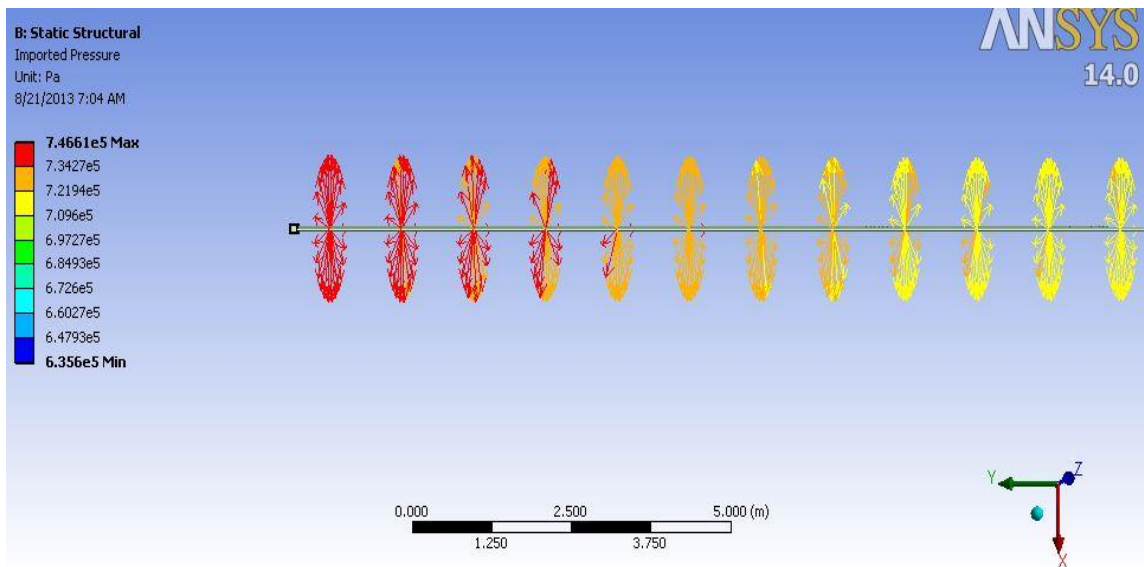


Figure 4.16: Pressure Exerted on the Tubing for Production Rate of 6500bbl/day at the Outlet Region

Maximum and minimum pressures exerted onto the tubing in Fig. 4.12 up to Fig. 4.16 are converted into Table 4.2, whereby the pressure difference is calculated. Then, from values in Table 4.2, the Fig. 4.17 is plotted to get the Graph of Difference of Pressure between Maximum and Minimum Pressure Exerted on Tubing at Different Production Rate.

Table 4.2: The Pressure Exerted on the Tubing at Different Production Rates

Production Rate (bbl/day)	Maximum Pressure Exerted on Tubing (Pa)	Minimum Pressure Exerted on Tubing (Pa)	Pressure Difference (Pa)
5000	575835	503550	72285
5500	627056	542865	84191
6000	685315	587927	97388
6500	746606	635598	111008

From the Figure 4.17 below, it can be seen that, the maximum difference of pressure between maximum and minimum pressure exerted on the tubing is 111kPa, while the minimum difference of pressure exerted on the tubing is 72kPa. And as the production rate increases, the pressure exerted on the tubing also increases, which causes the difference of pressure exerted on the tubing to increase. This is because the increase in production rate facilitates faster oil flow, which in turn causes increase in the collision between the oil molecules with the tubing.

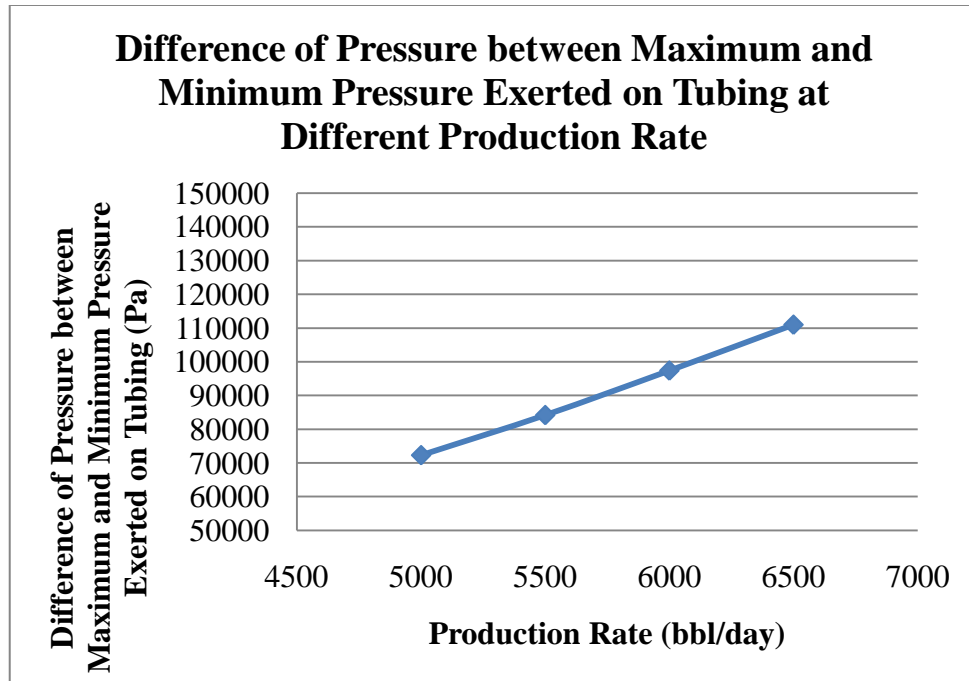


Figure 4.17: The Graph of Difference of Pressure Exerted on Tubing at Different Production Rates

4.3.2 DEFORMATION AND STRESS OCCURRING ON THE TUBING FOR DIFFERENT PRODUCTION RATES

After the simulation of Ansys Static Structural for production rate of 5000bbl/day is finished, the Von-Mises stress, shear stress, principal stress and deformation occurring on the tubing for production rate of 5000bbl/day (as shown in Fig. 4.18, 4.19, 4.20 and 4.21 below) are obtained.

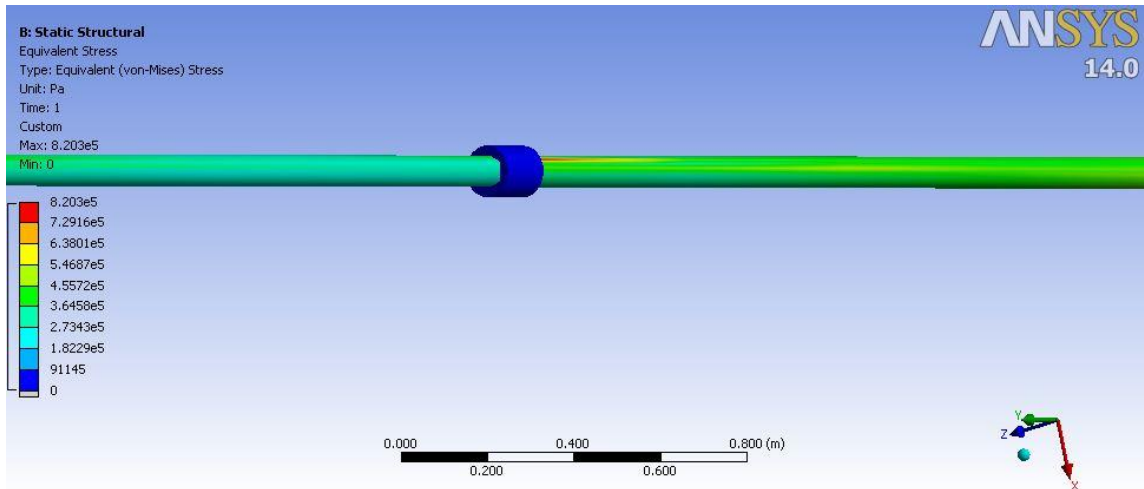


Figure 4.18: Von-Mises Stress Occurring on the Tubing for Production Rate=5000bbl/day at the Packer Region

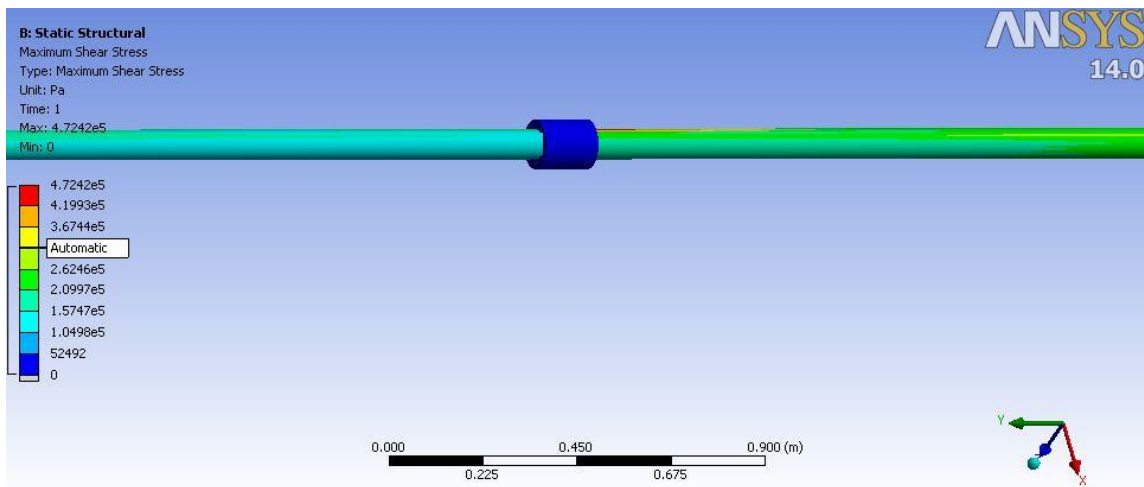


Figure 4.19: Shear Stress Occurring on the Tubing for Production Rate=5000bbl/day at the Packer Region

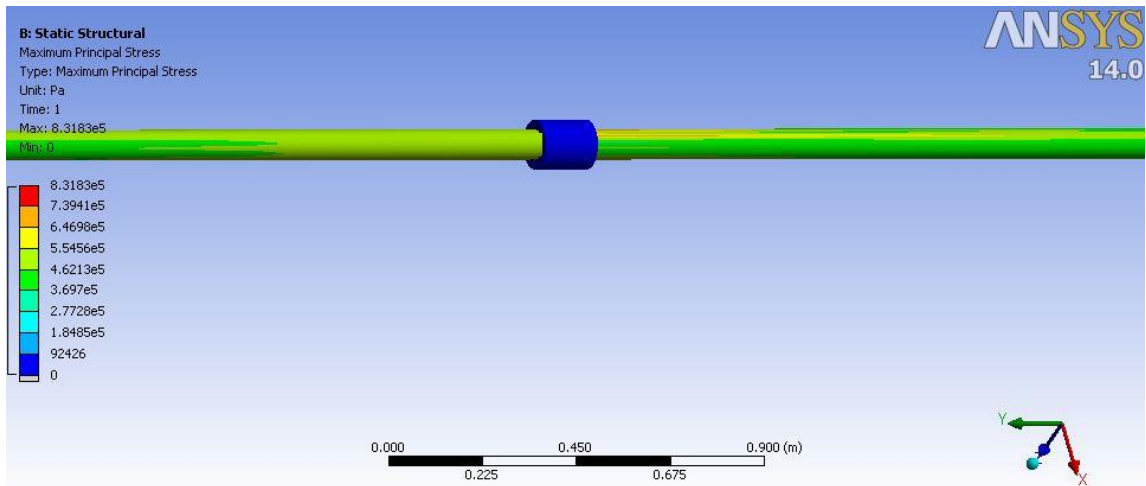


Figure 4.20: Principal Stress Occurring on the Tubing for Production Rate=5000bbl/day at the Packer Region

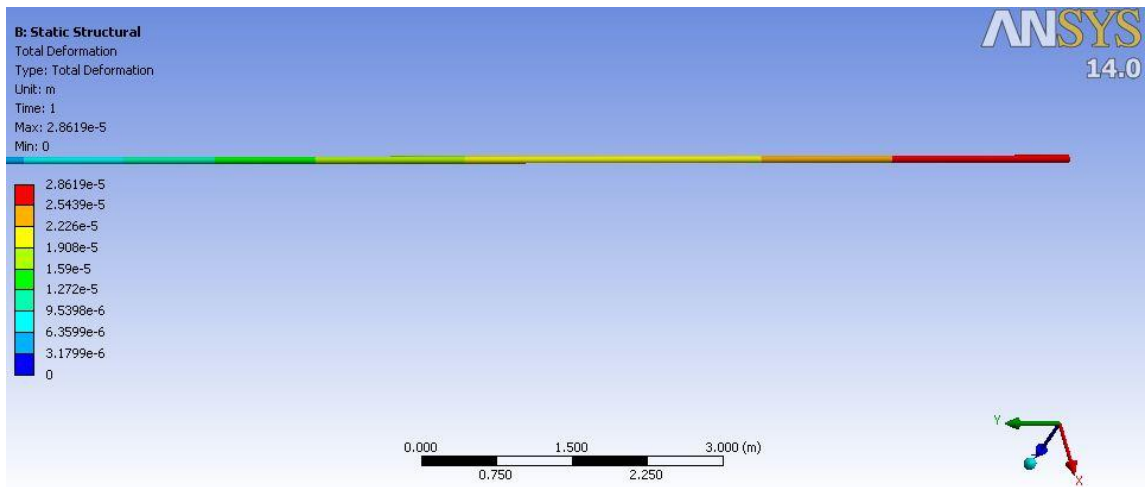


Figure 4.21: Deformation Occurring on the Tubing for Production Rate=5000bbl/day at the Inlet Region

After that, for the simulation of Ansys Static Structural for production rate of 5500bbl/day, the Von-Mises stress, shear stress, principal stress and deformation occurring on the tubing for production rate of 5500bbl/day (as shown in Fig. 4.22, 4.23, 4.24 and 4.25 below) are obtained.

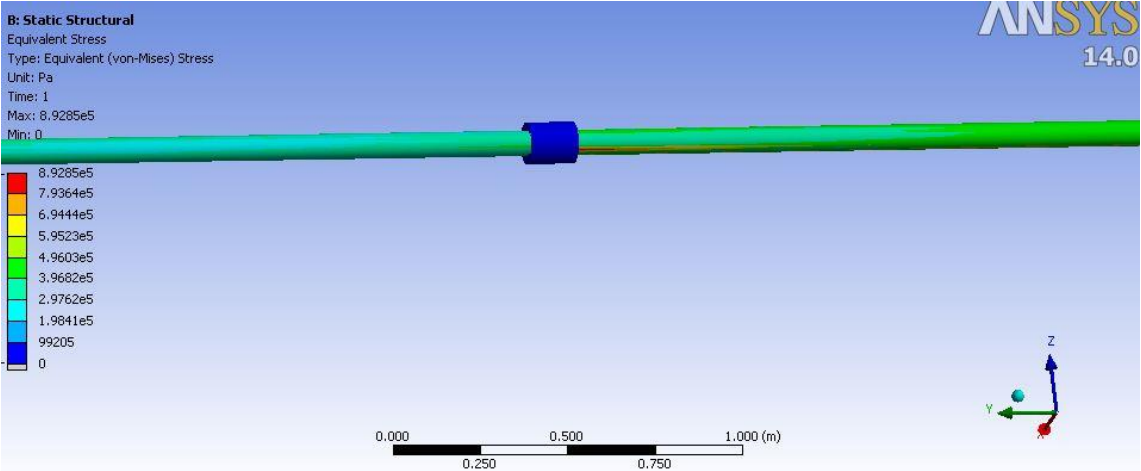


Figure 4.22: Von-Mises Stress Occurring on the Tubing for Production Rate=5500bbl/day at the packer region

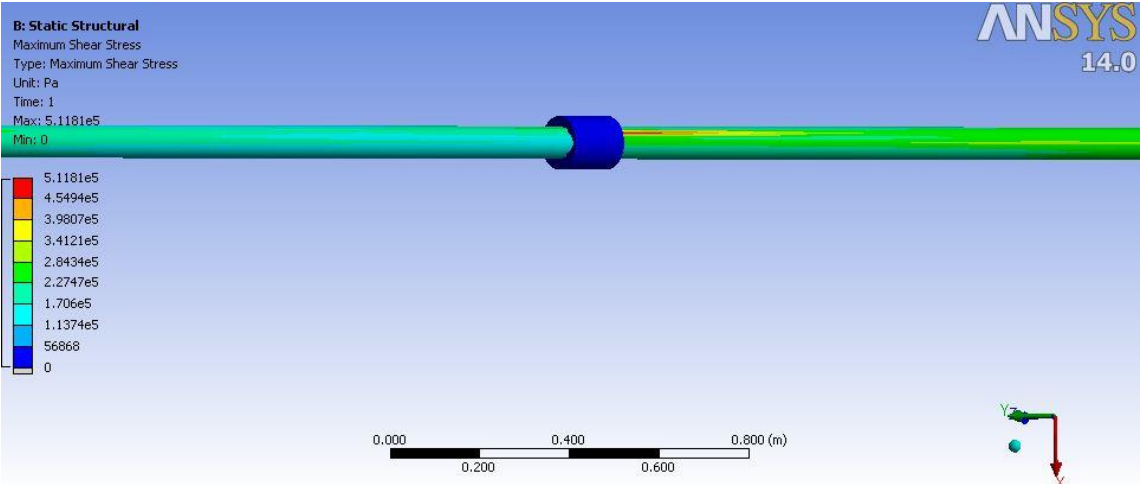


Figure 4.23: Shear Stress Occurring on the Tubing for Production Rate=5500bbl/day at the packer region

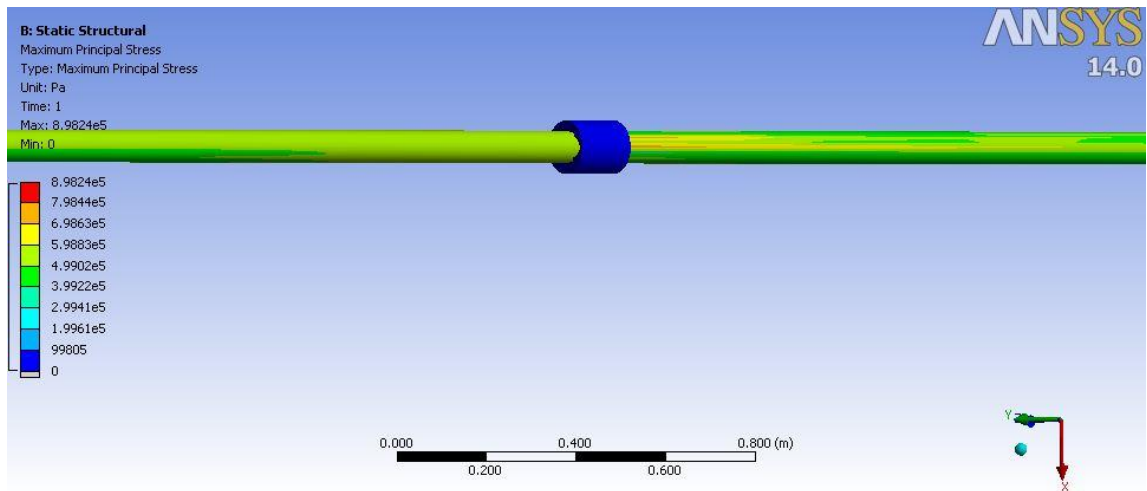


Figure 4.24: Principal Stress Occurring on the Tubing for Production Rate=5500bbl/day at the packer region

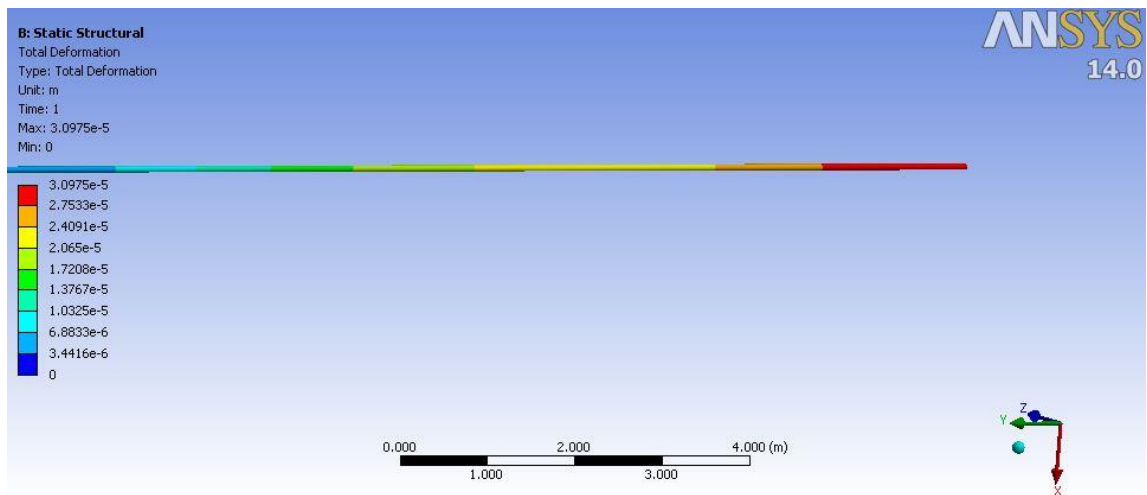


Figure 4.25: Deformation Occurring on the Tubing for Production Rate=5500bbl/day at the Inlet Region

After that, for the simulation of Ansys Static Structural for production rate of 6000bbl/day, the Von-Mises stress, shear stress, principal stress and deformation occurring on the tubing for production rate of 6000bbl/day (as shown in Fig. 4.26, 4.27, 4.28 and 4.29 below) are obtained.

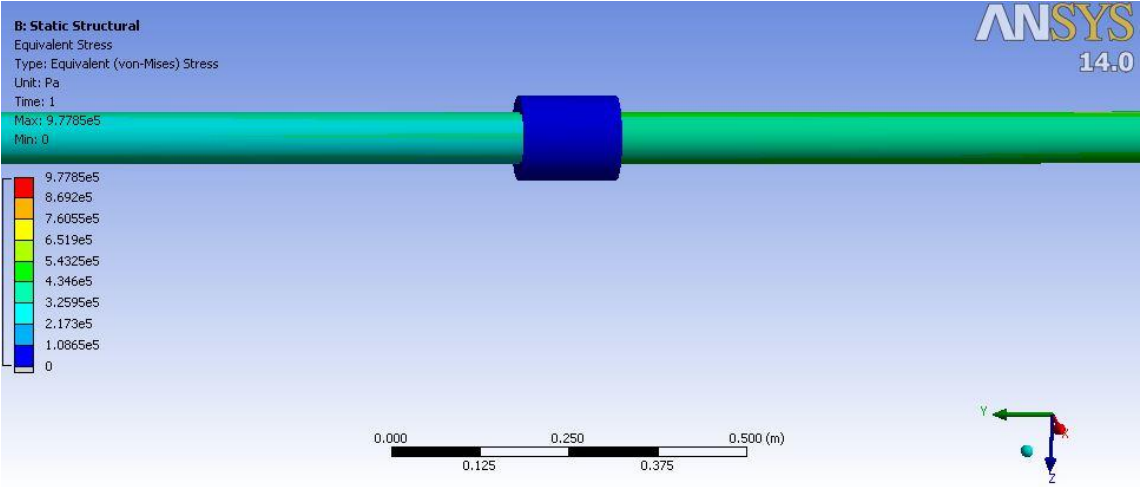


Figure 4.26: Von-Mises Stress Occurring on the Tubing for Production Rate=6000bbl/day at the Packer Region

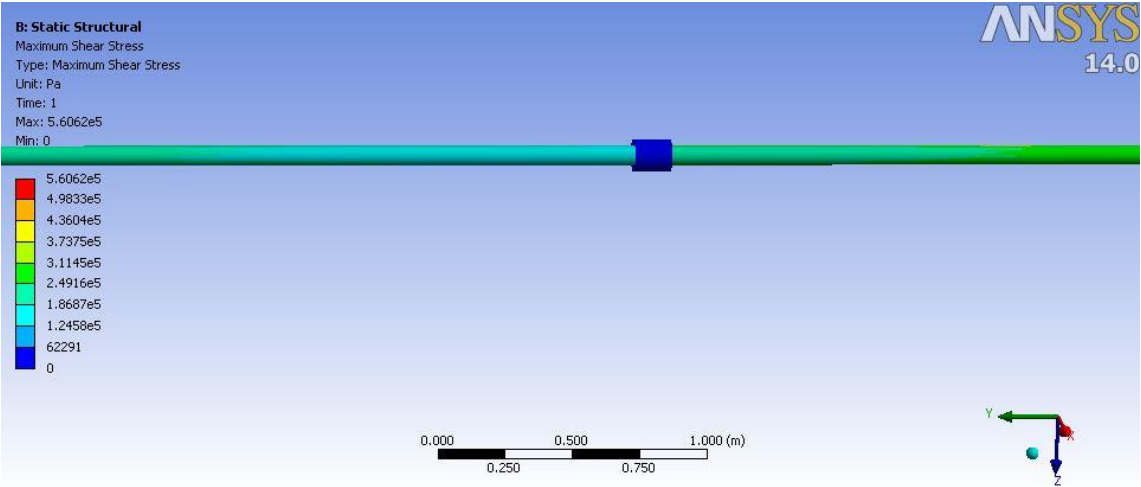


Figure 4.27: Shear Stress Occurring on the Tubing for Production Rate=6000bbl/day at the Packer Region

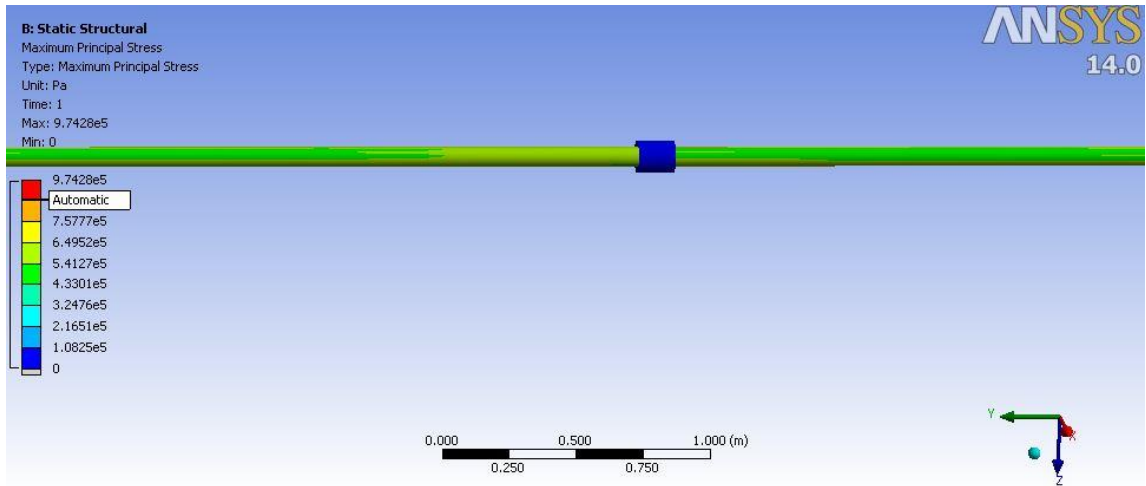


Figure 4.28: Principal Stress Occurring on the Tubing for Production Rate=6000bbl/day at the Packer Region

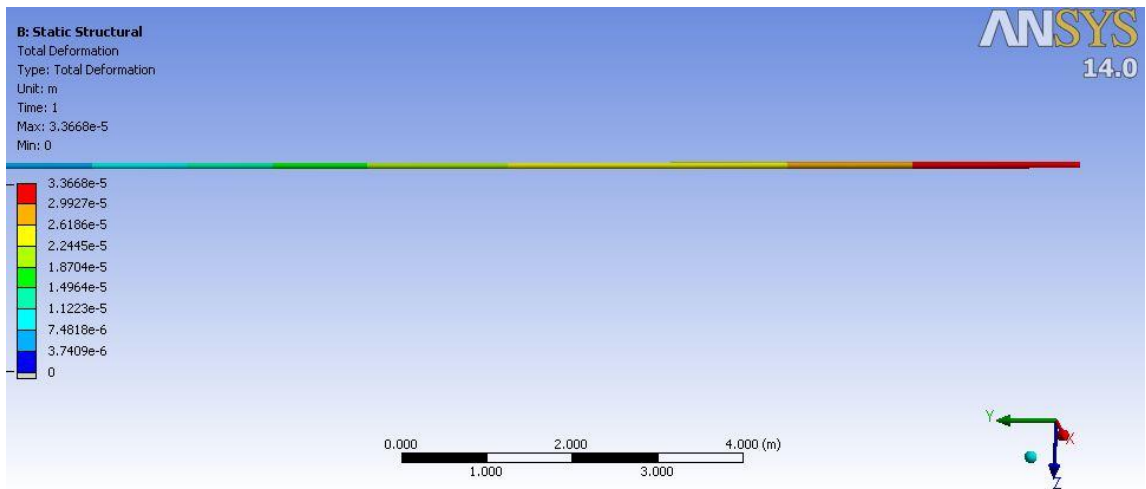


Figure 4.29: Deformation Occurring on the Tubing for Production Rate=6000bbl/day at the Inlet region

After that, for the simulation of Ansys Static Structural for production rate of 6500bbl/day, the Von-Mises stress, shear stress, principal stress and deformation occurring on the tubing for production rate of 6500bbl/day (as shown in Fig. 4.30, 4.31, 4.32 and 4.33 below) are obtained.

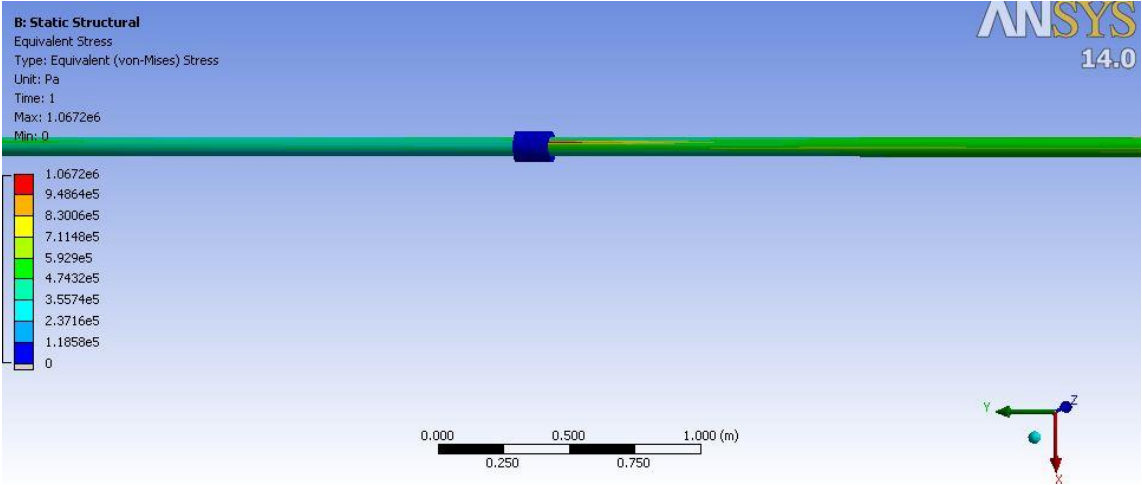


Figure 4.30: Von-Mises Stress Occurring on the Tubing for Production Rate=6500bbl/day at the packer region

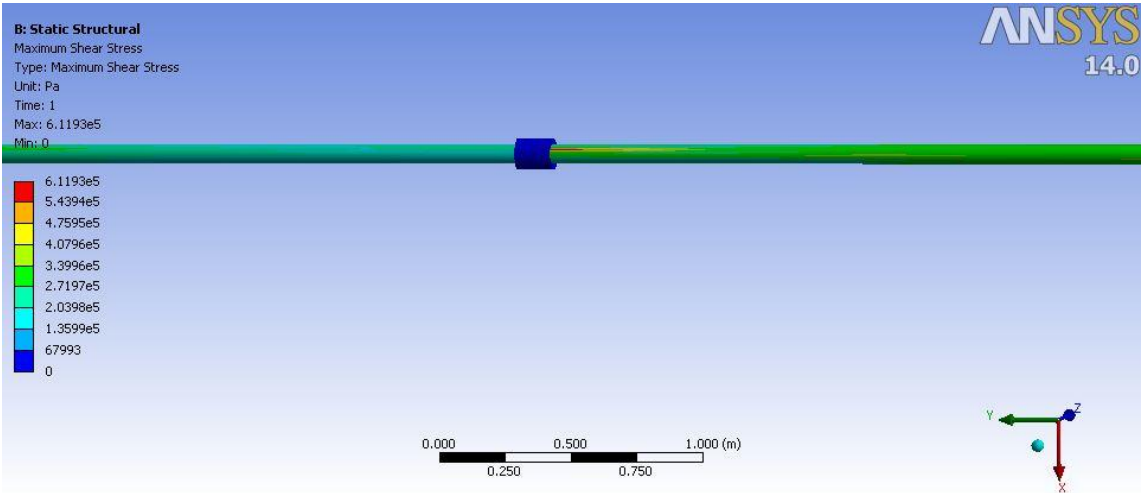


Figure 4.31: Shear Stress Occurring on the Tubing for Production Rate=6500bbl/day at the packer region

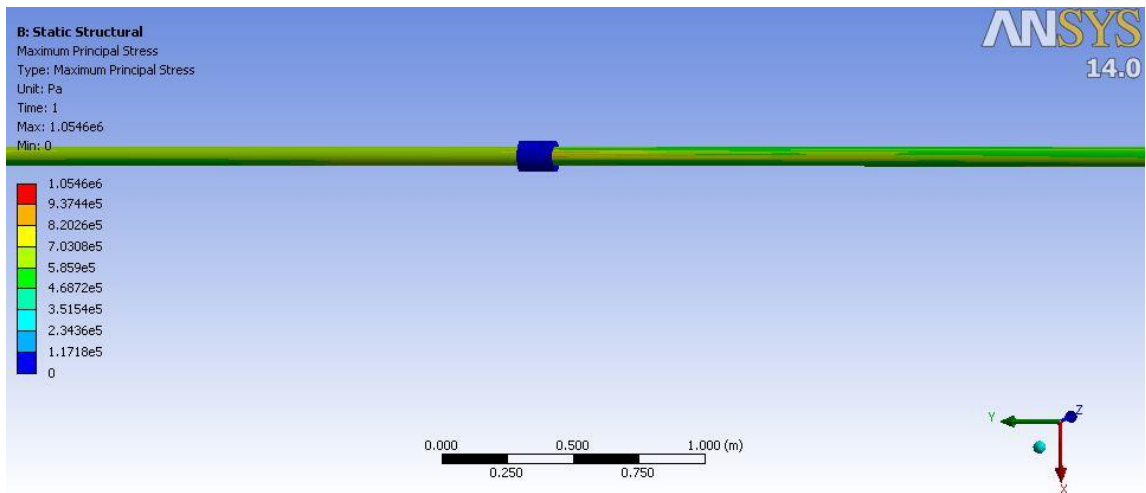


Figure 4.32: Principal Stress Occurring on the Tubing for Production Rate=6500bbl/day at the packer region

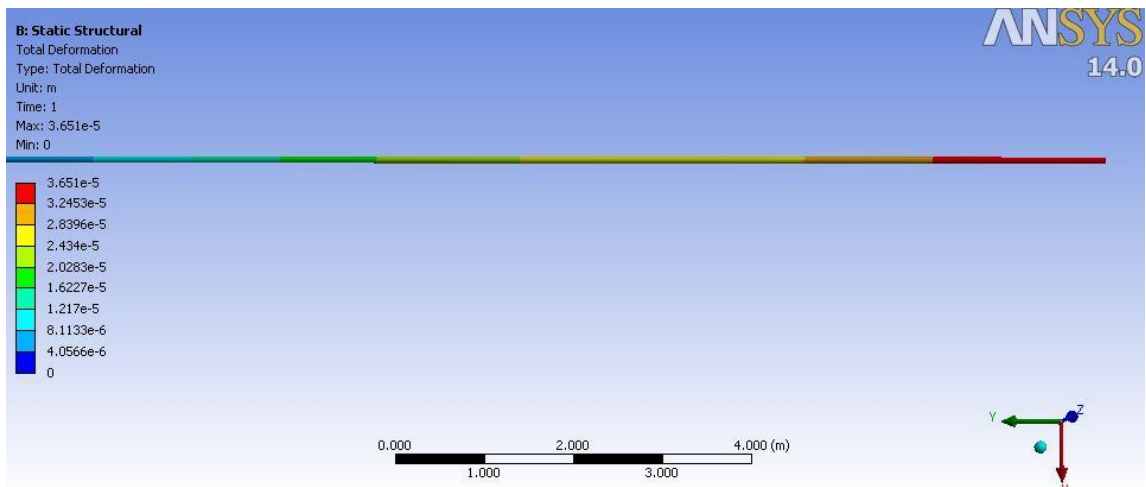


Figure 4.33: Deformation Occurring on the Tubing for Production Rate=6500bbl/day at the Inlet region

Then, using values in Fig. 4.18, 4.19, 4.20, 4.22, 4.23, 4.24, 4.26, 4.27, 4.28, 4.30, 4.31 and 4.32, the Table 4.3 is constructed. Table 4.3, as shown below is showing the maximum Von-Mises stress, maximum shear stress and maximum principal stress occurring on the tubing at production rates of 5000, 5500, 6000 and 6500bbl/day.

Table 4.3: The Stress Occurring on the Tubing at Different Production Rates

Production Rate (bbl/day)	Maximum Von-Mises Stress (E+5 Pa)	Maximum Shear Stress (E+5 Pa)	Maximum Principal Stress (E+5 Pa)
5000	8.203	4.7242	8.3183
5500	8.9285	5.1181	8.9824
6000	9.7785	5.6062	9.7428
6500	10.672	6.1193	10.546

After that, from values in Table 4.3, the Fig. 4.34 (as shown below) is plotted, showing the stress occurring on the tubing at production rates of 5000, 5500, 6000 and 6500bbl/day. From Fig. 4.34, it can be seen that, the higher the production rate, the higher the shear stress occurring on the tubing, the higher the principal stress occurring on the tubing, the higher the Von-Mises stress occurring on the tubing. For Von-Mises stress, the maximum stress is 10.672 E+5 Pa at 6500 bbl/day, while maximum shear stress is 6.1193E+5 Pa at 6500bbl/day, and the maximum principal stress is 10.546E+5 Pa at 6500bbl/day. The stress occurring on the tubing increases as the production rate increases. This is because the pressure exerted onto the tubing affects the stress and deformation. As the production rate increases, the pressure exerted onto the tubing also increases, which creates higher fluid loading as the production rate increases, resulting in higher stress. Therefore, as production rate increases, stress exerted onto the tubing increases.

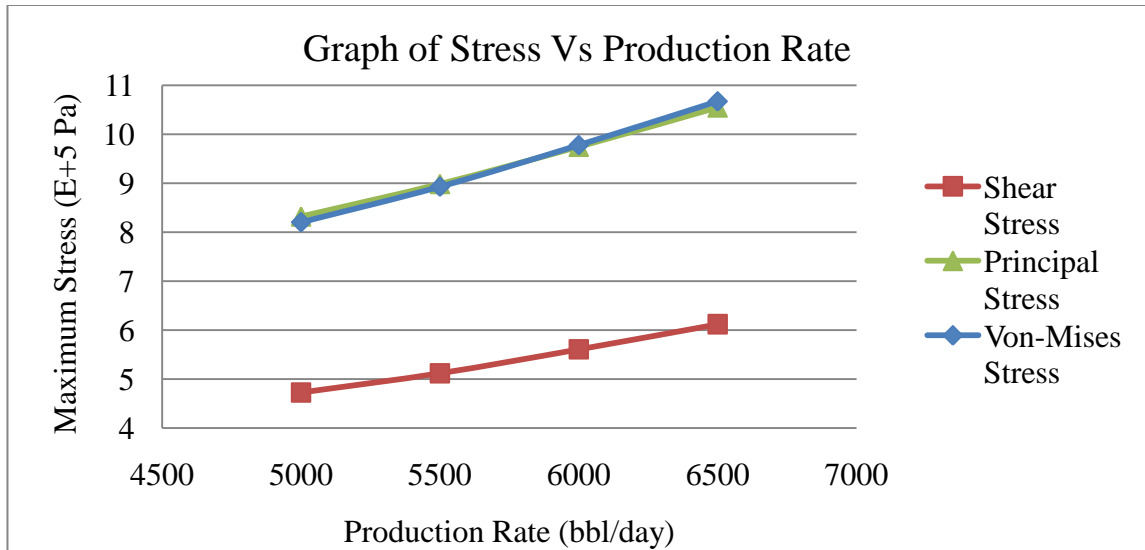


Figure 4.34: The Graph of Maximum Stress on the Tubing vs Production Rate

Then, using values in Fig. 4.21, 4.25, 4.29 and 4.33, the Table 4.4 is constructed. Table 4.4, as shown below is showing the maximum deformation occurring on the tubing at production rates of 5000, 5500, 6000 and 6500bbl/day.

Table 4.4: The Deformation Occurring on the Tubing at Different Production Rates

Production Rate (bbl/day)	Maximum Deformation (E-5 m)
5000	2.8619
5500	3.0975
6000	3.3668
6500	3.651

After that, from values in Table 4.4, the Fig. 4.35 (as shown below) is plotted, showing the maximum deformation occurring on the tubing at production rates of 5000, 5500, 6000 and 6500bbl/day. From Fig. 4.35, it can be seen that, the maximum deformation is 3.651E-5m at 6500bbl/day, while the minimum deformation is 2.8619E-5m at 5000bbl/day. Thus, the higher the production rate, the higher the deformation occurring on the tubing. The deformation occurring on the tubing increases as the production rate increases because the pressure and stress exerted onto the tubing affects the deformation. As the production rate increases, the pressure exerted onto the tubing also increases,

which creates higher fluid loading as the production rate increases, resulting in higher stress. Therefore, this increase in stress is causing the increase in deformation. Therefore, as production rate increases, deformation exerted onto the tubing increases.

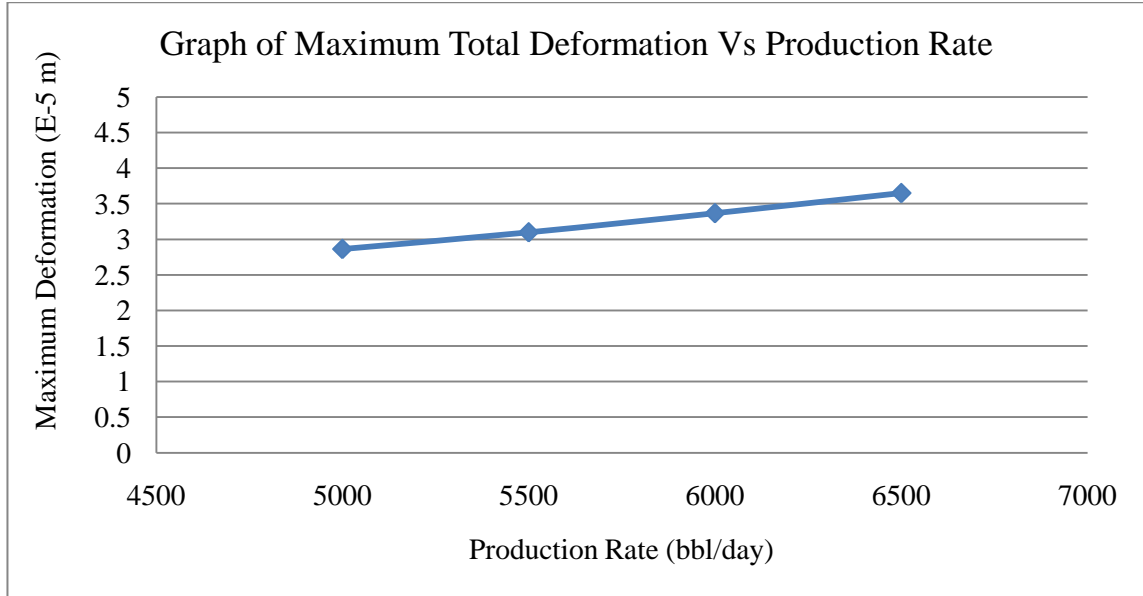


Figure 4.35: The Graph of Maximum Deformation vs Production Rate

However, as to whether the tubing experienced permanent or elastic deformation, it depends on the yield strength of the tubing. When the stress occurring on the tubing exceeds yield strength of the tubing, the tubing will experience permanent deformation, whereby the tubing will not return to original configuration even after the loading is released. On the other hands, when the stress occurring on the tubing is less than the yield strength of the tubing, the tubing experience elastic deformation, whereby the tubing will return to original configuration after the loading is released. Von-Mises stress is the stress which is usually applied for ductile material, and since the L80 steel is ductile material with yield strength of 80000psi or $5.5158E+8$ Pa, Von-Mises stresses are compared with the yield strength to determine the type of deformation. The maximum stress exerted onto the tubing is $10.672E+5$ Pa, which is less than the yield strength of the tubing, which is $5.5158E+8$ Pa. Therefore, for the production rates of 5000, 5500, 6000 and 6500bbl/day, the tubing only experience elastic deformation.

4.4 SIMULATION OF DYNAMIC CHARACTERISTICS OF THE TUBING FOR DIFFERENT PRODUCTION RATES

When the natural frequencies of the tubing are reached, the tubing resonates and begins to breakdown with irreversible deformation. For this project, the natural frequencies investigated are of lower modes of 1 and 2 and of a bit higher modes of 3 and 4. From the modal simulation, the natural frequencies of the first four modes for production rates of 5000, 5500, 6000 and 6500bbl/day are obtained and tabulated in Table 4.5 (as shown below).

Table 4.5: Natural Frequencies of First Four Modes for Different Production Rates

Production Rate (bbl/day)	Natural Frequency (Hz)			
	Mode 1	Mode 2	Mode 3	Mode 4
5000	68.679	68.894	84.384	85.877
5500	69.698	70.068	84.384	85.877
6000	70.773	71.455	84.384	85.877
6500	71.882	72.899	84.384	85.877

After that, by using the values in Table 4.5, the Fig. 4.36 is plotted, showing the natural frequencies at first four modes for production rates of 5000, 5500, 6000 and 6500bbl/day.

From Fig. 4.36 (as shown below), it can be seen that the natural frequency at the fourth mode is the biggest natural frequency, followed by natural frequency at mode 3, natural frequency at mode 2 and natural frequency at mode 1. And the natural frequencies of the tubing at lower modes of 1 and 2 increases as the production rate increases. The increase in natural frequency is due to turbulence effect. The turbulence effect from the flow increases the stiffness of the tubing, which causes increase in natural frequencies as the production rate increases. However, for mode 3 at different production rate, the turbulence effect in the tubing is not significant enough, which causes similar stiffness to be produced for the tubing at mode at different production rates. Therefore, the natural frequencies remain similar for different production rates. Same case also applies for mode 4 for different production rate.

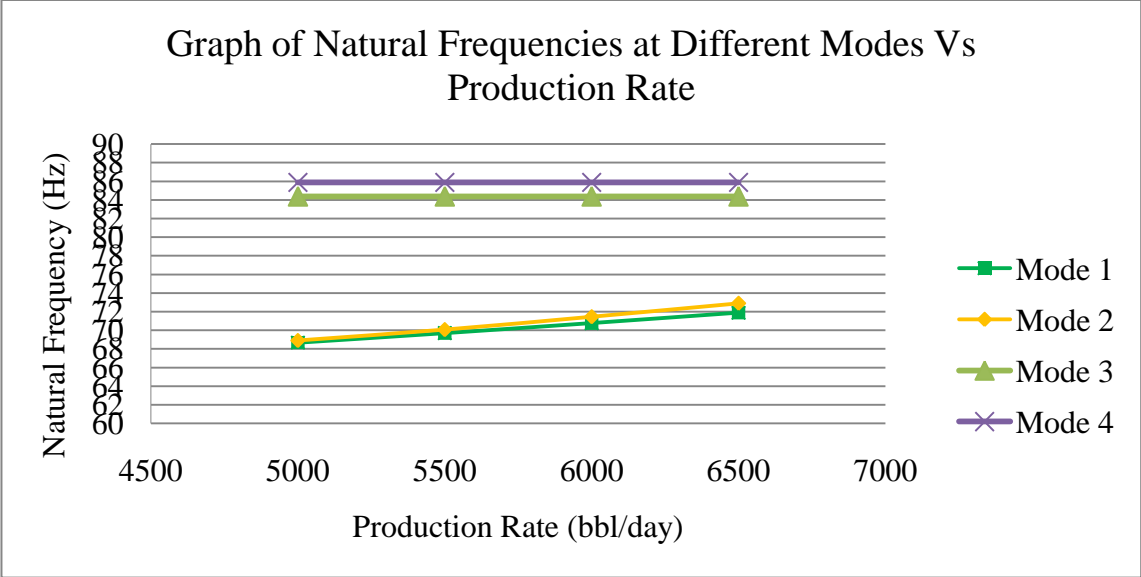


Figure 4.36: The Graph of Mode Natural Frequencies vs Production rate

After that, the maximum deformations of first four modes at production rate of 5000bbl/day are obtained with their pictures (as shown in Fig.4.37 to Fig. 4.44) are as shown below.

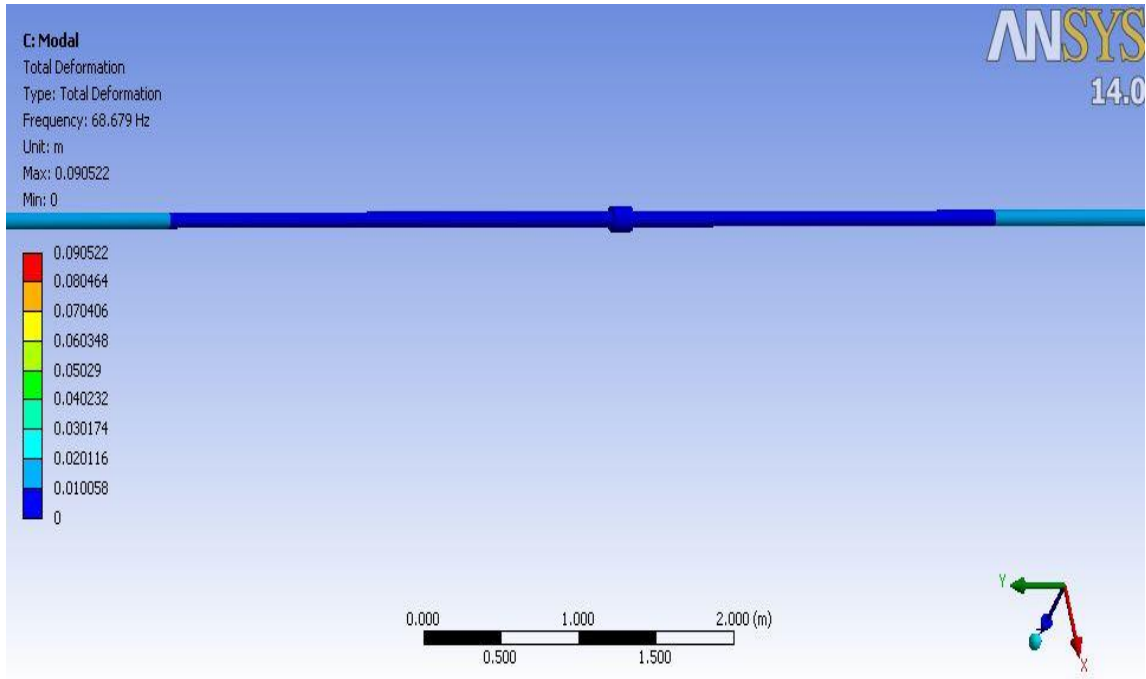


Figure 4.37: Deformation at Natural Frequency of Mode 1 at Production rate=5000bbl/day at Packer Region

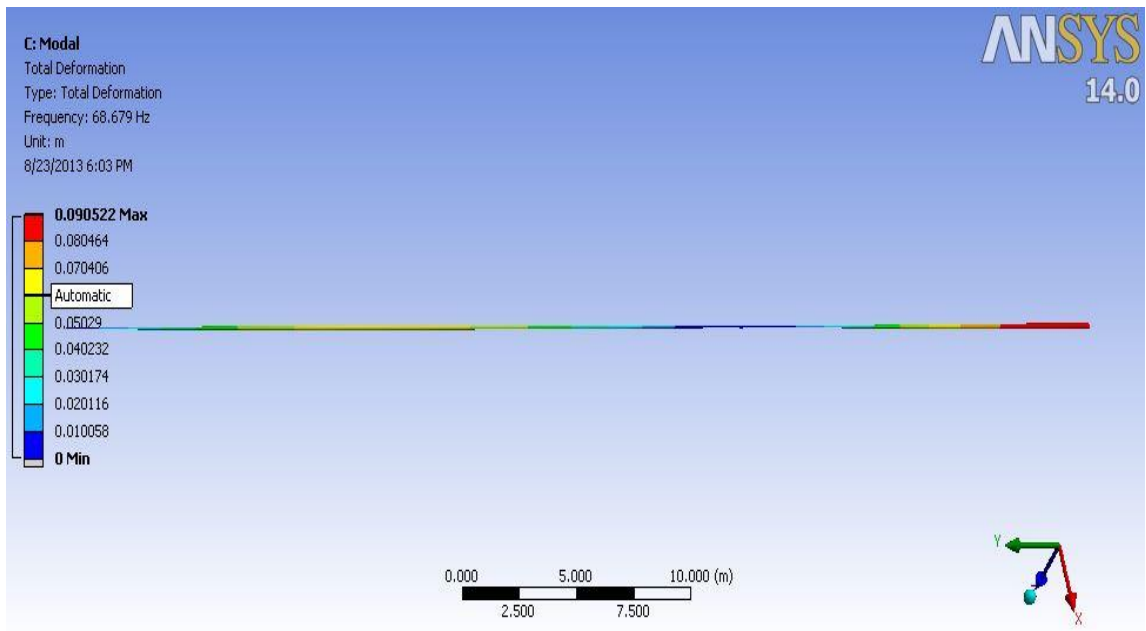


Figure 4.38: Deformation at Natural Frequency of Mode 1 at Production rate=5000bbl/day for the Whole 50m Tubing Length

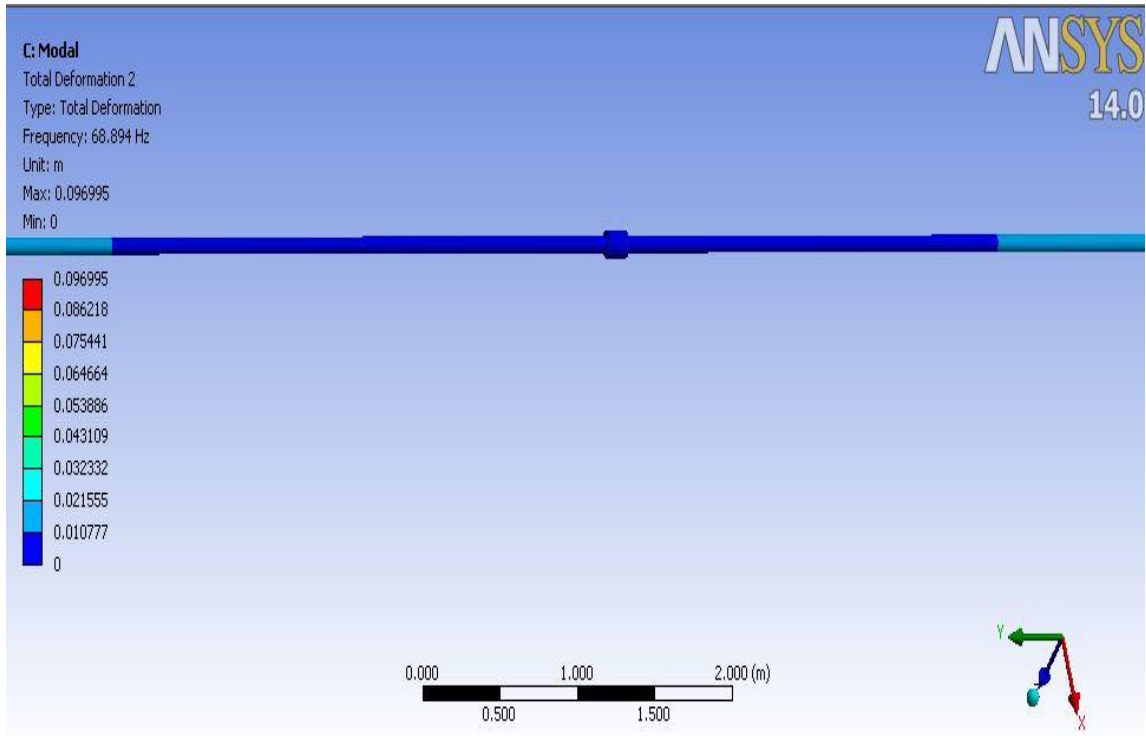


Figure 4.39: Deformation at Natural Frequency of Mode 2 at Production rate=5000bbl/day at Packer Region

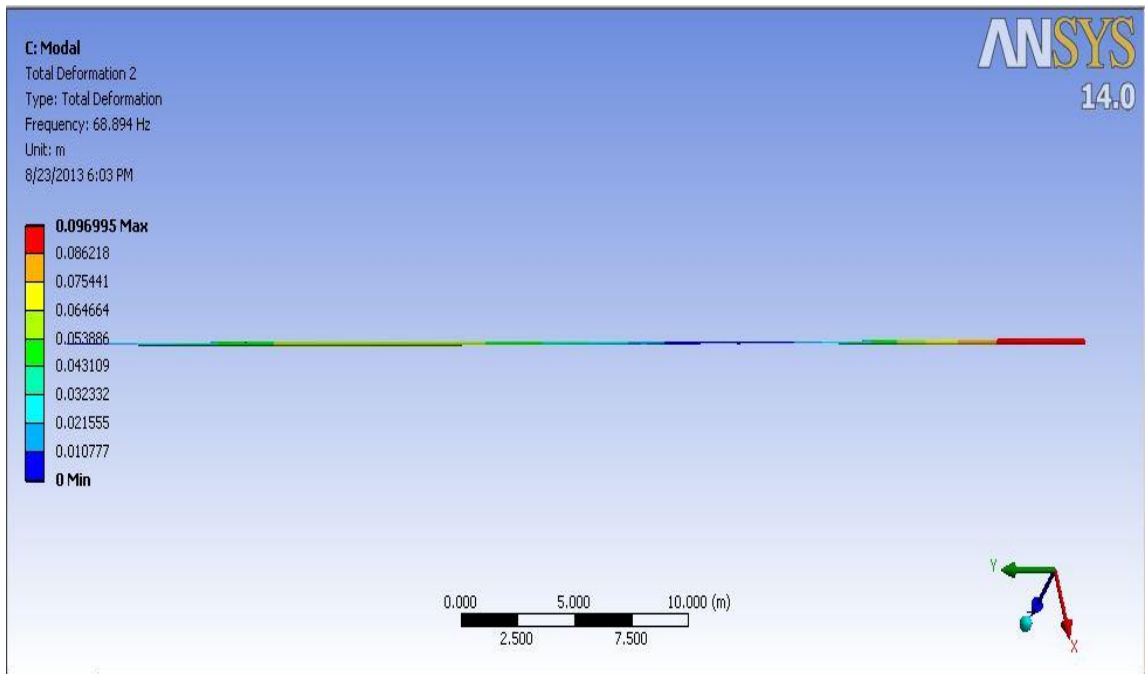


Figure 4.40: Deformation at Natural Frequency of Mode 2 at Production rate=5000bbl/day for the Whole 50m Tubing Length

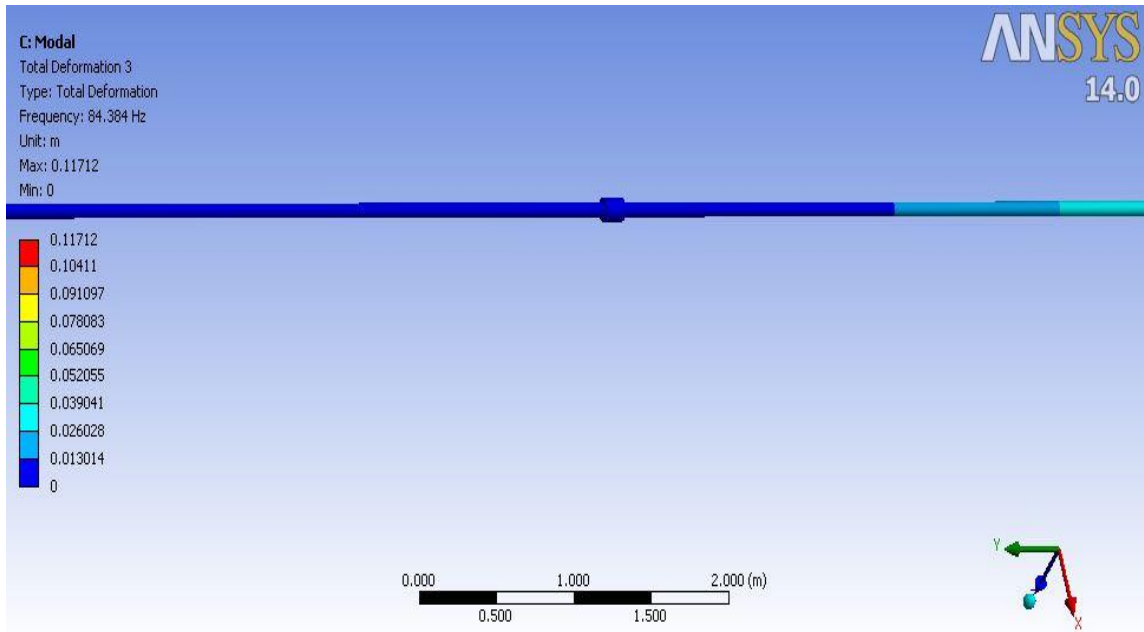


Figure 4.41: Deformation at Natural Frequency of Mode 3 at Production rate=5000bbl/day at Packer Region

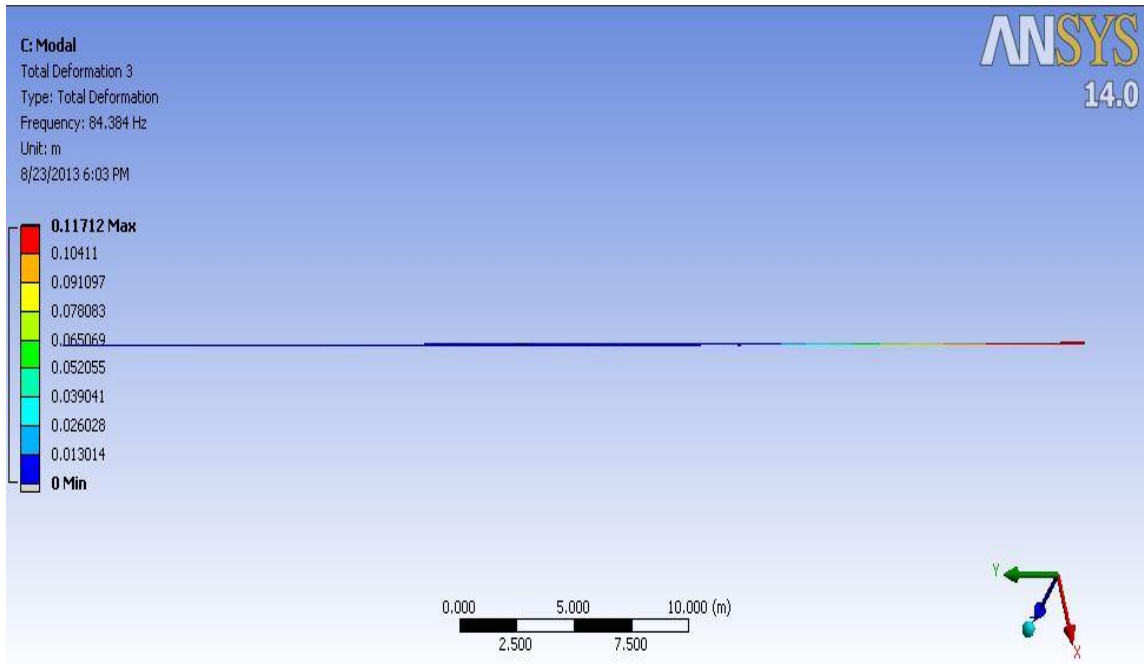


Figure 4.42: Deformation at Natural Frequency of Mode 3 at Production rate=5000bbl/day for the Whole 50m Tubing Length

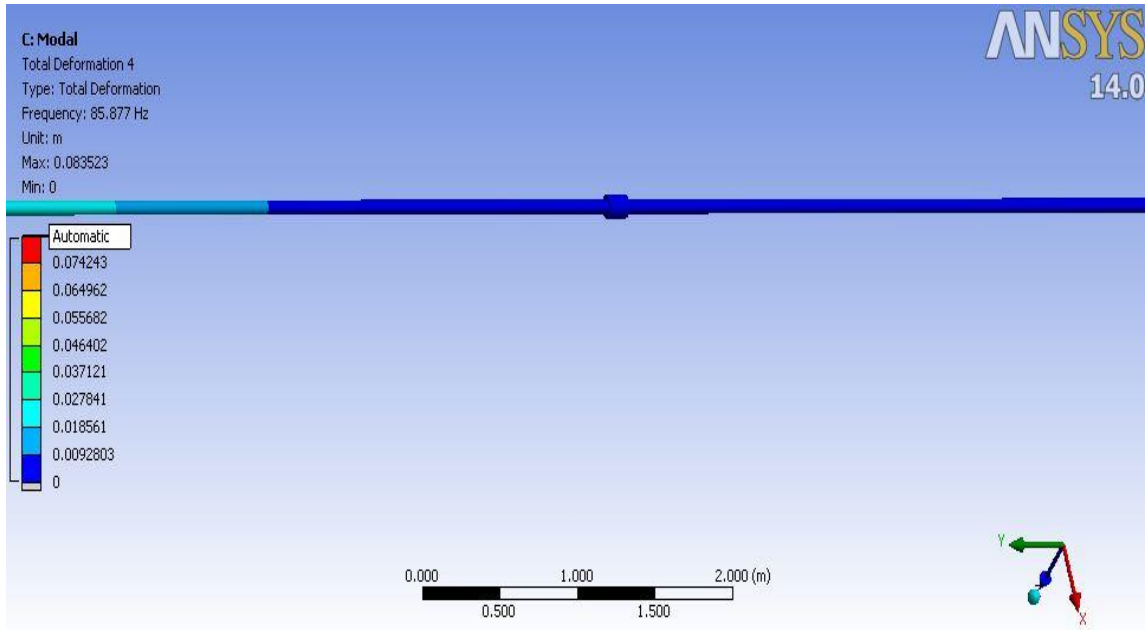


Figure 4.43: Deformation at Natural Frequency of Mode 4 at Production rate=5000bbl/day at Packer Region

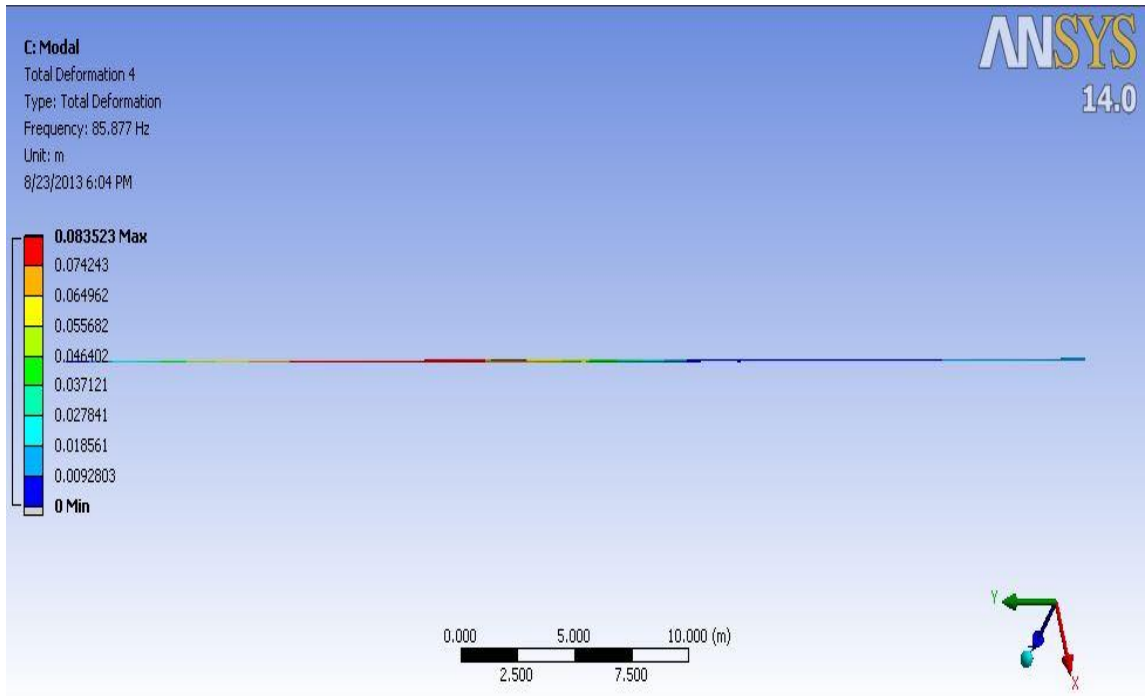


Figure 4.44: Deformation at Natural Frequency of Mode 4 at Production rate=5000bbl/day for the Whole 50m Tubing Length

After that, the maximum deformations of first four modes at production rate of 5500bbl/day are obtained with their pictures (as shown in Fig.4.45 to Fig. 4.52) are as shown below.

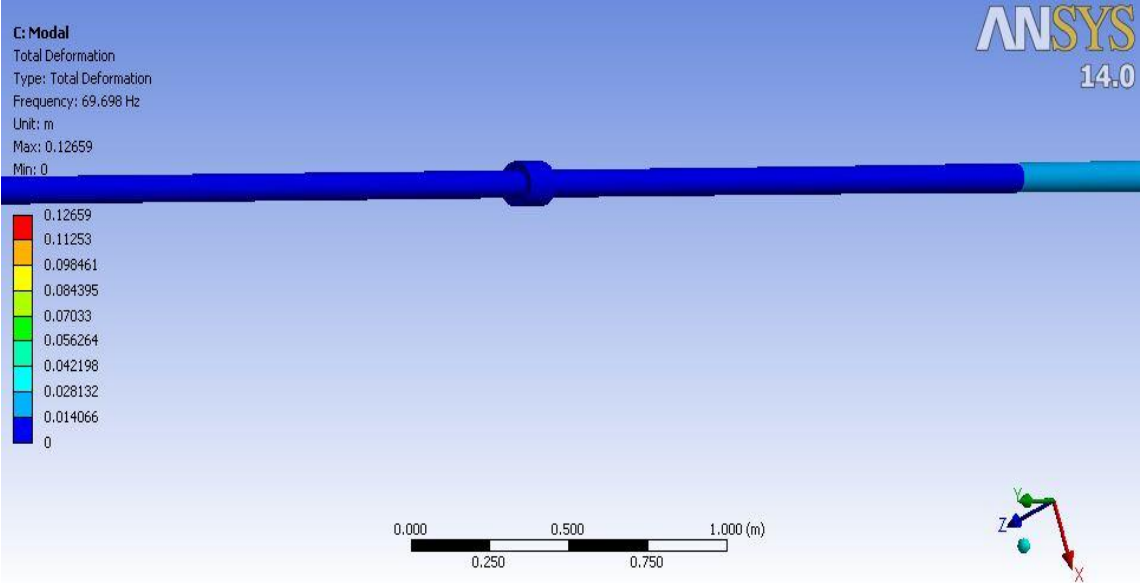


Figure 4.45: Deformation at Natural Frequency of Mode 1 at Production rate=5500bbl/day at Packer Region

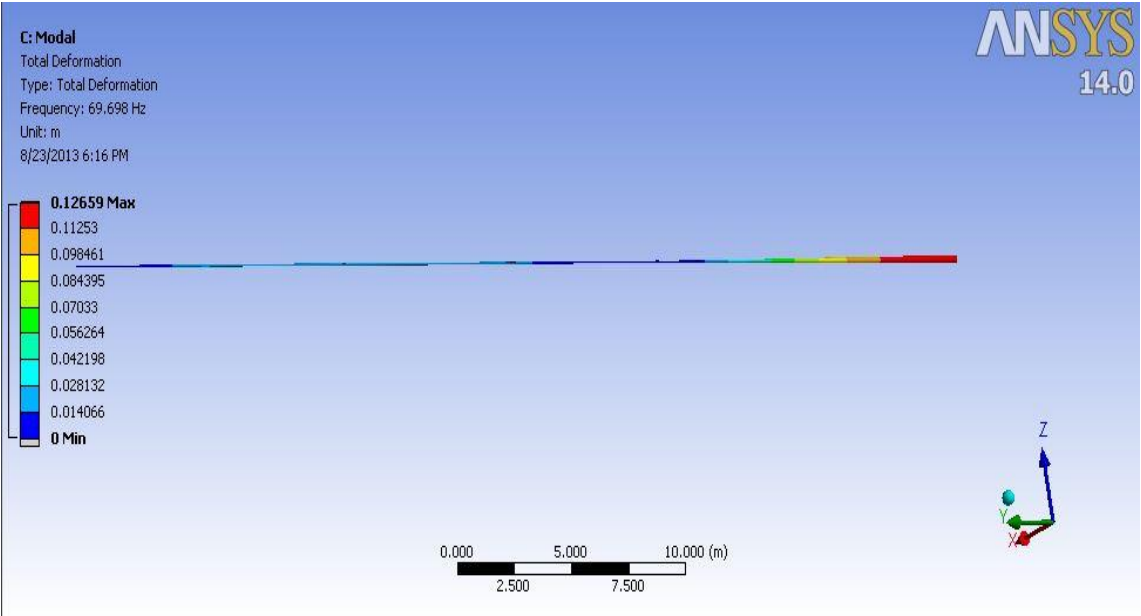


Figure 4.46: Deformation at Natural Frequency of Mode 1 at Production rate=5500bbl/day for the Whole 50m Tubing Length

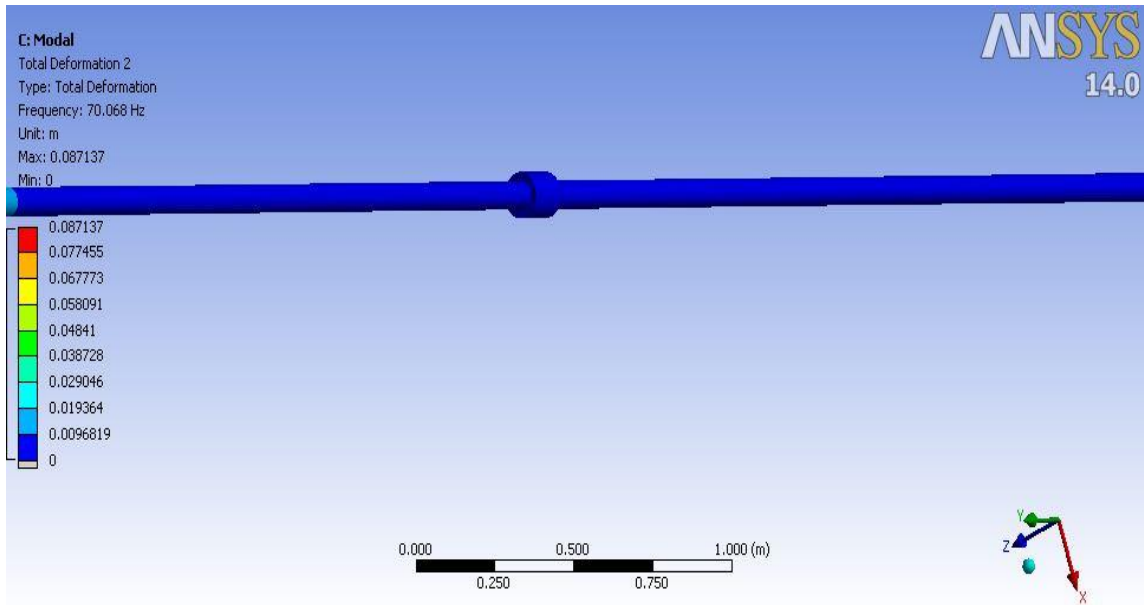


Figure 4.47: Deformation at Natural Frequency of Mode 2 at Production rate=5500bbl/day at Packer Region

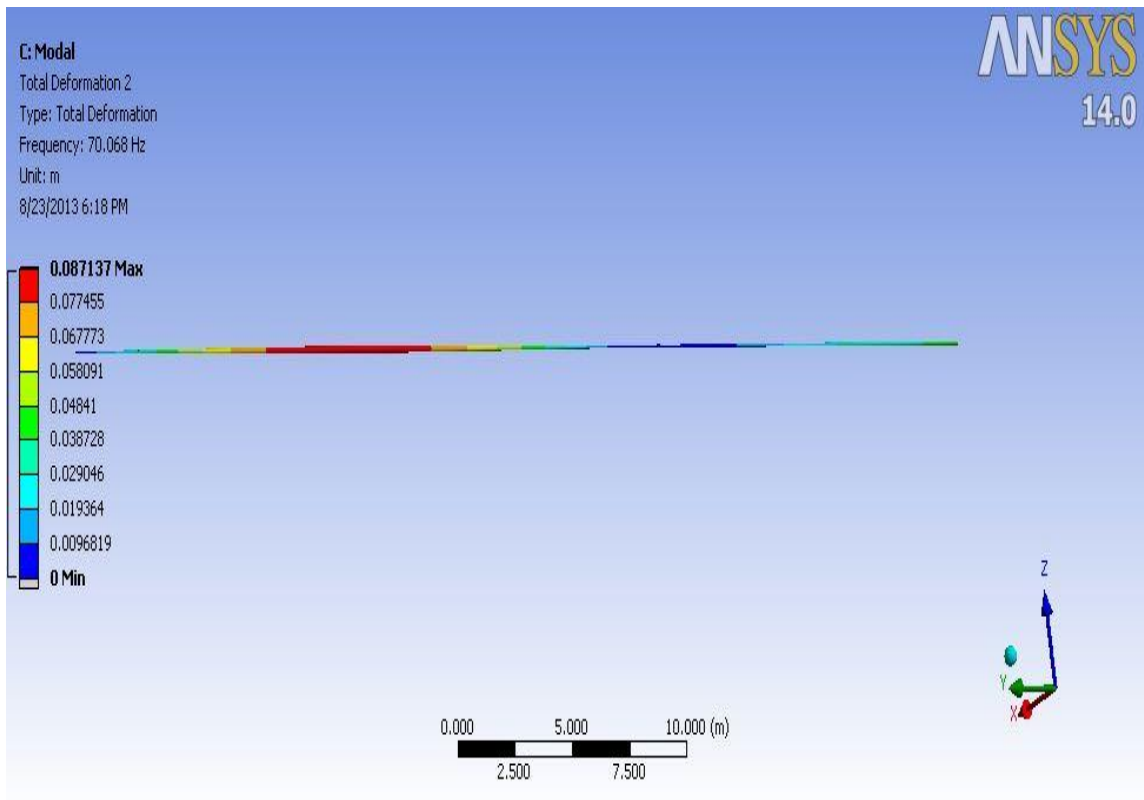


Figure 4.48: Deformation at Natural Frequency of Mode 2 at Production rate=5500bbl/day for the Whole 50m Tubing Length

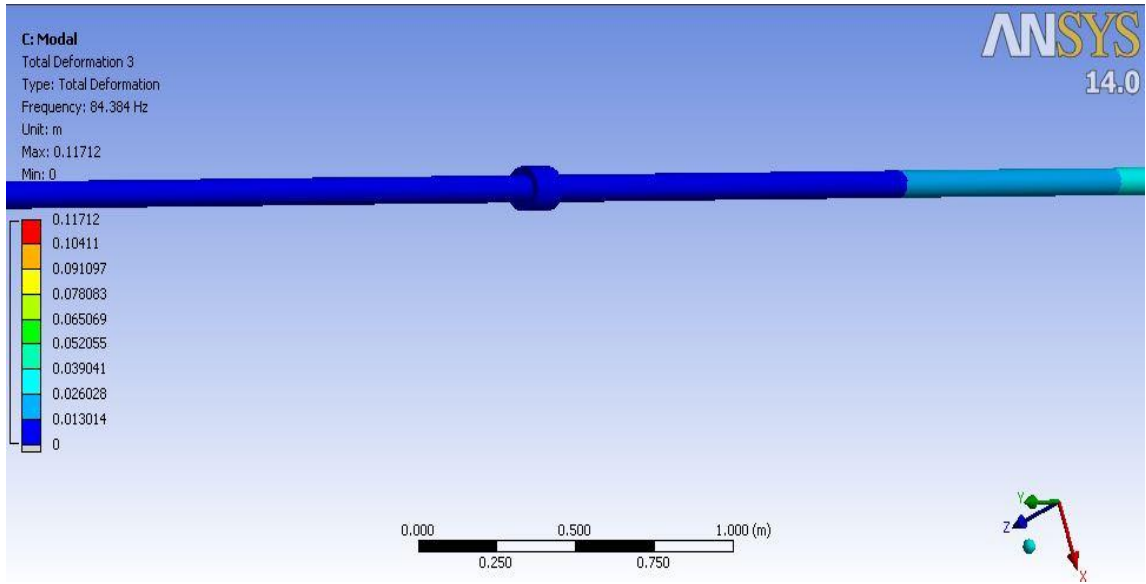


Figure 4.49: Deformation at Natural Frequency of Mode 3 at Production rate=5500bbl/day at Packer Region

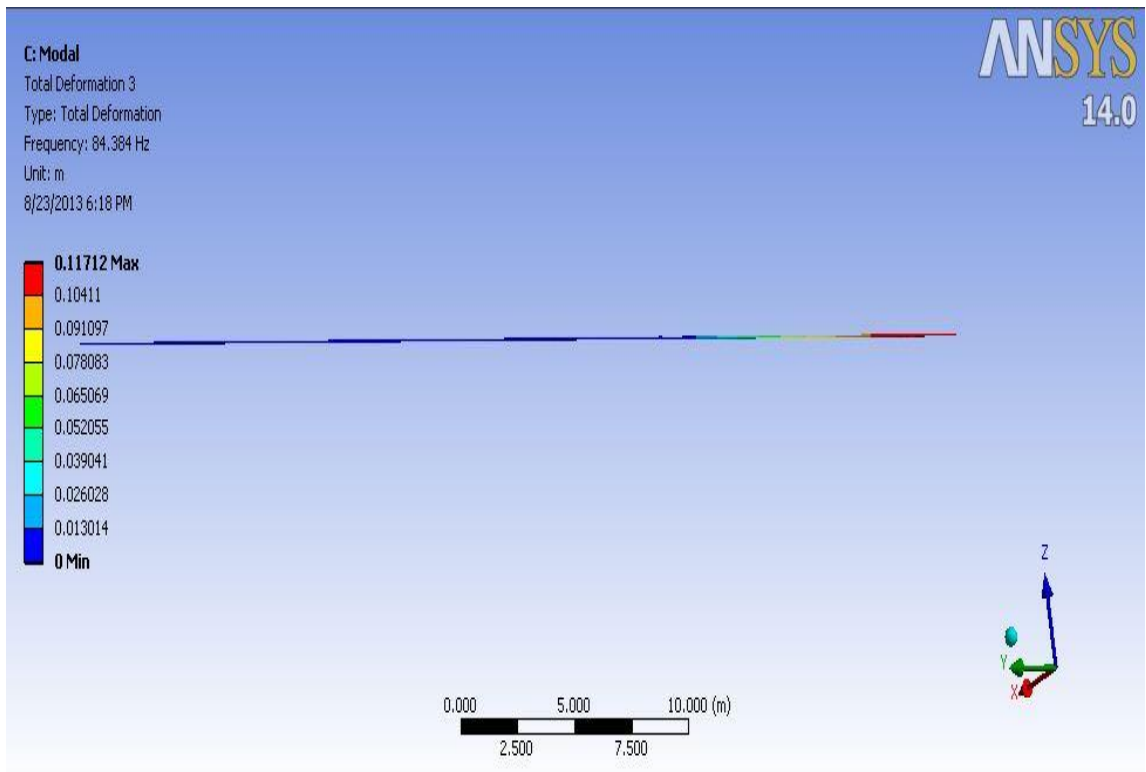


Figure 4.50: Deformation at Natural Frequency of Mode 3 at Production rate=5500bbl/day for the Whole 50m Tubing Length

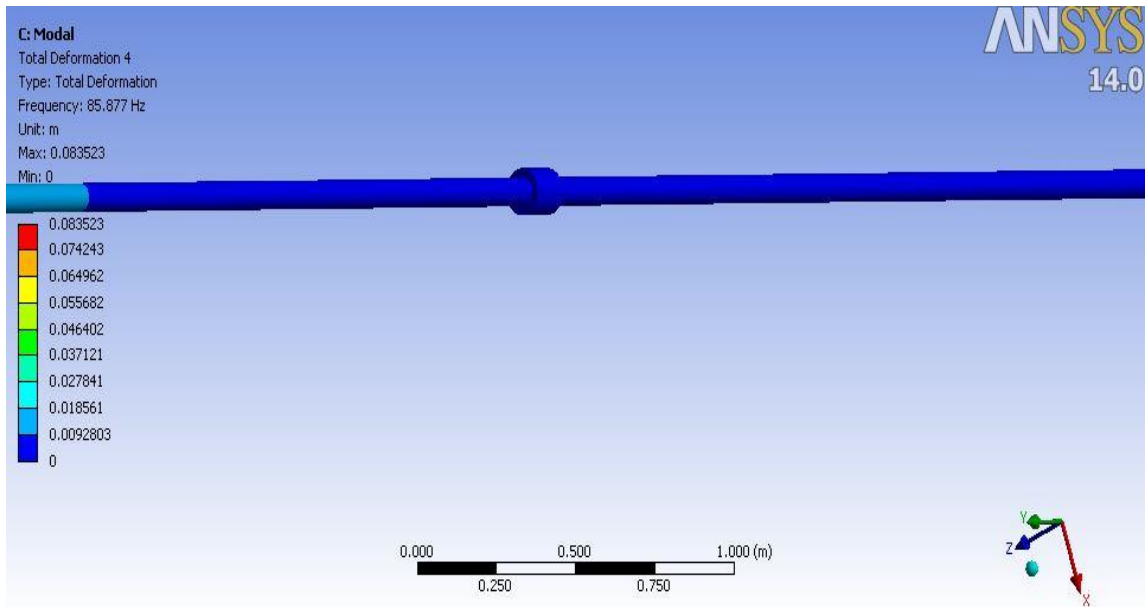


Figure 4.51: Deformation at Natural Frequency of Mode 4 at Production rate=5500bbl/day at Packer Region

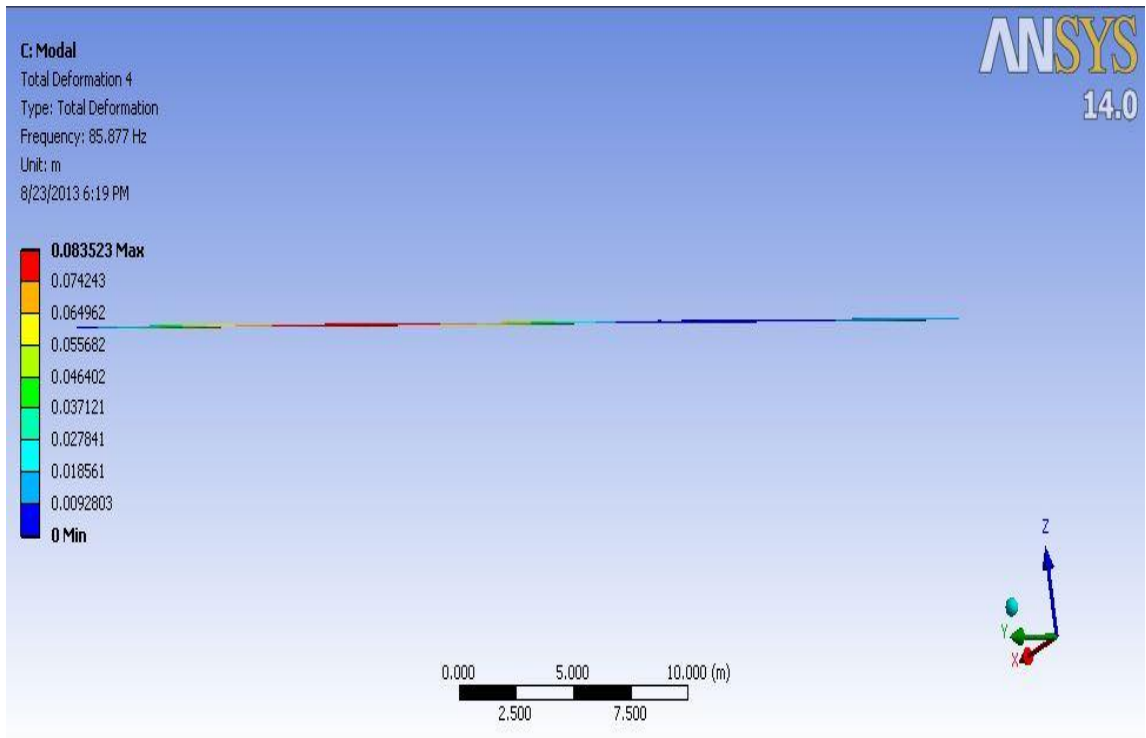


Figure 4.52: Deformation at Natural Frequency of Mode 4 at Production rate=5500bbl/day for the Whole 50m Tubing Length

After that, the maximum deformations of first four modes at production rate of 6000bbl/day are obtained with their pictures (as shown in Fig.4.53 to Fig. 4.60) are as shown below.

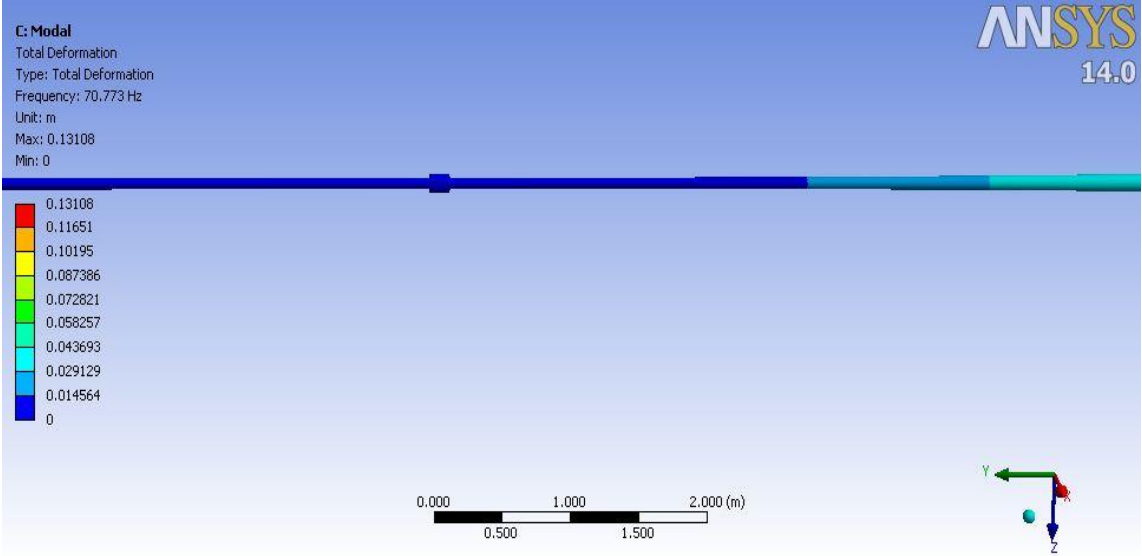


Figure 4.53: Deformation at Natural Frequency of Mode 1 at Production rate=6000bbl/day at Packer Region

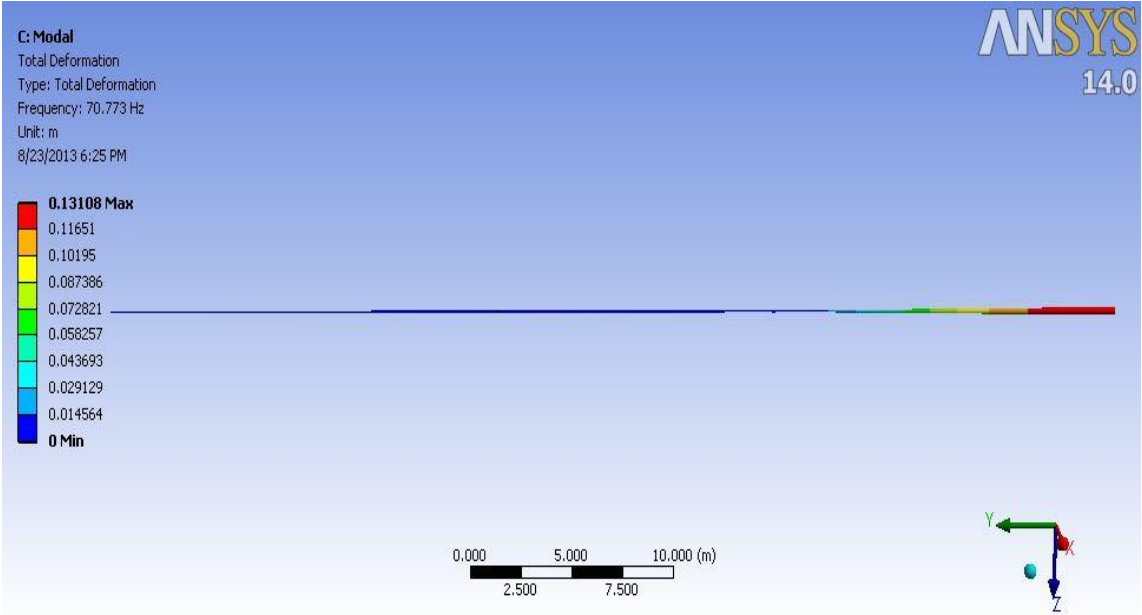


Figure 4.54: Deformation at Natural Frequency of Mode 1 at Production rate=6000bbl/day for the Whole 50m Tubing Length

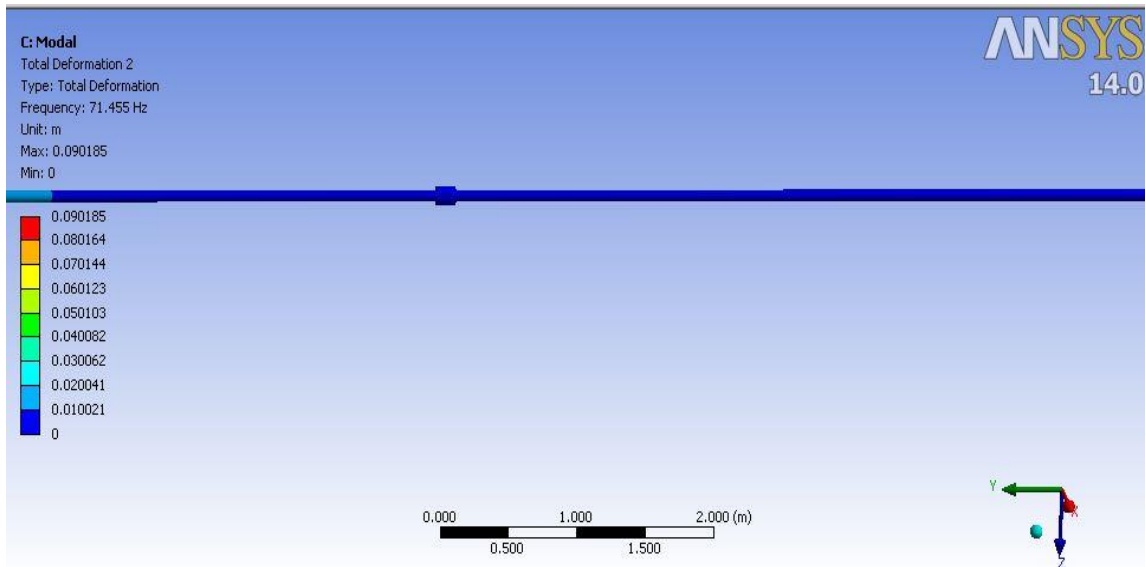


Figure 4.55: Deformation at Natural Frequency of Mode 2 at Production rate=6000bbl/day at Packer Region

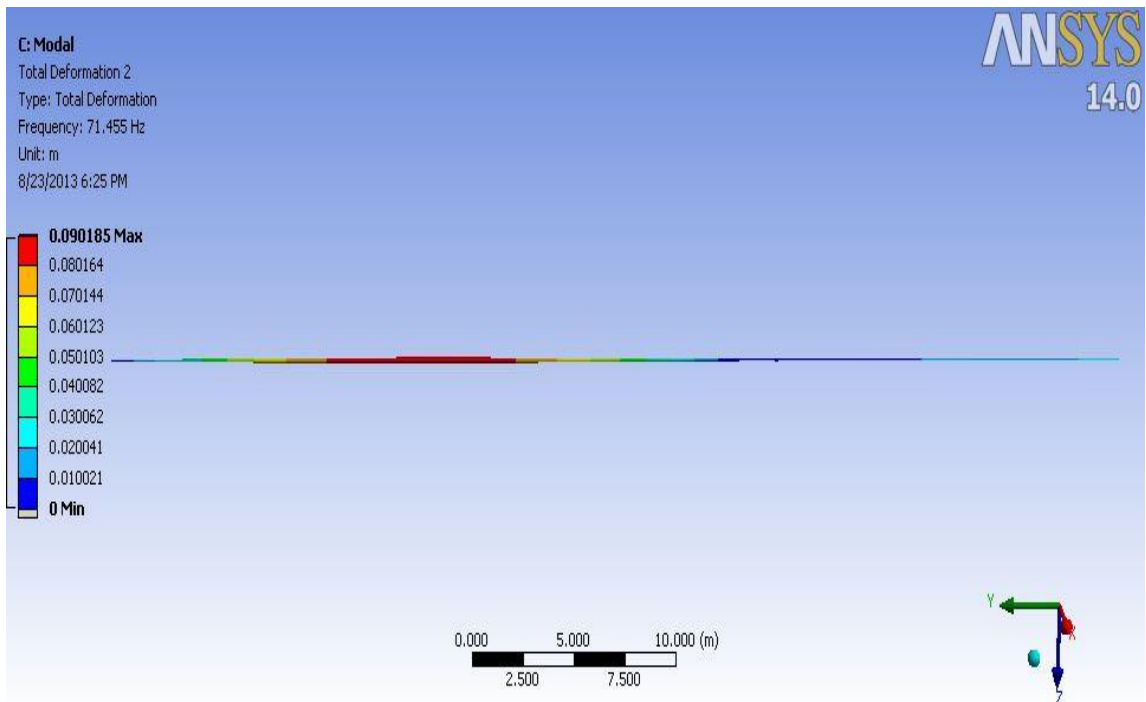


Figure 4.56: Deformation at Natural Frequency of Mode 2 at Production rate=6000bbl/day for the Whole 50m Tubing Length

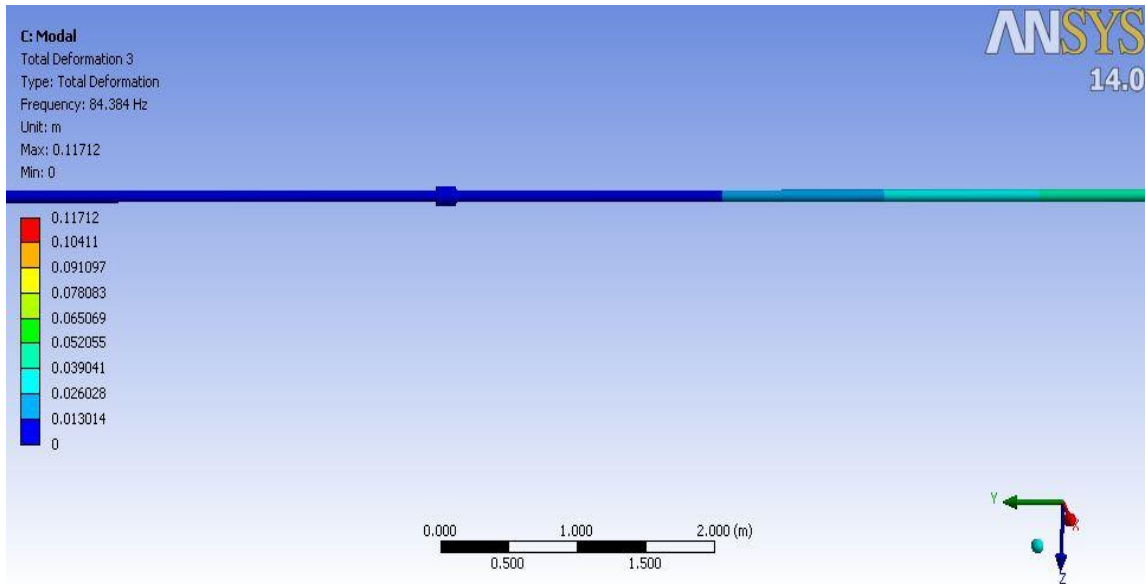


Figure 4.57: Deformation at Natural Frequency of Mode 3 at Production rate=6000bbl/day at Packer Region

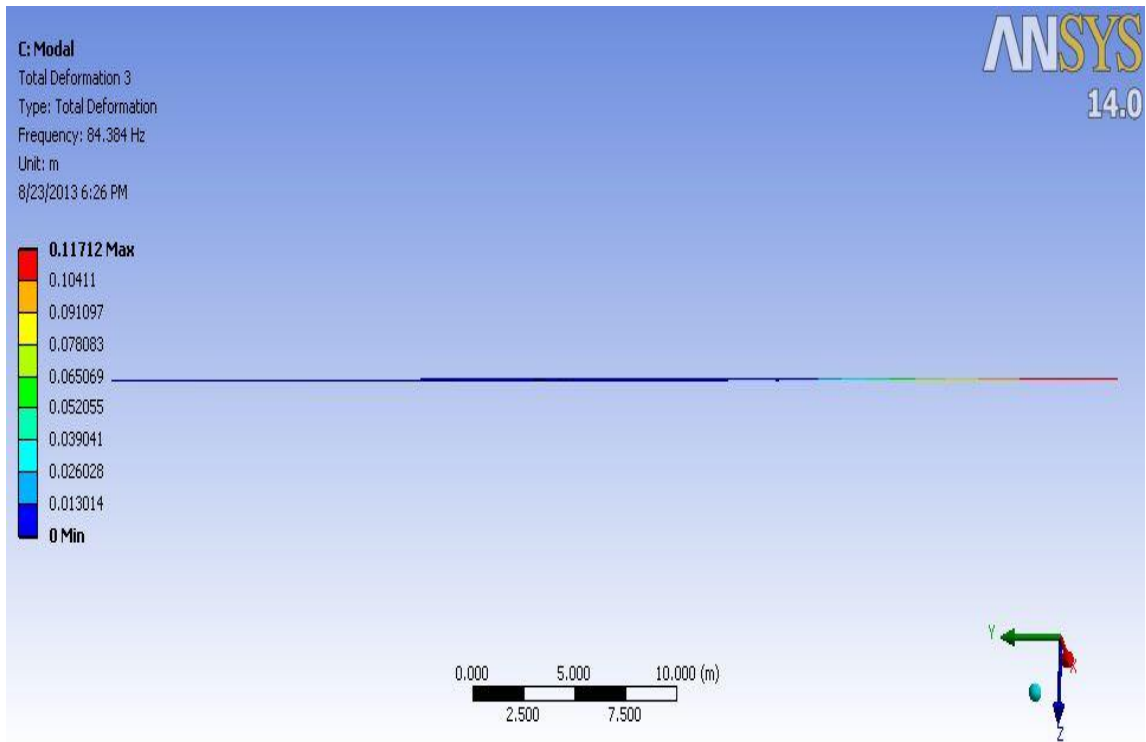


Figure 4.58: Deformation at Natural Frequency of Mode 3 at Production rate=6000bbl/day for the Whole 50m Tubing Length

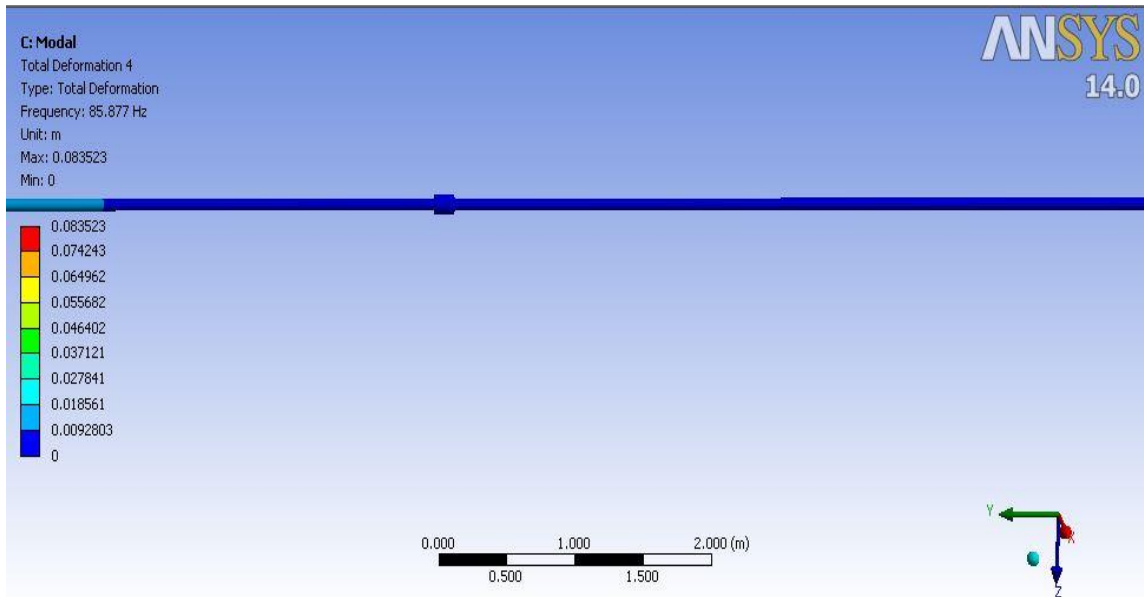


Figure 4.59: Deformation at Natural Frequency of Mode 4 at Production rate=6000bbl/day at Packer Region

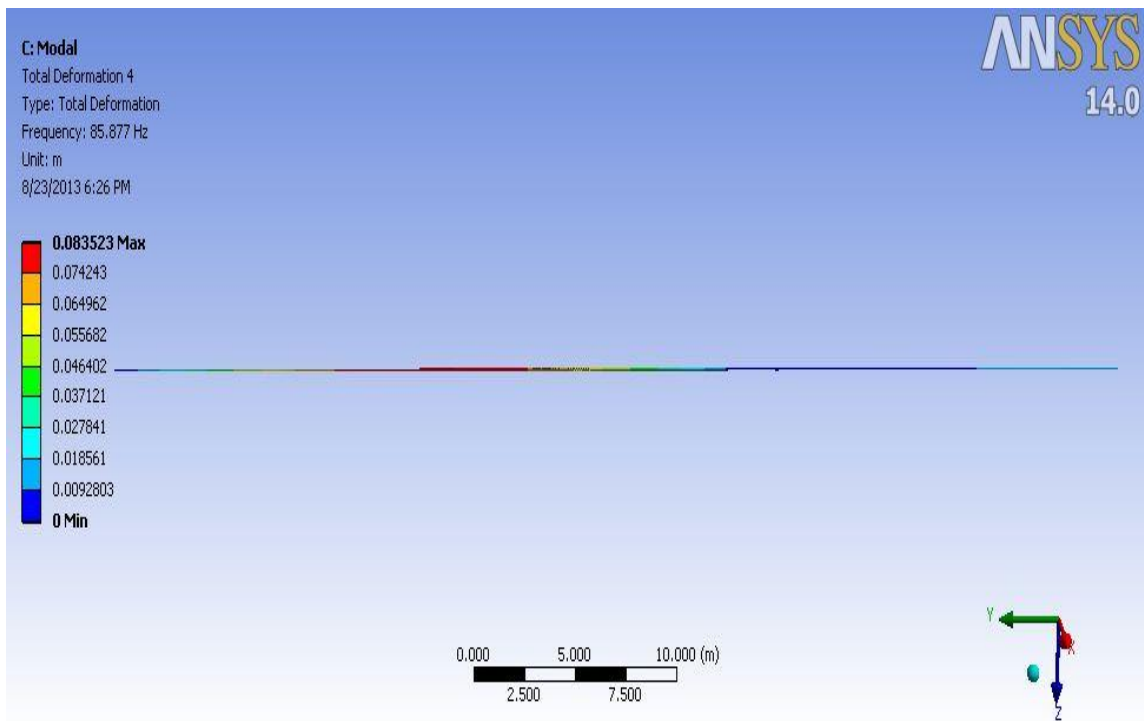


Figure 4.60: Deformation at Natural Frequency of Mode 4 at Production rate=6000bbl/day for the Whole 50m Tubing Length

After that, the maximum deformations of first four modes at production rate of 6500bbl/day are obtained with their pictures (as shown in Fig.4.61 to Fig. 4.68) are as shown below.

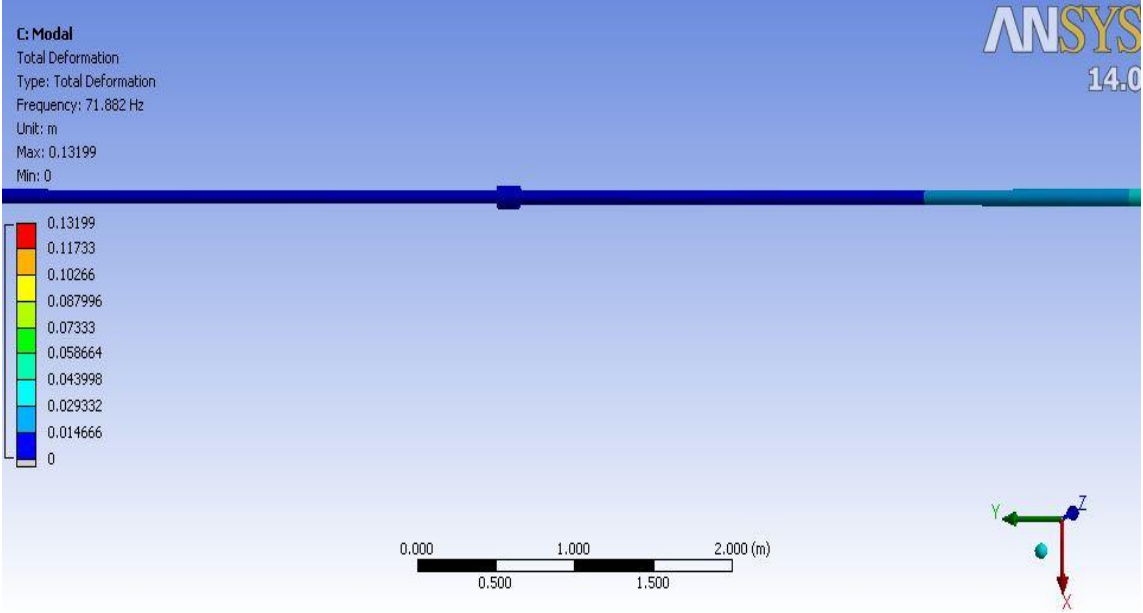


Figure 4.61: Deformation at Natural Frequency of Mode 1 at Production rate=6500bbl/day at Packer Region

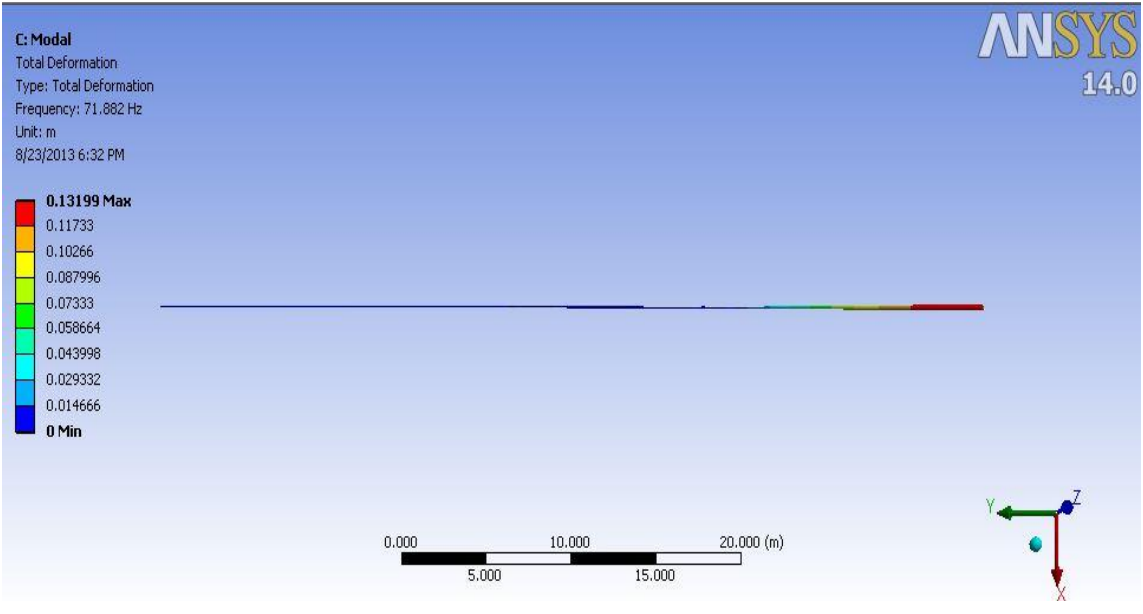


Figure 4.62: Deformation at Natural Frequency of Mode 1 at Production rate=6500bbl/day for the Whole 50m Tubing Length

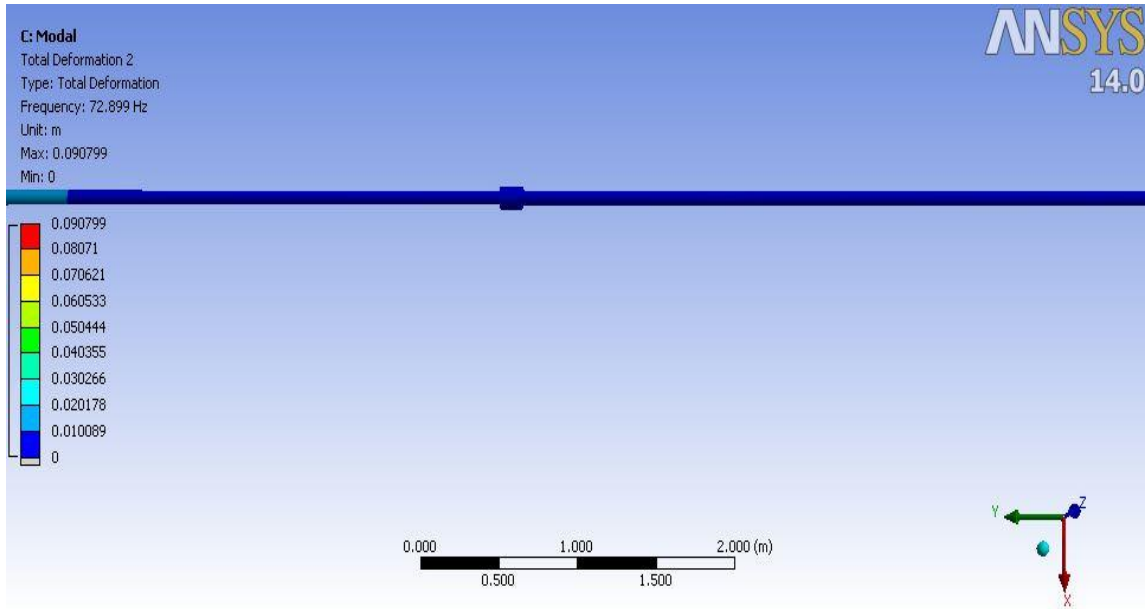


Figure 4.63: Deformation at Natural Frequency of Mode 2 at Production rate=6500bbl/day at Packer Region

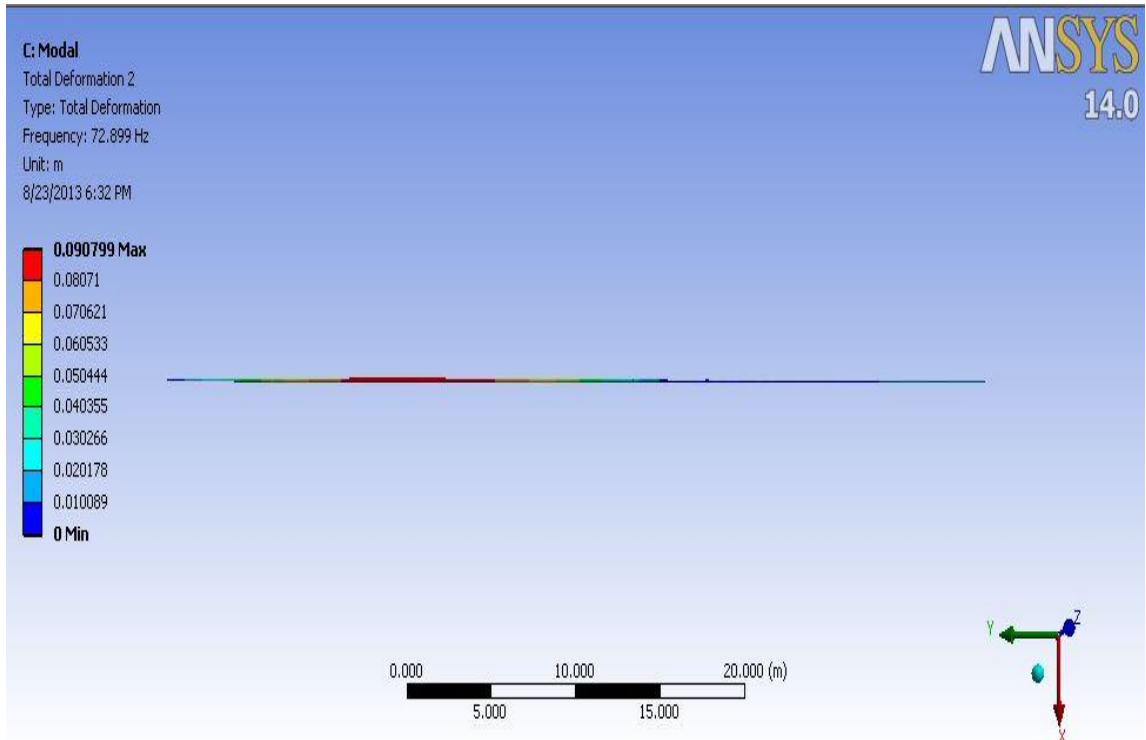


Figure 4.64: Deformation at Natural Frequency of Mode 2 at Production rate=6500bbl/day for the Whole 50m Tubing Length

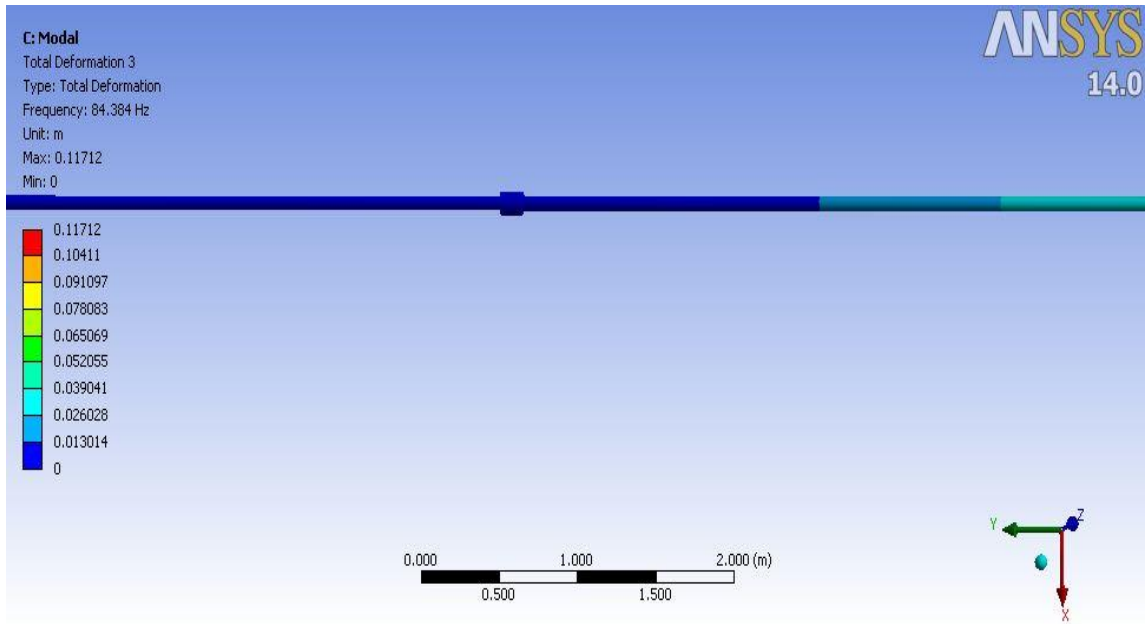


Figure 4.65: Deformation at Natural Frequency of Mode 3 at Production rate=6500bbl/day at Packer Region

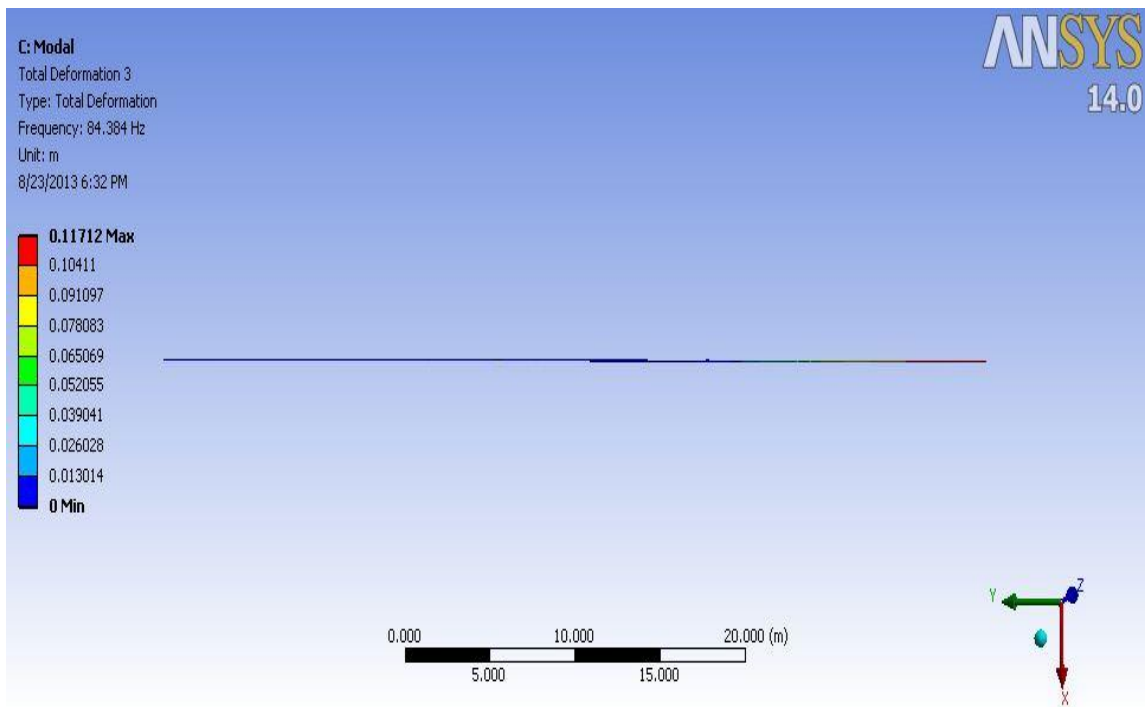


Figure 4.66: Deformation at Natural Frequency of Mode 3 at Production rate=6500bbl/day for the Whole 50m Tubing Length

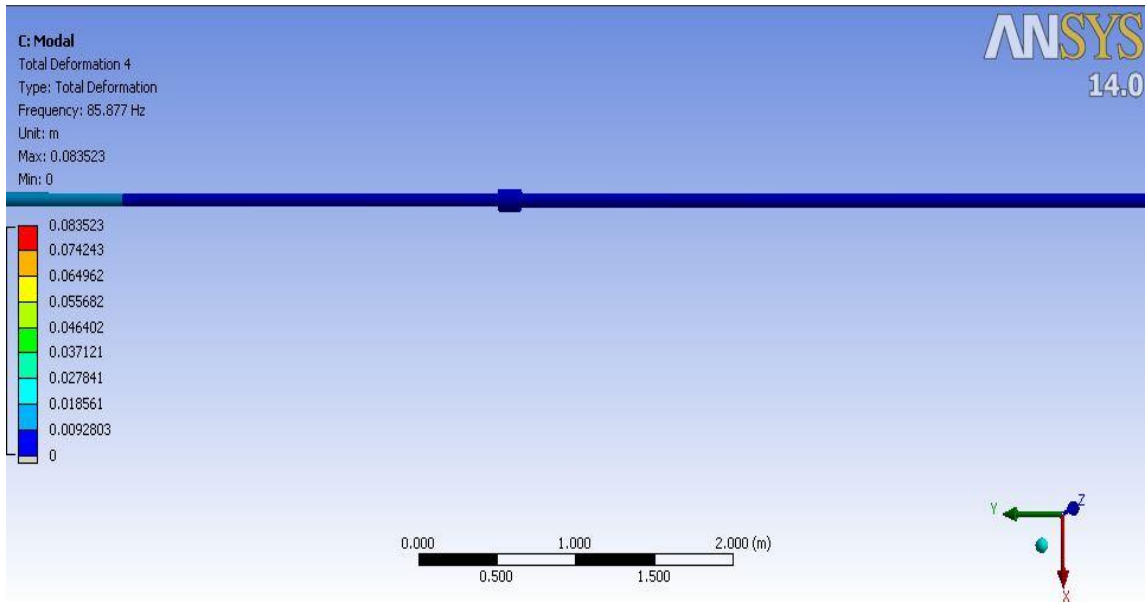


Figure 4.67: Deformation at Natural Frequency of Mode 4 at Production rate=6500bbl/day at Packer Region

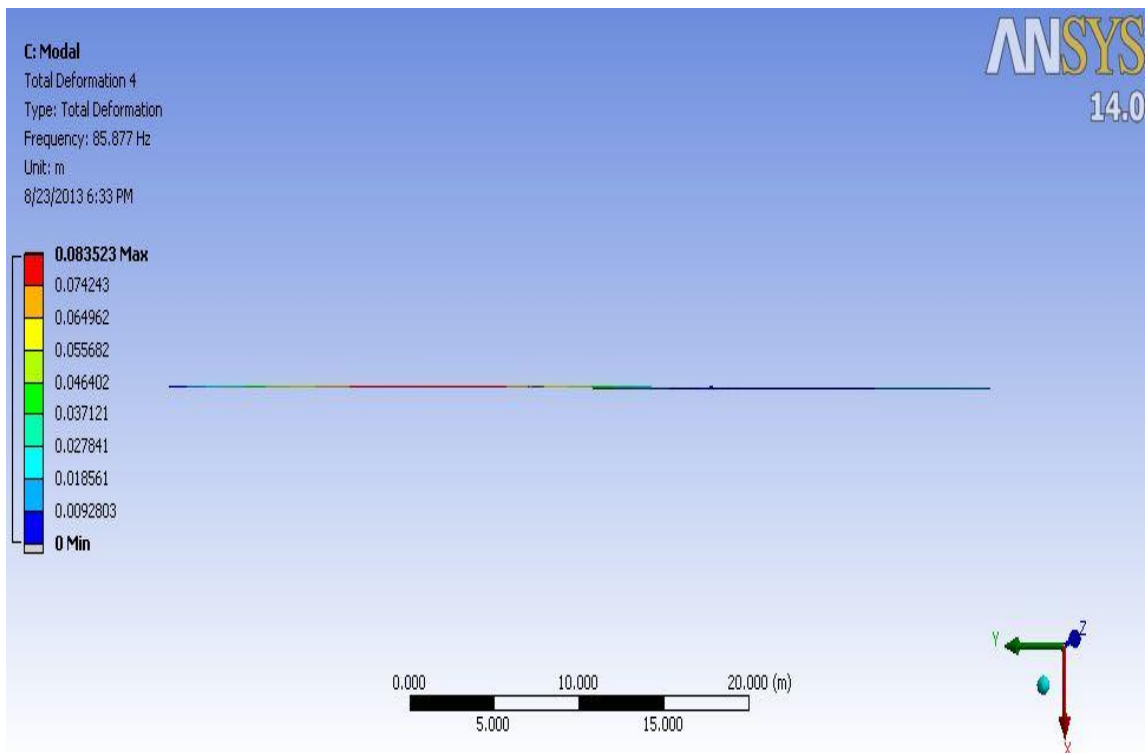


Figure 4.68: Deformation at Natural Frequency of Mode 1 at Production rate=6500bbl/day for the Whole 50m Tubing Length

Then, by using the values in Fig.37 up to Fig. 4.68, the Table 4.6 (as shown below) is tabulated, which is showing the maximum deformations at first four modes at production rates of 5000, 5500, 6000 and 6500bbl/day.

Table 4.6: The Maximum Deformation of Different Modes at Different Production rates

Production Rate (bbl/day)	Maximum Deformation (m)			
	Mode 1	Mode 2	Mode 3	Mode 4
5000	0.090522	0.096995	0.11712	0.083523
5500	0.12659	0.087137	0.11712	0.083523
6000	0.13108	0.090185	0.11712	0.083523
6500	0.13199	0.090799	0.11712	0.083523

After that, by using the values in Table 4.6, Fig. 4.69 (as shown below) is plotted, showing the Graph of Maximum Deformation of Different Modes vs Different Production rates. From Figure 4.69, it can be seen that the deformation at lower modes of 1 and 2 increases with increasing production rate. This is because the natural frequencies affect the deformation of the tubing. At higher natural frequencies, higher deformation is expected, and for similar natural frequencies, similar deformation is expected. Thus, for lower modes of 1 and 2, the increase in the natural frequencies causes the increase in the deformation occurring on the tubing as the production rate increases. However, for mode 3, the deformation is similar to each other because the natural frequencies are quite similar to each other for different production rates. The same case also applies to mode 4.

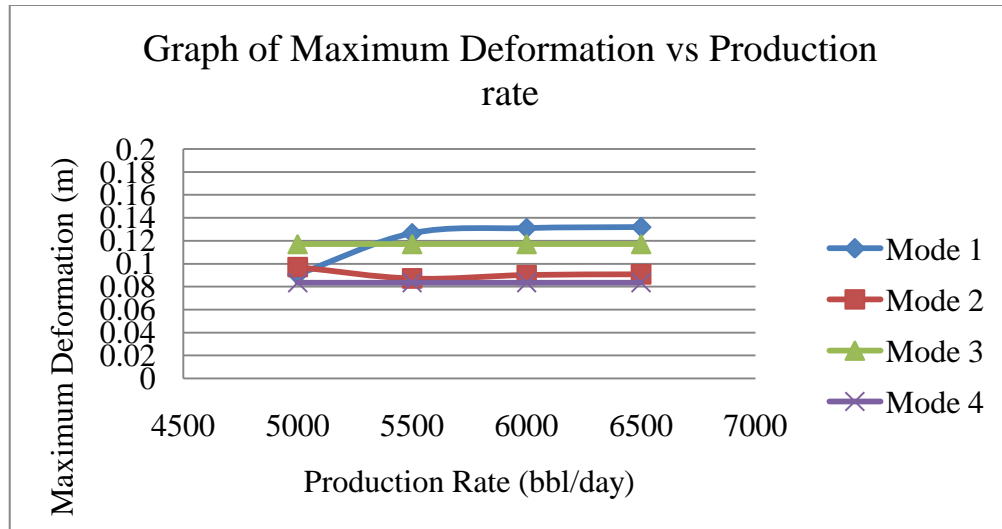


Figure 4.69: The Graph of Maximum Deformation of Different Modes vs Different Production rates

4.4.2 DEFORMATION ON THE DIFFERENT LOCATIONS OF THE TUBING WITH RESPECT TO THE NATURAL FREQUENCIES

The deformation at different locations of the tubing with respect to natural frequencies are investigated, however, only the natural frequencies at lower modes are considered, since the natural frequencies at a bit higher modes brings about quite similar deformation, which brings little significance as compared to the deformations produced by the natural frequencies at lower modes of vibration. For the investigation, the deformations at the length of $0.11L$, $0.23L$ and $0.33L$, which are between the inlet and the packer (Fig. 4.70), are obtained from the simulation conducted, with L is equivalent to total length. Then, the deformations at the length of $0.33L$, $0.56L$, $0.64L$, $0.86L$ and $1.0L$, which are between the packer and the outlet are obtained from the simulation conducted, with L is equivalent to total length. The investigation is focused on regions between the supports, whereby region between the packer and the outlet has 2 supports between it, while the region between the packer and the inlet has 1 support between it.

4.4.2.1 Between the Inlet and the Packer

The positioning between the inlet and the packer is shown in Fig. 4.70.

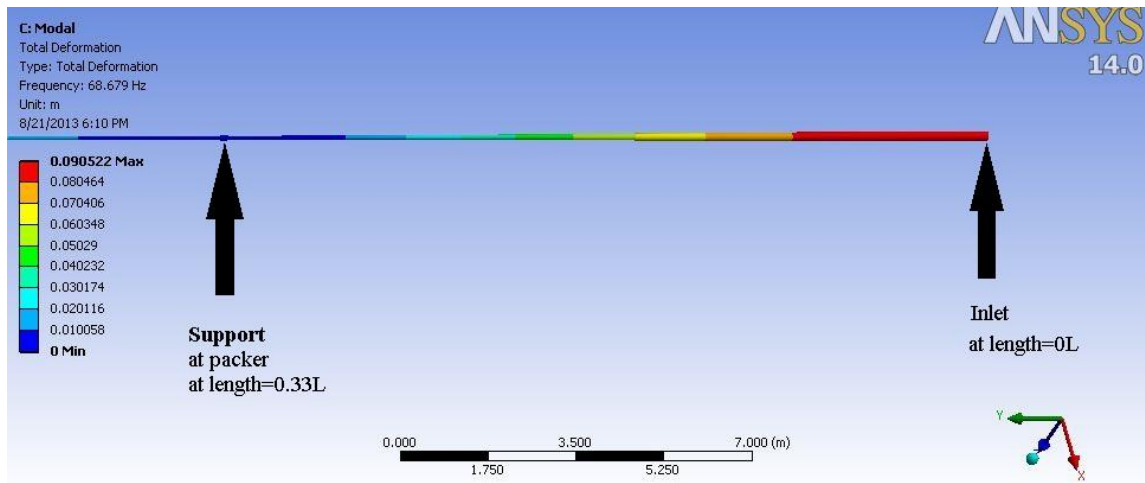


Figure 4.70: The Positioning of the Support between the Packer and the Inlet

And from the simulation, the deformations at different locations on the tubing at different natural frequencies between the inlet and the packer are shown in Table 4.7.

Table 4.7: The Deformation at Different Locations on the Tubing at Different Natural Frequencies between the Inlet and the Packer

Natural Frequencies	Deformation (m)		
	At Length=0.11L	At Length=0.23L	At Length=0.33L
68.679	0.07274600	0.03311000	0.00000000
68.894	0.07709800	0.03444500	0.00000000
69.698	0.10949000	0.05149400	0.00000000
70.068	0.03248700	0.01425700	0.00000000
70.773	0.09043400	0.02889200	0.00000000
71.455	0.01608300	0.00640690	0.00000000
71.882	0.10288000	0.05046600	0.00000000
72.899	0.01091400	0.00464690	0.00000000

After that, by using the values in Table 4.7, The Graph of Deformations at Different Locations on the Tubing between the Packer and the Inlet vs Natural Frequencies is plotted as shown in Fig. 4.71 below. From Fig. 4.71, it is seen that fluctuation of deformation occurs at different natural frequencies. This is because of the positioning of the support, whereby the support provides constraint to the system. At length=0.33L, which is located exactly at the packer region, the deformation is zero because the packer which envelops the tubing provides stability to the tubing at this particular region. However, the inlet is in free state, therefore, the inlet which is at 0L will experience deformation with quite high magnitude, which will slowly decreases in magnitude until it reaches the packer region, which is at 0.33L, since the packer region is supported by the stability effect of the packer.

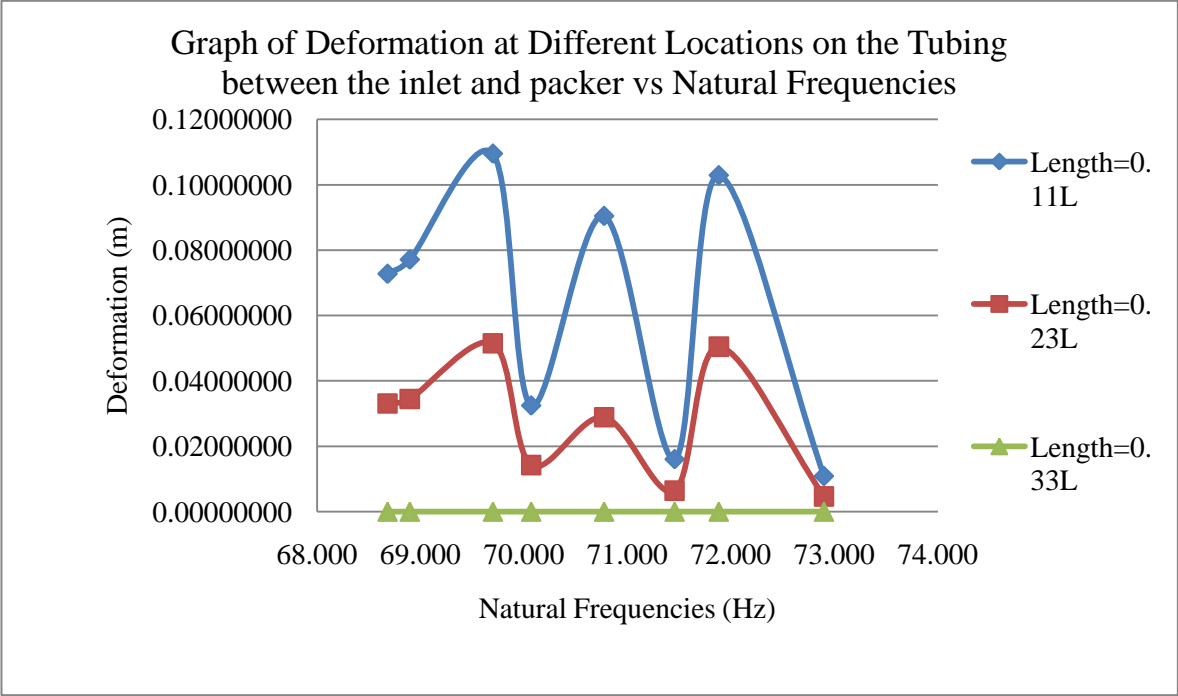


Figure 4.71: The Graph of Deformations at Different Locations on the Tubing between the Packer and the Inlet vs Natural Frequencies

4.4.2.2 Between the Packer and the Outlet

The positioning between the inlet and the packer is shown in Fig. 4.72.

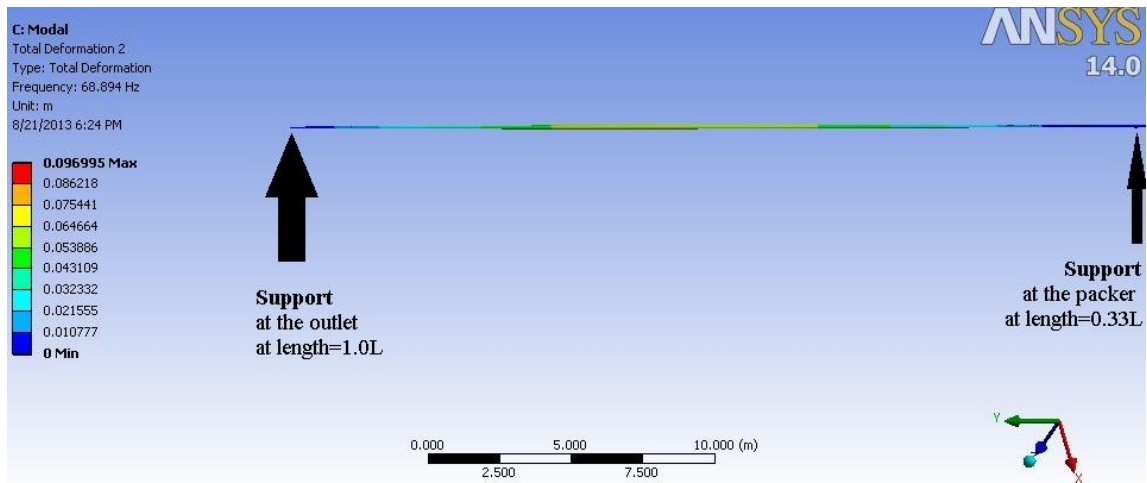


Figure 4.72: The Positioning of the Support between the Packer and the Outlet

And from the simulation, the deformations at different locations on the tubing at different natural frequencies between the inlet and the packer are shown in Table 4.8.

Table 4.8: The Deformation at Different Locations on the Tubing at Different Natural Frequencies between the Packer and the Outlet

Natural Frequencies	Deformation (m)				
	At Length=0.33L	At Length=0.56L	At Length=0.64L	At Length=0.86L	At Length=1.0L
68.679	0.0000000	0.0525980	0.0661670	0.0597040	0.0000000
68.894	0.0000000	0.0484950	0.0620140	0.0566660	0.0000000
69.698	0.0000000	0.0216680	0.0269640	0.0242230	0.0000000
70.068	0.0000000	0.0688170	0.0865490	0.0787650	0.0000000
70.773	0.0000000	0.0110120	0.0138350	0.0123370	0.0000000
71.455	0.0000000	0.0777860	0.0899860	0.0742210	0.0000000
71.882	0.0000000	0.0075489	0.0090425	0.0078407	0.0000000
72.899	0.0000000	0.0863500	0.0872340	0.0671290	0.0000000

After that, by using the values in Table 4.7, The Graph of Deformations at Different Locations on the Tubing between the Packer and the Outlet vs Natural Frequencies is plotted as shown in Fig. 4.73. From Fig. 4.73, it is seen that fluctuation of deformation occurs at different natural frequencies. This is because of the positioning of the supports, whereby the support provides constraint to the system (Fig. 4.72). At length=0.33L, which is located exactly at the packer region, the deformation is zero because the packer which envelops the tubing provides stability to the tubing at this particular region. At length=1L, which is located at the outlet region at the depth of 1585m, there is actually a packer just exactly above this location at other oil production zone. Therefore, in the simulation, a support is placed here at the outlet region. And the deformation at this region of 1L is zero because it has support to provide stability to the tubing at this particular region. Therefore, deformation will become zero at the packer region, which is at 0.33L, and slowly increases in magnitude until it reaches approximately at the middle region between the outlet and the packer, and then the deformation will start to decrease in magnitude until it reaches the outlet region, where the deformation will finally becomes zero.

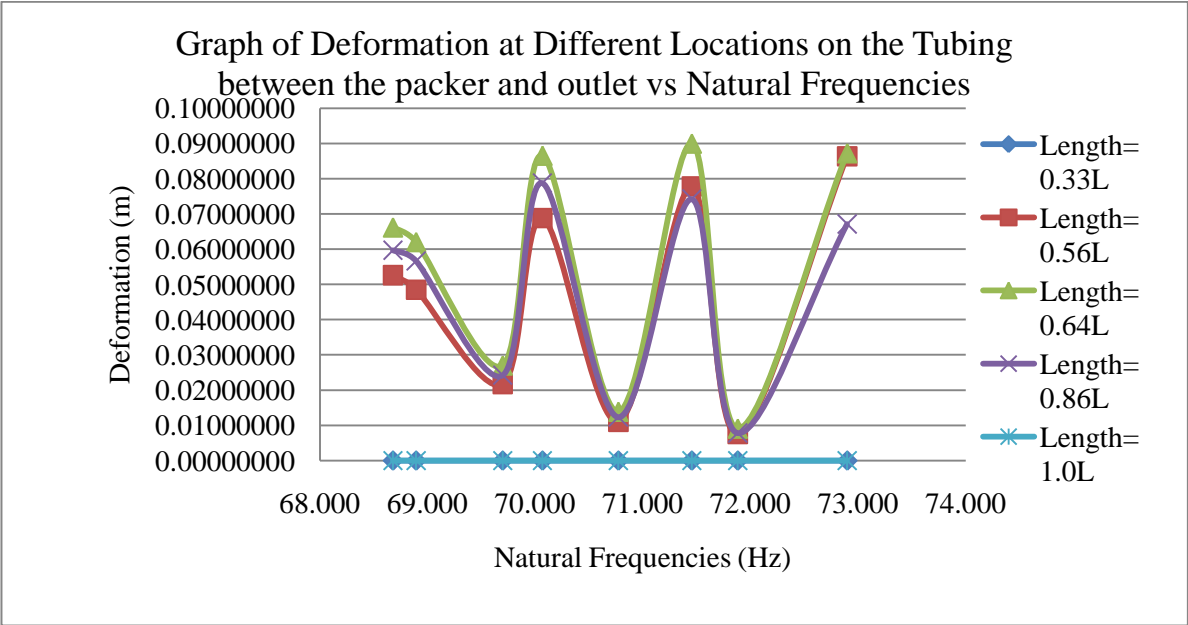


Figure 4.73: The Graph of Deformations at Different Locations on the Tubing between the Packer and the Outlet vs Natural Frequencies

CHAPTER 5

CONCLUSION

5.1 CONCLUSION

The objectives of this project which are to determine the dynamic characteristics (natural frequencies at different modes) and static characteristics (stress and deformation) of the tubing due to fluid dynamic loading with respect to different production rates have been achieved. For static characteristics of the tubing, the stress is increasing when the production rate is increasing with their relationship is almost linear. This is because the pressure exerted onto the tubing increases as production rate increases. For deformation, the deformation is increasing when the production rate is increasing with their relationship is almost linear because the pressure and stress exerted onto the tubing increases as the production rate increases. For dynamic characteristics of the tubing, the natural frequency at lower modes is increasing when the production rate is increasing with their relationship is almost linear because the turbulence effect is causing the increase in stiffness as the production rate increases. However, the natural frequencies at a bit higher modes are not affected much when the production rate is increasing due to insignificant effect of turbulence effect. Plus, different positioning of support affects the tubing system and produces different deformations at different locations of the tubing since support provided by the packer provides stabilizing effect which can help reduce deformation at the area of contact between packer and the tubing. Therefore, the summary of this project are, the stress, deformation and the natural frequency at lower modes of vibration increases with increasing production rates, which signifies that stress, deformation and natural frequency at lower modes are proportional to the production rate. However, natural frequencies at higher modes are receiving less effect from the turbulence effect, which cause the deformation to be similar even though the production rate is increased.

5.2 RECOMMENDATIONS FOR FUTURE WORK AND CONTINUATION

It is recommended to do the simulation for multiphase fluid flow, by choosing the oil production zone with multiphase fluid flow, so that comparison can be made between the dynamic and static characteristics of the tubing for multiphase and single phase fluid flow.

It is recommended that instead of doing simulation, the project is continued with experiments, because the experiment results can be used to make correlation between the simulation and experimental side of this project. Plus, with experiments, different kinds of oil can be used for the experiments, which can provide results for different kinds of oil and comparison can be made between the different kinds of oil involved.

REFERENCES

- [1] William, C.L., & Gary, J.P., *Standard Handbook of Petroleum and Natural Gas Engineering*, 2nd Ed. Texas, United States of America: Gulf Professional Publishing, 2004.
- [2] Norman, J. H., *Nontechnical Guide to Petroleum Geology, Exploration, Drilling and Production*, 3rd Ed. Oklahoma, United States of America: Penn Well, 2001.
- [3] Bradley, H.B., *Petroleum Engineering Handbook*, Rev Ed. Texas, United States of America: Gulf Publishing, 1987.
- [4] Layton, B.E., "A Comparison of Energy Densities of Prevalent Energy Sources in Units of Joule per Cubic Meter," *International Journal of Green Energy*, vol. 5, pp. 438-455, 2008.
- [5] Hasan, A.R., & Kabir, C.S., *Fluid Flow and Heat Transfer in Wellbores*. 1st Ed. Texas, United States of America: Society of Petroleum Engineers, 2002.
- [6] Cullender, M.H., & Smith, R.V., "Practical Solution of Gas Flow Equations for Wells and Pipelines with Large Temperature Gradients. Trans," *Trans. ASME*, pp.281-287, 1956.
- [7] Kelkar, M., *Natural Gas Production Engineering*. Oklahoma, United States of America: Penn Well, 2008.
- [8] Farshad, F., Rieke, H. & Garber, J., "New Developments in Surface Roughness Measurements, Characterization and Modelling Fluid Flow in Pipe," *Journal of Petroleum Science and Engineering*, vol. 29, pp.135-150, 2001.
- [9] Romeo, E., Royo, C. & Monzon, A, "Improved Explicit Equations for Estimation of the Friction Factor in Rough and Smooth Pipes," *Journal of Chemical Engineering*, vol. 86, pp.369-374, 2002.
- [10] Munson, B.R., Young, D.F., Okiishi, T.H. & Huebsch, W.W., "Fundamentals of Fluid Mechanics," New Jersey, United States of America: John Wiley & Sons, 2010.
- [11] Tijsseling, A.S. , "Fluid –Structure Interaction in Liquid-Filled Pipe Systems: A Review," *Journal of Fluids and Structures*, vol. 10, pp. 109-146, 1999.
- [12] Wiggert, D.C. & Tijsseling, A.S., " Fluid Transients and Fluid Structure Interaction in Liquid-Filled Piping," PhD thesis, Eindhoven University of Technology, Netherlands, 2001.

- [13] Zhang, L., Tijsseling, A. S. & Vardy, A.E., “FSI Analysis of Liquid-Filled Pipes,” *Journal of Sound and Vibration*, vol. 224, pp. 69-99, 1999.
- [14] Zhang, H., Ji, S.& Bathe, K.J, “Finite Element Analysis of Fluid Flows Fully Coupled with Structural Interactions,” *Computers and Structures*,pp. 1-16, 1999.
- [15] Torres Monzon, C.F., “Modeling of Oil Water Flow in Horizontal and Near Horizontal Pipes,” PhD thesis, University of Tulsa, United States of America, 2006.
- [16] Moaveni, S., *More ANSYS. Finite Element Analysis : Theory and Application with ANSYS*, 3rd Ed. New Jersey, United States of America: Prentice Hall, 2007.
- [17] Hibbler, R.C., *Mechanics of Materials*. New Jersey,United States of America: Prentice Hall, 2010.R. E. Sorace, V. S. Reinhardt, and S. A. Vaughn, “High-speed digital-to-RF converter,” U.S. Patent 5 668 842, Sep. 16, 1997.
- [18] Zhang, Y.L.& Chen, L.Q., “Internal Resonance of Pipe Conveying Fluids in the Supercritical Regime,” *Dynamics*, vol. 67, pp.1505-1514, 2012.

APPENDICES

Appendix 1: The Software Used for the Project (ANSYS)

